博士論文

Fermentation-associated extracellular electron transport mechanism in human pathogens

(ヒト病原細菌による発酵代謝と共役した細胞外電子移動機構の研究)

ナラダス　デイビア
NARADASU DIVYA
Department of Advanced Interdisciplinary Studies.
The Research Center for Advanced Science and Technology (RCAST)
The University of Tokyo

2018

Contents **Page No**

Abbreviations

AA	:	*Aggregatibacter actinomycetemcomitans*
AI	:	Auto-inducers
ATP	:	Adenosine Triphosphate
BHI	:	Brain heart infusion broth
CA	:	Chronoamperometry
CE	:	Counter electrode
CO	:	*Capnocytophaga ochracea*
DAB	:	3, 3'-diaminobenzidine
DM	:	Defined medium
DPV	:	Differential pulse voltammogram
ETP	:	electron transport phosphorylation
EET	:	Extracellular electron transfer
ET	:	Electron transmission
IC	:	Ion chromatography
ITO	:	Tin-doped Indium oxide
LB	:	lysogeny broth
LSV	:	Linear sweep voltammogram
MFC	:	Microbial fuel cell
μA	:	Micro ampere
mM	:	Milli molar
mV	:	milli volts
NADH	:	Nicotinamide adenine dinucleotide
NanoSIMS	:	Nanoscale secondary ion mass spectroscopy
OCV	:	Open-circuit voltage
OD	:	Optical density
OM	:	Outer membrane
OMV	:	Outer membrane vesicles
PBS	:	Phosphate buffer saline

PG	:	*Porphyromonas gingivalis*
REX	:	Redox enzyme repressor
RE	:	Reference electrode
RF	:	Riboflavin
ROI	:	Regions of interest
rRNA	:	ribosomal Ribonucleic acid
SEM	:	Scanning electron microscopy
SHE	:	Standard hydrogen electrode
SLP	:	substrate-level phosphorylation
SM	:	*Streptococcus mutans*
TEM	:	Transmission Electron Microscopy
TW239	:	REX deleted *S. mutans*
WE	:	Working electrode
WT	:	Wild type

Chapter 1

General Introduction, Research Objective and methodology

1. Introduction to bacterial metabolic electron transfer

My research has inspiration from a quotation "Life is nothing but an electron looking for a place to rest" by a noble laurate Albert Szent Györgyi, electron transfer processes are key for living organisms from macro to micro scale especially microorganisms like bacteria. Bacteria are omnipotent and influences the human (inside your body and on your skin) and non-human (air, soil, water) environments in the nature. Adapting to the extracellular environment associated with various energy sources, redox potentials, pH, and/or temperature challenges the bacteria's survival. Oxidation reduction reactions involved in these bacterial energy acquisition processes comprises their metabolism and electron transfer processes through which they maintain the intracellular redox homeostasis. Understanding of these microorganism's electron transfer processes has become a focal point in-order to identify the key mechanisms helping these microbe's survival in the nature especially in human environments. Because bacteria co-exist with human environments in polymicrobial communities, some are beneficial, and some are harmful by causing diseases. Scientists/biologists studies the bacterial disease enhancement from host point of view, but electrochemists and microbiologists are more focused on electron transfer pathways to look at the underlying mechanism of survival by understanding their metabolic energy acquisition. As in environmental bacteria of non-human environments, a novel electron transfer process is being studied in which metabolism is linked with extracellular electron acceptors like insoluble metal oxides. In this section the history and importance of bacterial electron transfer processes are introduced.

Of the many challenges bacteria face in-order to make in making a living, are more importantly adenosine triphosphate (ATP) generation, maintaining redox balance, and generating primary metabolites by acquiring basic elements like carbon and nitrogen [1].

Nitrogen fixation and oxidation of inorganic compounds such as Sulphur and iron are one of the many numbers of metabolic pathways which have been described for microorganisms [2],[3]. Today, it is well recognized that the energy deriving capacity by catalyzing diverse chemical reactions is one of the mechanisms of the microbes for growth. Most of the microorganisms can convert simple sugars, such as glucose, fructose, and galactose, to pyruvate through the glycolytic Embden-Meyerhoff pathway as shown in schematic Figure 1-1 [4,5]. The glycolysis produced pyruvate is then metabolized further through fermentative pathways to become lactic acid, acetic acid, formic acid and ethanol. Chemotrophic organisms utilize redox reactions in catabolic pathways to couple energy conservation. In the oxidative part or branch, ATP is generated via substrate-level phosphorylation (SLP) from "energy-rich" compounds that are formed. The electron carriers are reoxidized by a terminal acceptor in the reductive branch; in this way ATP is synthesized by generating an electrochemical ion gradient at the cytoplasmic membrane, transport across membranes, and motility. This second type of energy conservation is called respiration or electron transport phosphorylation (ETP).

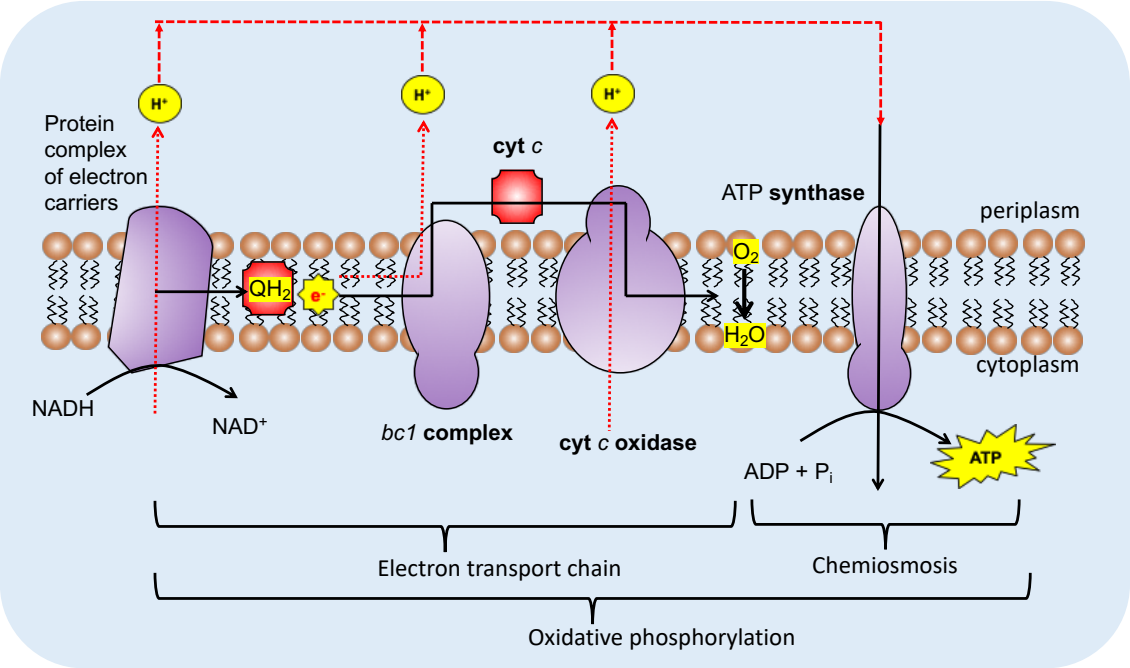

Figure 1-1. Electron transport chain coupled with ATP generation through oxidative phosphorylation

Bacterial fermentations are considered distinct from these type of energy conversions because they do not require terminal electron acceptors for reoxidation of electron carriers and are thought to lack ETP [6-8]. In these fermentations the substrate serves not only as an electron donor but also as a terminal acceptor for regeneration of electron cofactors such as NAD^+, since oxygen, nitrate, fumarate, etc. are absent [9-11] (Figure. 1-2). In recent years, much attention is towards the microbial metabolisms that involve electron transfer between cells and extracellular substrates, such as minerals termed as extracellular electron transfer (EET), turned out to be a promising area for future biochemical, genetic and cell biological research.

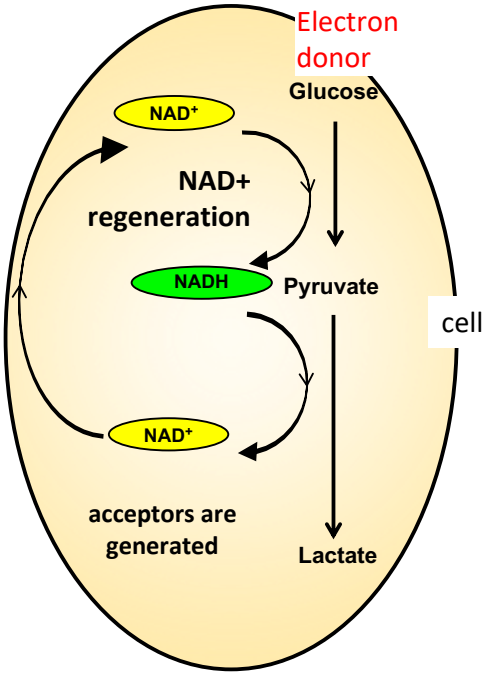

Figure 1-2. Fermentative metabolism in which electron acceptors are generated

1.1 Extracellular electron transfer

Extracellular electron transfer is defined as the process in which electrons derived from the oxidation of electron donors are transferred to the outer surface of the cell to reduce an extracellular terminal electron acceptor. Extracellular electron acceptors may be soluble yet reduced outside the cell because they are too large to enter the cell, as is probably the case for humic substances like iron, manganese oxides (Figure. 1-3, [12-17]). There are well studied model EET microbes called *Shewanella* and *Geobacter*. Unlike other metabolisms where the final electron acceptor is a freely diffusible gas such as oxygen or a readily soluble species that the cell can easily access such as nitrates, sulphate, metal reducers face the task of transferring electrons to a solid form present at the outside of the cell surface. Although Fe (III) is almost insoluble at neutral pH, it serves as one of the most important electron acceptors for microorganisms in anaerobic environments[18]. Using an outer-membrane reductase to receive and transfer the reducing power in terms of energy cofactors like NADH, generated by internal metabolism to the insoluble oxidant outside is one way to respire iron

minerals. For example, *G. sulfurreducens* transports the electrons to iron by using a membrane-bound NADH dehydrogenase coupled to a c-type cytochrome [19]. A series of electron carriers such as cytochromes and menaquinones are required to transport the electrons to iron down a long respiratory chain in *Shewanella* species [20,21]. Although the specifics of energy generation have not yet been determined, a proton-motive force is presumably established by proton pumping by electron carriers such as menaquinone and/or the NADH dehydrogenase of electron transport chain [1,22] Whether in *Geobacter* or *Shewanella* species, all of these pathways assume direct contact between microbes and minerals. Extracellular electron transfer is most likely to take place in an environment where a terminal oxidant is not easily accessible (e.g., poorly soluble and/or diffusion limited) and where excreted shuttles can be efficiently recycled. Hence a for high density bacterial biofilms, a terminal acceptor can be replaced to a soluble quinones which can shuttle and reduce molecular oxygen outside of the biofilm and conducts EET.

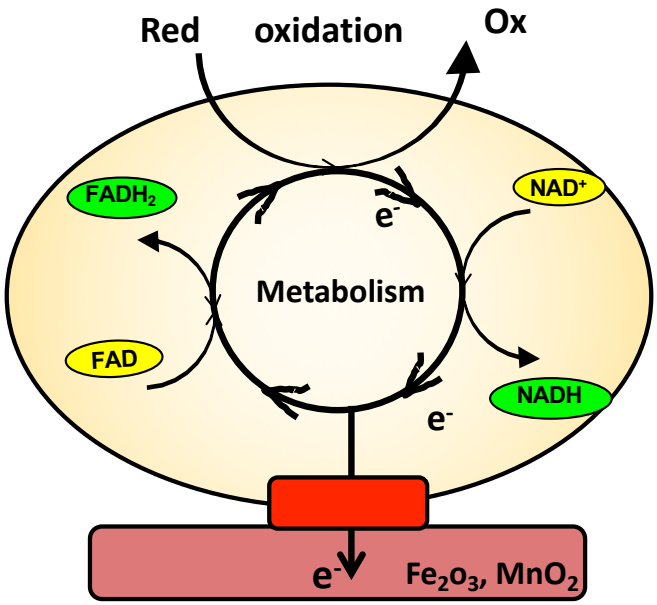

Figure 1-3. Extracellular electron transport mechanism which requires external electron acceptors like insoluble minerals

1.2 Importance of EET in human bacterial biofilms

Polymicrobial fermentative communities have a critical impact on human health by causing various illnesses [23]. Bacterial biofilms contribute to host health and disease and are complex systems that rely on the biofilm matrix to provide the structural and functional properties that distinguish this state from free-living bacterial cells [23-25] by attaching to host surface such as gut lumen or tooth surfaces. The dynamics of biofilm formation are dependent on many factors for example nutrient availability, oxygen gradients, environmental stress, social competition, and the generation of extracellular matrix materials. These extracellular polymeric substances provide the architecture surrounding the bacterial cells enabling emergent properties such as resource capture, tolerance to antimicrobial compounds, cooperation or competition, and localized gradients of nutrient, pH and oxygen. Biofilm-associated infections have increased tolerance to antimicrobials and immune clearance and can be especially difficult to treat or eradicate them completely [25]. In a polymicrobial biofilm, there exists the development of gradients and can create anoxic and acidic zones in the interior of biofilm clusters [26-29]. Bacteria can develop a stationary phase -like dormancy in nutrient-depleted zones within the biofilm, which may be responsible for the general resistance of biofilms to antibiotics [30,31]. In such energy scarce conditions survival and electron transfer mechanism of these bacteria are poorly understood. While most of the human bacteria rely on fermentation, which is the primary microbial metabolism for the redox cycling of biological electron carriers such as nicotinamide adenine dinucleotide (NADH) that drives the intracellular oxidation and reduction of organic substrates. Because fermentation does not require extracellular electron acceptors to terminate the metabolism, energy gain under such conditions is potentially lower than respiratory metabolisms; And fermentative metabolites such as hydrogen creates redox environment in dense biofilms and inhibits the reoxidation of NADH, hinders continuation of fermentation process. Therefore, EET capability to increase the rate of NAD^+ regeneration and fermentative metabolism may be important for them to increase net energy gain and compete with other respiratory bacteria [18]. In fact, a few studies have shown that the fermentative microbes are capable of EET using soluble electron carrier molecules [32,33].

1.3 Research background and objective of this study

Microbial communities have a critical impact on human health by causing various diseases with major energy mechanism of fermentation [34]. The microbially generated fermentative metabolites such as hydrogen hamper the re-oxidation of pyridine nucleotides (NADH), hence individual cells encounter the challenge of sustaining the redox homeostasis to maximize energy production [34,35]. Hydrogen consumption by niche-specific symbiotic bacteria has been considered as an alternative for balancing the intracellular energy [36], rather than the capability of individual bacteria. While, in environmental microbes, electron transfer is used for the regeneration of NAD^+ by a phenomenon called extracellular electron transfer (EET) through redox enzymes, where metabolically generated electron are transferred to an external electron acceptor [18,37]. However, the ability of electron transfer to balance intracellular potential has not been widely investigated in fermentative bacteria as bacterial fermentation doesn't require electron acceptor. In this study, we hypothesized that exporting reductive energy via electron transfer can be energetically conservative for the fermentative bacteria to sustain the redox balance. However, the capability of EET in human environmental oral pathogens and the physiological significance of such electron export in biofilm was not explored before.

We tested our hypothesis in an enormously studied fermentative pathogen of the oral environment *Streptococcus mutans (S. mutans)*, with the application of bioelectrochemical and biochemical methods. The capability of EET by *S. mutans* and its associated mechnaism along with its physiolocal role of EET in redox homeostasis was identified and discussed in detail in chapter 2. Known, *S. mutans* has low-pH tolerance associated virulence properties and survives in acidic redox conditions by causing chronic periodontic diseases [38], yet its survival mechanism is ambiguous. Thus, we specifically examined the pH dependence on the electron transfer capability which could give insights into the mechanism of this acid tolerant pathogen presented in chapter 3.

Understandig the implication of extracellular electron trnasport in oral biofilms is critical, where exists a diverse oxygen gradients creating anaerobic, anoxic and aerobic interfaces in which bacteria are spanned over a range of more than 200 micrometer length on tooth surface. The oral biofims were found to be arranged in an architectured manner, where anaerobes exists in deep anaerobic spaces, faculttaive anaerobes in anoxic and aero tolerants near the surface where plenty of oxygen is available [39]. Biofilms extracted from a patient having a bisphosphonate related osteonecrosis of jaw, were found to have electrically conductive nanowires conencting the bacteria [40]. The existance of oxygen gradients and electric conductive nature of biofilm suggesteing the possibility of a long range extracellular electron trnapsort in oral biofilms, where anaerobes in depth of biofilm can transfer electrons to the aerobic space to utilise oxygen as an electron acceptor. To this end we tested the generality of EET capability on other predominent oral pathogens [38,39], such as *capnocytophaga ochracea, Porphyromonas gingivalis* and *Aggregatibacter actinomycetemcomitans* to understand the ecophysiological role and associated energetics of EET in human pathogenic bioiflms. Since, model EET capable bacteria such as *shewanella,* and *Geobacter* utilise the cell surface bound cytochromes for direct electron trnasport along with secretion of redox mediator molecules like flavins to use as electron shuttles [32,33]. Specifically identifying the electron transport associated mechanism and energy level determination in these pathogens is explored in chpater 4. Extracellular electron trnasport nature of electrode respiring bacteria is being applied and studied in various researches such as energy conservation or waste water treatments by using microbial fuelc ells (MFC), such EET capability was used as a tool to scrutinize and study the pathogens of other human environments, for example, the human gut by integrating the electrochemical analysis. In chapter 5, using the electrochemical systems EET capable bacteria were enriched and isolated from a microbial community from human gut samples. While similar methods and analyses techniques were used while characterizing the human oral pathogens throughout this dessertation such as the microbal growth preceded by Electrochemical analyses conditions were listed in the following sections.

1.4 Methods and Materials

Cell culture preparation

Streptococcus mutans UA159, purchased from ATCC, was precultivated in 20 ml of brain heart infusion (BHI) medium in butyl-rubber-stoppered vials at 37°C with an anoxic headspace of CO_2/N_2 (20:80 v/v). For pH7 cultures *S. mutans* was grown in buffered (pH7±0.2) BHI medium. The *rex* gene (*SMU_1053*) deleted *S. mutans* termed as Δ*rex* was previously constructed using a PCR-ligation-mutation strategy [41], and kindly provided by Assoc. Prof. Zezhang T. Wen, at Louisiana State University Health Sciences Center. The BHI medium containing kanamycin (1mg/mL) was used for the growth of Δ*rex*. *Capnocytophaga ochracea* ATCC 27872 was propagating in 80 mL of DSMZ 340 medium supplied with 1g/L sodium bicarbonate at 37°C. The medium excluding glucose and hemin was autoclaved for 15 min and 121 °C before use. Glucose and hemin were separately prepared, and filter sterilized prior to inoculation. To maintain the anaerobic growth condition, 20 min of N_2/CO_2 sparging was done prior to glycerol stock inoculation. In the electrochemical experiments, *Capnocytophaga* at late exponential growth phase or early stationary phase, pH= 5.3-5.5, was collected for current production study. Electrochemical experiments were established using a single-chamber three-electrode reactor in the anaerobic chamber (COY glovebox). Three electrodes include: 1-Working electrode (WE), a glass substrate attached with Tin-doped indium oxide (ITO) by spray pyrolysis deposition (SPD Laboratory, Inc., Japan); 2- Counter electrode (CE), platinum wire of 0.1 mm thickness; and 3- Reference electrode (RE), Ag/AgCl (sat. KCl). *Aggregatibacter actinomycetemcomitans* y4 and *Porphyromonas gingivalis* W83 were grown anaerobically in Brain Heart Infusion broth (with 1% yeast extract) and Gifu anaerobic medium respectively.

The cultures were grown till the growth reached the late exponential phase, at which point the OD_{600} was 1.0. Cells were centrifuged at 7800 rpm and 37°C for 10 min, and the resultant cell pellet was washed with defined medium (DM) twice. DM was prepared according to previously described methods with some modification [17] DM contained (per

litre) the following components: $NaHCO_3$, 2.5 g; $CaCl_2 \cdot 2H_2O$, 0.09 g; NH_4Cl, 1.0 g; $MgCl_2 \cdot 6H_2O$, 0.2 g; NaCl, 10 g; HEPES, 7.2 g; and yeast extract, 0.5 g.

Whole-cell electrochemical analysis

Electrochemical measurements were conducted as reported [42,43] in single-chamber, three-electrode reactors. ITO grown on a glass substrate by spray pyrolysis deposition (SPD Laboratory, Inc., Japan) was used as the working electrode (resistance, 8Ω/square; thickness, 1.1 mm; and surface area, 3.14 cm^2) and was placed at the bottom of the reactor. Platinum wire and Ag/AgCl (sat. KCl) were used as counter and reference electrodes, respectively. DM containing 10 mM glucose/Lactate (4.8 mL) was injected into the electrochemical cell as an electrolyte, and the solution was purged with N_2 gas for at least 15 min to remove the dissolved oxygen. Then, 0.2 mL of freshly prepared cell suspension of *S. mutans* pre-washed with DM with an optical density (OD) of 2.5 at 600 nm was injected into the electrochemical cell under a potentiostatic condition of 0.4 V vs a standard hydrogen electrode (SHE) to a final OD_{600} of 0.1. During the electrochemical measurements, the reactor temperature was maintained at 37°C, and the reactor was operated without agitation. Single-potential amperometry (SA), cyclic voltammetry (CV) and differential pulse voltammetry (DPV) were measured with an automatic polarization system (VMP3, Bio Logic Company, France). DPV was measured under the following conditions: −0.6 V to +0.7 V vs. SHE at a pulse height of 50 mV, pulse width of 0.3 s, step height of 5 mV s^{-1}, and step time of 5 s [44]. SOAS software, which is an open source program to analyze experimental electrochemical data was used for our analysis on CV and DP voltammograms. The background current was subtracted by fitting the baseline from regions sufficiently far from the peak assuming continuation of a similar and smooth charging current throughout the peak region. The background-subtracted data were further analyzed for deconvolution to fit the shapes of the peaks with the functions of a model function by finding the parameters that minimized the sum of the square weighted orthogonal distances from a set of observations to a curve determined by the parameters[45].

Antibiotic treatment

A stock solution of Ampicillin sodium 1.86 g/L (with demineralized water as solvent) was prepared and 0.1 mL of the stock solution was added into the *S. mutans* electrochemical reactor to a final concentration about 0.04 mg/mL. This is higher than the minimum inhibitory concentration (MIC) and minimum bactericidal concentration (MBC) for both planktonic or biofilm-detached cells [46]. Triclosan was dissolved in 100% dimethyl sulfoxide (DMSO) solvent at a concentration of 30 mg/mL and 0.1 mL was then added to the electrochemical reactor to a final concentration of 0.6 mg/mL [47]. A control experiment of 100% DMSO was also carried out by adding the same volume of it to a reactor as in case of Triclosan experiment to check the effect of organic solvent. A stock solution of 50 mg/mL Kanamycin (Sigma-Aldrich) was added to a final concentration of 1 mg/mL.

Supernatant exchange experiments during current producing condition

The role of cell-secreted soluble redox mediator was evaluated using a supernatant medium replacement experiment as reported in environmental model microbes *Shewanella* [48] and *Geobacter* species [49]. Here, the medium in the electrochemical cell was removed; the biofilm was gently rinsed with N_2-sparged DM twice at each replacement; and the headspace was continuously sparged with N_2 during each replacement to avoid the leakage of oxygen into the electrochemical cell. The cell was refilled with N_2-sparged sterile medium. The accumulation of soluble mediators in the medium was also evaluated using spent-medium experiments. Culture broth was removed from the surrounding biofilm, centrifuged to remove cell debris, introduced into a fresh electrochemical cell, and sparged with nitrogen. Filters were not used to avoid losing organic molecules by adsorption, and DPV measurements were performed as to detect the redox molecules.

Quantification of metabolite concentration

Aliquots (approximately 200 µL) were collected from the reactors at every 8-hour time intervals for 24 hours, passed through 0.22-µm-pore-size filters to remove cells and stored at -20°C until further analysis. Glucose concentrations were measured by using a

glucose assay kit (GAGO-20, Sigma-Aldrich) according to the manufacturer's instructions, and concurrent results from two different sets of experiments are shown. Samples were diluted 100 times with distilled water prior to metabolite analysis. Lactate, formate and acetate production were analysed by using ion chromatography. As the pH of the medium in the electrochemical cell dropped to 6.8 from the initial pH of 8, the sample pH was adjusted with NaOH to 8, *i.e.,* to that of standards, prior to the analysis. The lactate, acetate and formate concentrations in the samples were quantified using an ion chromatography system (HIC-20Asuper, Shimadzu corporation, Japan). Fifty-microliter samples were injected, and the anions were analysed in non-suppressor mode. Shim-pack IC-A3 and Shim-pack IC-GA3 (Shimadzu corporation, Japan) were used as the analytical column and guard column, respectively. The mobile phase contained 8 mM p-hydroxy benzoic acid, 3.2 mM Bis-Tris, and 50 mM boric acid, and the flow rate was 1.2 mL/min. The column temperature was maintained at 40°C, and the detector (CDD-10A_{SP}) parameters were set according to manufacturer's guidelines. Peak area analysis was conducted by Shimadzu analytical workstation software LabSolutions provided by the manufacturer. The retention times of acetate, lactate and formate were approximately 2.4, 3.25 and 3.4 min respectively, and the standard curves showed sufficiently high linearity (R^2 = 0.999). We could not detect any other visible peak of metabolite by ion chromatography.

Ethanol quantification assay by acid dichromate titration.

Ethanol was quantified in the samples by using standard acid dichromate titrimetric analysis as previously described [50] and the solutions were prepared as follows: 1) Acid dichromate solution (0.01 mol L^{-1} in 5.0 mol L^{-1} sulfuric acid): to prepare the solution, 125 mL of water was added to a 500-mL conical flask. Carefully, 70 mL of concentrated sulfuric acid was added with constant swirling. The flask was cooled under cold water tap. Then, 0.75 g of potassium dichromate ($K_2Cr_2O_7$) was added, and the mixture was diluted to 250 mL with distilled water. 2) Starch indicator solution (1.0%): 1.0 g of soluble starch was added to 100 mL of freshly boiled water and stirred until it dissolved. 3) Sodium thiosulfate solution ($Na_2S_2O_3.5H_2O$; 0.03 mol L^{-1}): 7.44 g of $Na_2S_2O_3.5H_2O$ was added to a 1 L volumetric flask,

dissolved in distilled water and diluted up to the mark. 4) Potassium iodide solution (KI; 1.2 mol L^{-1}): 5 g of KI was dissolved in 25 mL of water. Samples were diluted 1:50 with distilled water. Then, 10 mL of the acid dichromate solution was transferred to a 50- mL Falcon tube. One millilitre of the diluted sample was pipetted into an Eppendorf sample tube, and the sample tube was suspended in a sample holder over the dichromate solution. The sample tubes were stored overnight at 37°C (this incubation should ideally be performed in an incubator). Next morning, the flask was allowed to cool to room temperature, then the cap was loosened carefully, and the sample holder was removed and discarded. The walls of the Falcon tube were rinsed with distilled water, and then approximately 100 mL of distilled water and 1 mL of potassium iodide solution were added, and the tube was swirled to mix the contents. A burette was filled with sodium thiosulfate solution, which was used to titrate each flask. When the brown iodine colour faded to yellow, 1 mL of starch solution was added, and titration was continued until the blue colour disappeared. The blank titration indicated how much acid dichromate was present at the start, as no alcohol was added, thus the full amount of the dichromate was present in contrast to the sample titrations. The average volume of sodium thiosulfate used for the sample was determined from the concordant sample results. The average volume of sodium thiosulfate used for the blank titration was determined from the concordant blank results. The volume of sodium thiosulfate solution used for the sample titration was subtracted from the volume used for the blank titration. This volume of sodium thiosulfate solution was used to determine the alcohol concentration. The number of moles of sodium thiosulfate in this volume was calculated. The relationship between the moles of sodium thiosulfate and the moles of ethanol was calculated as follows: 6 mol of $S_2O_3^{2-}$ is equivalent to 1 mol of $Cr_2O_7^{2-}$, and 2 mol of $Cr_2O_7^{2-}$ - is equivalent to 3 mol of C_2H_5OH; therefore, 1 mol of $S_2O_3^{2-}$ is equivalent to 0.25 mol of C_2H_5OH. This ratio was used to calculate the moles of alcohol in the sample solution.

Total protein assay after electrochemical measurements

After the electrochemical operation for 8 hours, the electrode attached cells were scratched and collected into a 200 µL volume of 0.1 M phosphate buffer saline (PBS)

containing 1% sodium dodecyl sulphate (SDS). Similarly, non-attached cells were centrifuged and resuspended in same volume. The samples were boiled at a temperature of 95°C and total protein was estimated by using the bicinchoninic acid assay (BCA protein assay kit, Thermo fisher) against a standard of bovine serum albumin (BSA) following the manufacturer's instructions.

Riboflavin reduction by fluorescence spectroscopy and coulombic efficiency estimation

Given oxidized flavins are fluorescent, riboflavin reduction by *S. mutans* was quantified by measuring the fluorescence intensity of oxidized riboflavin in an anaerobic quartz cuvette as described previously (riboflavin reduction assay) [51,52]. Ten μM oxidized riboflavin was added to 3 mL of deaerated DM and emission spectrum of oxidized riboflavin (RF) measured by excitation at 450 nm. Given decrease in emission peak intensity at 530 nm corresponds to the reduction of riboflavin, we estimated the amount of electron transported from *S. mutans* in the presence of 10 mM glucose. Coulombic efficiency was calculated with charge transported to RF and the amount of glucose consumed in the cuvette after 24 hours. For other conditions, coulombic efficiency of *S. mutans* in the presence and absence of RF and in Δ*rex* was determined by the consumed glucose, and time vs. current profile after 24 hours.

Sample preparation for scanning electron microscopy

After conducting the electrochemical measurements, the ITO electrodes were removed from the reactors, fixed with 2.5% glutaraldehyde and then washed by immersing the electrodes three times in 0.1 M phosphate (pH 7.4) buffer. The washed samples were dehydrated in 25%, 50%, 75%, 90%, and 100% ethanol gradients in the same buffer, exchanged three times with t-butanol and then freeze-dried under vacuum. The dried samples were coated with evaporated platinum and then viewed using a Keyence VE-9800 microscope.

Sample preparation for nanoscale secondary ion mass spectroscopy (NanoSIMS)

We prepared the NanoSIMS samples and analysed data as described previously [53]. After the current vs. time measurement in the presence of $^{15}NH_4Cl$ as a sole nitrogen source, the ITO electrode with the biofilm was fixed in 2.5% glutaraldehyde in 0.1 M phosphate buffer for 10 min, washed with fresh buffer, dehydrated with an ethanol gradient and t-butanol, dried under vacuum, coated with platinum using Quick Coater SC-701 (Sanyu Electron), and analysed with a CAMECA NanoSIMS 50 L system (CAMECA, Gennevilliers, France) at The University of Tokyo. A Cs^+ beam was irradiated on the sample surface, and the amounts of secondary ions ($^{12}C^{14}N^-$, and $^{12}C^{15}N^-$) were determined. Regions of interest (ROIs) were drawn by hand to mark each individual cell, and the sum of the ion signals in each ROI was calculated with the ImageJ plugin OpenMIMS (http://nano.bwh.harvard.edu/openmims), from which the isotopic ratio of N in each individual cell was calculated as $^{15}N/N_{total}$, which is the ratio of ^{15}N to total nitrogen.

$$^{13}C\text{- ratio}=\frac{^{13}C\text{-pixel}}{(^{13}C+^{12}C)\text{-pixel}}\times 100\% \quad (1)$$

$$^{15}N\text{- ratio}=\frac{^{12}C^{15}N\text{-pixel}}{(^{12}C^{15}N+^{12}C^{14}N)\text{-pixel}}\times 100\% \quad (2)$$

Construction of 16*S* rRNA phylogenetic tree based on Rossman-like folding sequences in the Rex proteins

Initially Rossman-like folding sequences in the Rex proteins of the bacteria were identified and NAD binding was predicted by the bioinformatics software Cofactory v.1.0 [54], with a minimum of 35 residues. The identity of the predicted NAD binding site in the Rossman-like folding motifs of Rex sequences obtained by NCBI blastp searches was compared to that of *S. mutans.* For the construction of a 16*S* rRNA phylogenetic tree, 16*S* rRNA sequences of the bacteria, having Rex Rossman-like folding with NAD binding site, were collected from the NCBI nucleotide database, aligned using MUSCLE [55] and analyzed by the neighbor- joining method [56] using Molecular Evolutionary Genetics Analysis package (MEGA 7) [57].

Membrane Vesicle Isolation and Staining

Membrane vesicles of C. *ochracea* were isolated by growing the cells to late exponential phase and collected by centrifugation at 7,500g for 10 min at 4°C followed by filtration through a 0.22-µm pore size filters to remove residual bacteria. Finally, vesicles were collected by ultracentrifugation at 126,000g for 2 h at 4°C and resuspended in defined medium used for ECs. Bacterial concentrations were determined with a Protein Assay Kit (Bio-Rad, Hercules, CA). For TEM of C. *ochracea* vesicles, vesicles were suspended in 25 µL ddH_2O and applied to a copper microgrid for 60 second and were air-dried. The vesicles were then negatively stained with 0.5% ammonium molybdate for 1 min, and observed under a JEM-1400 microscope operated at 80 kV.

Electrochemical enrichment of human guts sample

Gifu Anaerobic Medium (GAM Broth), which is known for providing reducing conditions and adequate anaerobiosis was used as a rich medium for enrichment of gut microbes. Defined medium 1 (DM1) used as an electrolyte for EET strains enrichment and initial electrochemical characterization experiments had the following composition (L^{-1}): NH_4Cl, 1 g; $MgCl_2.6H_2O$, 0.8 g; $CaCl_2.2H_2O$, 0.1 g; KH_2PO_4, 0.5 g; yeast extract, 1 g; $NaHCO_3$, 1 g, trace mineral mix, 10 mL; and trace vitamin mix, 10 mL. Acetate (30 mM) or lactate (30 mM) were used as electron donors. DM1 exclusive of $NaHCO_3$, trace mineral, and trace vitamin was autoclaved first and after adding remaining components pH was adjusted to 7.2. Final medium was syringe filtered and deaerated by purging it with 100% N_2 for 15 min prior to use for experiment. Defined minimum medium 2 (DM2) used as an electrolyte for EET experiments prepared as previously[17]. Acetate (10 mM) or lactate (10 mM) was used as electron donor for EET experiments with DM2. This medium was also autoclaved and deaerated prior to experiments. A total of 5 ml of medium (including strain culture) was used in the electrochemical reactor for all experiments. During the electrochemical measurements, the reactor was operated without any agitation.

This study was approved by RIKEN Ethics Committee. A fecal sample was obtained from a healthy volunteer (45-50 years old). A written informed consent agreement signed by

the volunteer was obtained before the experiment. 0.5 g of fecal sample was suspended in 4.5 ml of pre-reduced phosphate buffer saline (PBS) and then serially diluted in 10-fold steps. We initiated electrochemical enrichment in rich GAM medium with microbial consortium sample collected from human gut and diluted to the concentration of 10^{-7} (v/v) at 37°C. Electrode surface was washed twice with PBS, and finally electrode-attached biomass from each WE were streaked on separate δ-MnO_2 agar plates after electrochemical enrichment with GAM, or DM1 containing acetate or lactate. The plates were incubated at 37°C under a $H_2/CO_2/N_2$ (1:1:8, by vol.) gas mixture. Given the microbial reduction of δ-MnO_2 generate transparent spot in the dark brown agar plate, this visual clue was used to identify the colony of EET-capable bacteria. After 2-4 days of incubation, the colonies formed transparent spot were sub-cultured on Eggerth Gagnon agar (Merck) supplemented with 5% horse blood at 37°C under the same conditions, and single colonies were picked up. Isolated strains *Gut-S1* and *Gut-S2* were precultivated in 40 ml of lysogeny broth (LB) medium in butyl-rubber-stoppered vials at 37°C with an anoxic headspace of CO_2/N_2 (20:80 v/v). Microbial cultures were harvested in the late exponential phase when OD_{600} was about 1.0. The culture was centrifuged at 7800 rpm and 37°C for 10 min in 50 ml plastic tubes, and the resultant cell pellet was washed with defined mediums twice, resuspended in defined mediums, and then added into the reactors to a final OD_{600} of 0.1.

DNA isolation and phylogenetic tree

The discrete colonies were analyzed by 16S rRNA gene sequences. The forward and reverse primers for PCR were 27 F (5-AGA GTT TGA TCC TGG CTC AG-3) and 1492 R (5'-GGT TAC CTT GTT ACG ACT T-3). The 16S rRNA gene sequences were compared with the sequences of closely related strains by using BLAST program in GenBank database. These sequence data were deposited in NCBI GenBank under accession numbers MK051424 and MK051423 for *Gut-S1* and *Gut-S2*, respectively. For the construction of a 16S rRNA phylogenetic tree, 16S rRNA sequences were collected from the NCBI nucleotide database, aligned using MUSCLE [55] and analyzed by the neighbor- joining method [56] using Molecular Evolutionary Genetics Analysis package (MEGA 7) [57].

Chapter 2

Low Electron Transport Regulates Metabolic Pathways in *Streptococcus mutans* UA159: a physiological importance

Introduction

Extracellular electron transport (EET) is the process in which electrons are transported from electron donors to the electron acceptors outside the microbial cell wall [44,48,58-61], thus opening new metabolic windows of opportunity for electron acceptor limited respiratory cells. However, many fermentative bacteria have been shown to exhibit low levels of EET [32,62-64]; levels that are far below those needed to stoichiometrically impact metabolism, and the role of EET in such microbes has not been elucidated. Here we demonstrate that a Gram-positive fermentative bacterium, *Streptococcus mutans,* alters its fermentation pattern via a mechanism dependent on both a very low level of electron flux via EET, and a functional redox regulator (Rex), found in many Gram-positive bacteria [41,65-69]. Although the apparent coulombic efficiency of EET was less than 0.02%, its impact was large, resulting in a shift in the fermentation pathway from ethanol to lactate production in *S. mutans*. Single-cell mass spectrometry analysis for cell-specific stable isotope fixation [53,70,71] showed that the low EET also significantly enhanced the anabolic activity of cells on the electrode. None of these effects were observed in a deletion mutant (Δ*rex*) of *S. mutans*. Amino acid alignment of the Rossman-like folding motif in the NAD-binding site of Rex[72] suggests that the critical coupling of EET and Rex observed in *S. mutans* is broadly conserved among pathogens with EET capability [32,62-64]. Given that Δ*rex* is also deficient in biofilm formation [73], EET may support sensing the presence of other cells that affect redox environments in addition to chemical sensing mechanism [74]. These findings suggest a greater prevalence of highly sensitive capabilities for redox compounds in pathogens, and establishes the importance of previously overlooked low EET and sensing potential across diverse processes via Rex, including interspecies symbiosis, coupled with anaerobic methane oxidation [71] and electro fermentation [75].

The extent of EET in the fermentative microbes is often low, wherein the number of electrons is less than 1% of the total metabolic electron flux. Even though the low extent of EET facilitates their growth [62,63,76,77], this low EET cannot significantly impact their metabolic activity, which is distinct from bacteria with high EET capability [32,52,59]. In addition to coupling with metabolism, EET impacts the NADH/NAD$^+$ ratio [75,78], and may activate regulation mechanisms [41,66]. Therefore, we posit that EET in fermentative pathogens aids metabolic activation through gene regulation mechanisms rather than stoichiometric support for fermentation metabolism. Our study evaluated EET and its impact on fermentation activity in *Streptococcus mutans* UA159, an etiological bacterium of human dental caries, with a defined redox regulator system, encoding Rex protein [65]. *S. mutans* utilizes a mixed-acid fermentation pathway controlled by a redox regulator, triggered by the NADH/NAD$^+$ ratio-sensing Rex protein, which enhances ethanol production by regulating the expression of pyruvate dehydrogenase (*pdhAB*). Through mediation of Rex protein, high NADH/NAD$^+$ ratios enhance ethanol in comparison to lactate production (Figure. 2-1) [41,66].

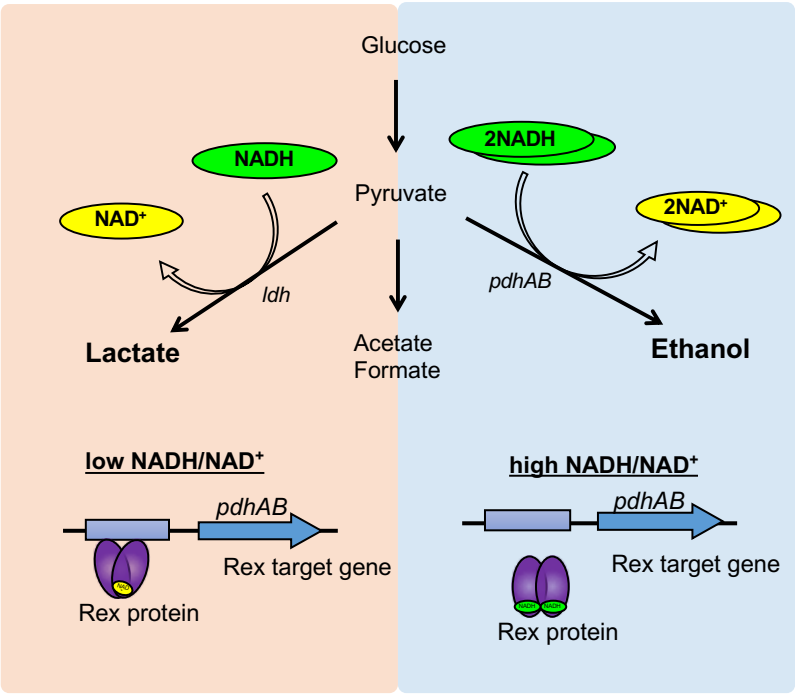

Figure. 2-1. Schematic depiction of metabolic pathways coupled with the Rex protein in *Streptococcus mutans* UA159. The NADH redox sensor Rex represses the transcription of pyruvate dehydrogenase (*pdhAB*) upon sensing a low NADH/NAD$^+$ ratio and enhances the lactate fermentation pathway. However, in case of high NADH accumulation, Rex does not bind the target genes, thus enhancing ethanol production.

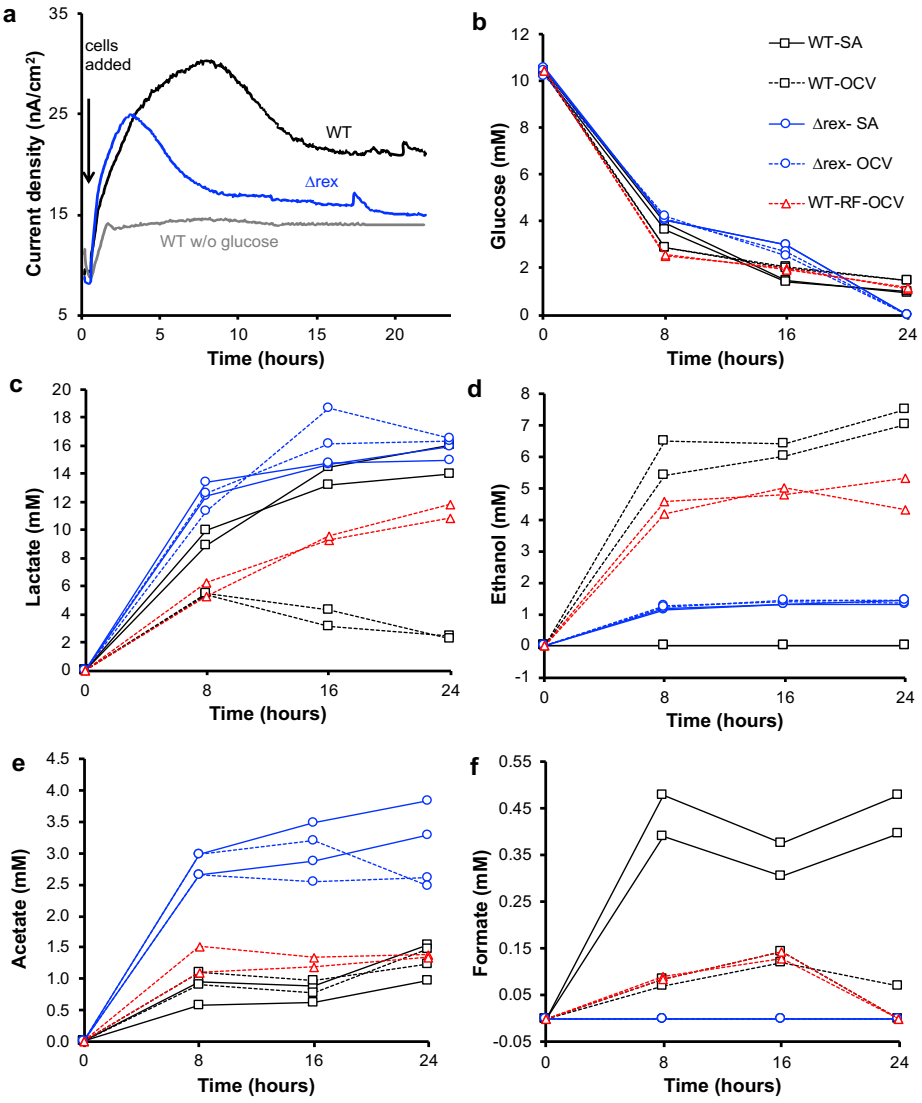

Figure. 2-2. Extracellular electron transfer coupled with glucose metabolism by *S. mutans* (SM) and a mutant strain lacking the *rex* gene (Δ*rex*). a, production of current for SM and Δ*rex* over time in anaerobic reactors equipped with ITO electrodes at +0.4 V (SHE) in the presence of 10 mM glucose and in the absence of 10 mM glucose. b–f, Glucose (b), Lactate (c), Ethanol (d), Acetate (e), and Formate (f) concentrations versus time by single-potential amperometry (SA, solid lines) and open circuit voltage (OCV, dotted lines) conditions in the

presence of 10 μM riboflavin and absence of 10 μM riboflavin (RF). Values from two independent experiments are shown, and the same trend was observed in more than four separate experiments for each condition.

Results & Discussion

Shift in metabolic pathways via Extracellular electron transfer

Ethanol production from glucose fermentation was monitored as an indicator of the reductive cytoplasmic state, and a cell-specific stable isotope fixation assay was used to analyze single cell activity on an electrode during electron transport in an anaerobic electrochemical system. We first examined the EET capability of *S. mutans* in a three-electrode electrochemical system, setting the potential of an indium tin-doped oxide (ITO) electrode to +0.4 V versus a standard hydrogen electrode (SHE) in the presence of 10 mM glucose as the sole electron donor. A significant but low current density (~20 nA cm^{-2}) was observed for *S. mutans* in the presence of glucose during single-potential amperometry (SA) (Figure. 2-2a). Replacement of the spent culture medium from the electrochemical cell with N_2-sparged, glucose-amended sterile medium did not significantly change either the current production or the voltammetric redox signal by *S. mutans* (Figure. 2-3a and 2-3b). Removal of planktonic cells and secreted soluble redox mediators or the yeast extract did not significantly impact the current density (Figure. 2-3a and 2-3c), indicating that EET is primarily due to bacterial cells that are directly attached to the electrode surface. As *S. mutans* lacks genes encoding the cell-surface *c*-type cytochromes, flavin-based enzymes, and the type IV pili [32,60,61,65], direct electron transport to the electrode is most likely mediated by unidentified redox proteins. Furthermore, current production increased up to 30% in the presence of riboflavin, an electron shuttle (Figure. 2-4a) [48,64]. These data suggest that *S. mutans* is capable of both direct EET and indirect EET via soluble riboflavin reduction.

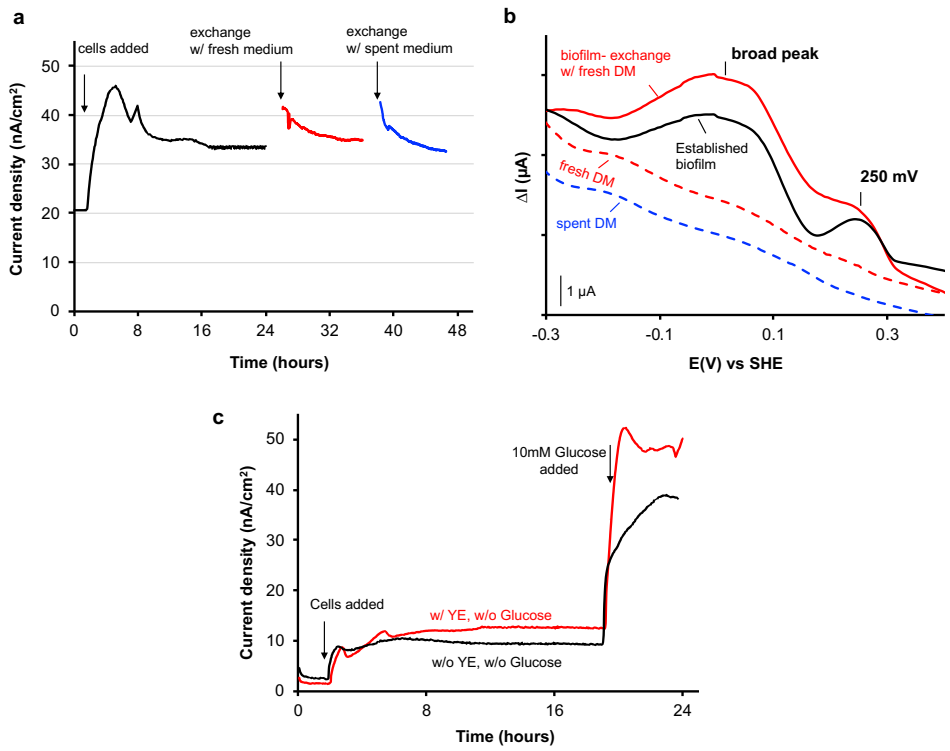

Figure. 2-3. Evidences for direct electron transfer by *S. mutans*. a, Supernatant replacement during the current production of *S. mutans* at +0.4 V (versus SHE). At the indicated times, the medium was removed and replaced with sterile defined medium containing 10 mM glucose (red line) or cell free spent medium (blue line), leading to no decrease in current production. The same tendency was confirmed in three individual experiments. b, Baseline-subtracted differential pulse voltammograms in the presence of *S. mutans* before (black solid line) and after medium exchange (red solid line). Data for sterile DM (red dotted line) and cell free spent medium (blue dotted line) are also represented. c, Effect of the removal of yeast extract (YE) on the current production of *S. mutans*. In the absence of YE, the glucose oxidation current production after the addition of 10 mM glucose reached to the value approximately 15 % smaller than that in the presence of YE. Because YE provides essential nutrients for protein synthesis, a little less current production is explainable by not only shuttling of riboflavin contained in the YE but also less cellular protein synthesis for direct electron transport mechanism.

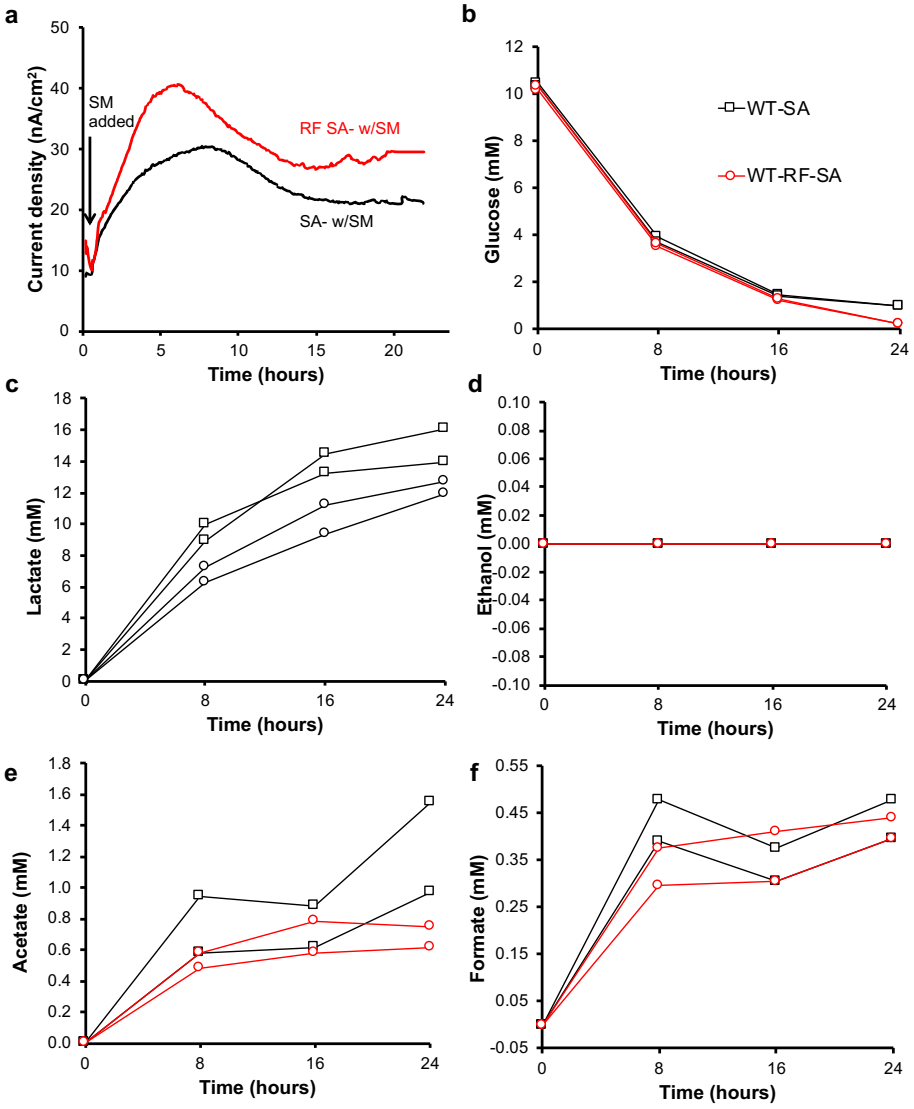

Figure. 2-4. Effect of electron transport via diffusible riboflavin (RF) on EET and metabolites in S. mutans (SM). a, Current production versus time measurements conducted in anaerobic reactors equipped with ITO electrodes (surface area: 3.14 cm^2) poised at +0.4 V (versus SHE) , single-potential amperometry (SA) condition for SM in the presence (WT-RF-SA) and absence of 10 µM RF (WT-SA). b-f, Glucose (b), lactate (c), ethanol (d), Acetate (e) and Formate (f) concentrations versus time during current production. The data points represented were values from two individual experiments.

While the production of current in this system was less than one percent of that commonly seen in environmental EET-capable bacteria (1 µA cm^{-2}–100 µA cm^{-2}) with the same electrode material and potential [44,49], the low level EET markedly impacted the fermentation products of *S. mutans*. The generated current reached saturation after 7–8 hours, corresponding to decreases in the rate of glucose consumption and lactate production (Figure. 2-2b and 2-2c), whereas ethanol, acetate, and formate were scarcely produced (Figure. 2-2d, 1e, and 1f), suggesting that EET may be coupled with lactic acid production and glucose fermentation. In contrast, when current production was maintained at zero under open-circuit voltage (OCV) conditions, 6 mM ethanol was produced (Figure. 2-2d) in 8 hours, and the trends in glucose and lactate concentrations over time were consistent with those observed under current-generating conditions. Electron export to the electrode via diffusive riboflavin also caused a metabolite shift similar to that in the absence of riboflavin (Figure. 2-4). Quantification of cellular proteins in solution and on the electrode revealed that most bacteria were in suspension, but the cellular protein amount on the electrode was nearly identical in all conditions (Figure. 2-5). Therefore, the observed variation in metabolites did not result from the number of cells; cells on the electrode surface likely increased and stopped ethanol production in OCV and SA conditions, respectively.

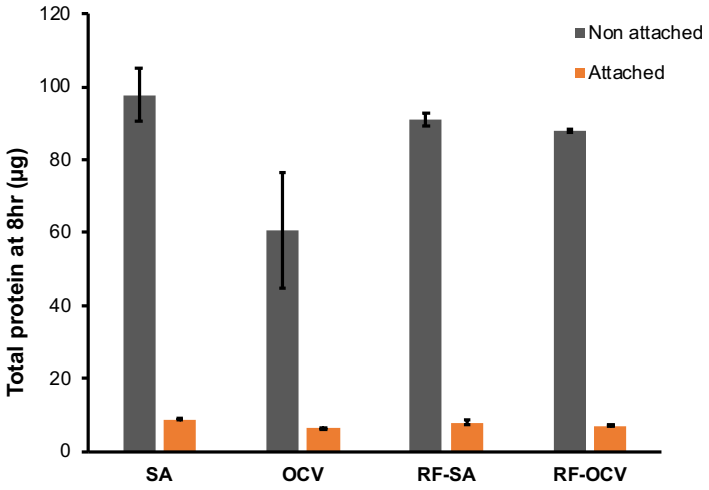

Figure. 2-5. The total protein amount of electrode attached and non-attached *S. mutans* cells collected after 8 hours of electrochemical operation.

The reduction of riboflavin under OCV conditions also strongly influenced the metabolic pathway (Figure. 2-2). As determined by metabolite levels, the presence of riboflavin under OCV conditions decreased ethanol production by 40% (Figure. 2-2d) and increased the lactate production after 8 hours compared to the levels observed in the absence of riboflavin (Figure. 2-2c: WT-OCV, WT-RF-OCV), whereas the trend in glucose consumption was the same, irrespective of riboflavin (Figure. 2-2b). A fluorescence assay to quantify oxidized riboflavin revealed that the coulombic efficiency for riboflavin reduction was about 6 times lower than that in SA conditions (Figure. 2-6). Although riboflavin is considered an essential nutrient in growth media, the quantity of yeast extract was sufficient in our experimental conditions (contained less than 3 nM riboflavin); thus, externally added riboflavin mainly impacted electron transport.

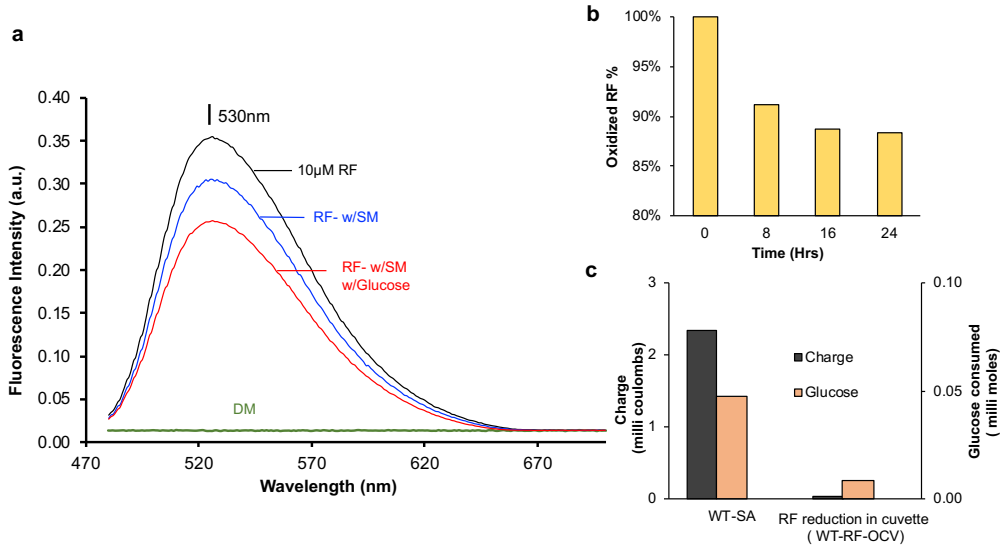

Figure. 2-6. Quantification of riboflavin reduced, and charge transported by *S. mutans* in the presence of glucose in an anaerobic cuvette. a, Emission spectrum of oxidized riboflavin (RF) measured by excitation at 450 nm, showing the fluorescence intensity peak of 10 μM RF (black line) at 530 nm. Upon the addition of *S. mutans* (SM) to 3 mL of deaerated DM at OD_{600} = 0.1 (blue line), and subsequent addition of 10 mM glucose. b, The time course of oxidized RF fluorescence intensity (red line) in cuvette measured at every 8 hours. c, The graph showing the charge estimated from RF reduction and amount of glucose consumed

after 24 hours in the cuvette, from which we estimated the columbic efficiency in the open circuit condition with SM in the presence of RF (WT-RF-OCV). Electrochemical single-potential amperometry (WT-SA) condition is also shown as a reference.

Extracellular electron transfer enhanced the low active cells

We further confirmed the impact of EET on metabolism by a single cell activity analysis of *S. mutans* attached to the electrode surface. The extent of isotopically labeled nitrogen incorporation into cells is directly correlated with overall anabolic activity [53,70,71]. We therefore incubated *S. mutans* on the electrode surface as in the above experiments, replacing NH_4Cl with N-labeled $^{15}NH_4Cl$ as the sole nitrogen source. Following current generation with some isotopic effect (Figure. 2-7), we analyzed the ^{15}N ratio ($^{15}N/N_{total(15N+14N)}$) in more than 200 bacterial cells attached to the electrode surface by nanoscale secondary ion mass spectrometry (NanoSIMS) (Figure. 2-8, Figure. 2-9a and 2-9b, Table. 2-1). In riboflavin-free OCV conditions, 42% of the cells exhibited relatively low activity (^{15}N ratio <10%, Figure. 2-9a, Table. 2-2), whereas the cell count in the same activity range was significantly lower in the other three conditions with electron export (SA w/ and w/o riboflavin and OCV w/ riboflavin) (Figure. 2-9a and 2-9b, Table 2-2). Further, pH exhibited similar trends in all four conditions (Figure. 2-10) and ethanol was present in the two OCV conditions, cell deactivation for OCV in the absence of electron acceptor (without riboflavin) could not result from pH or membrane permeation of the resulting weak acids.

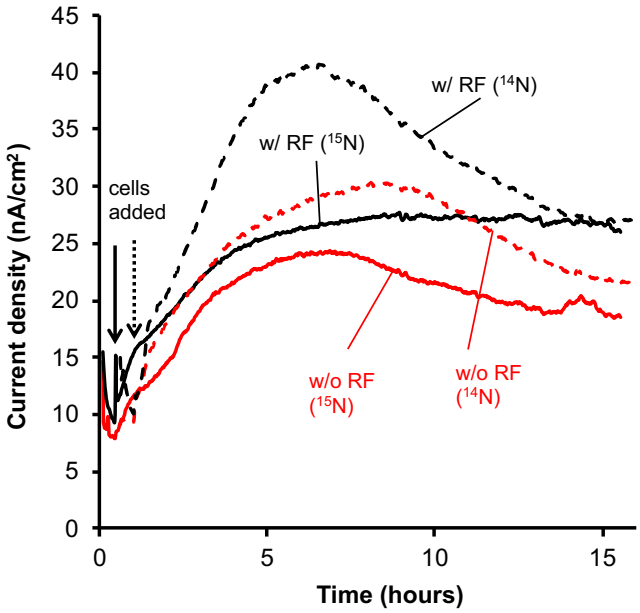

Figure. 2-7. Effect of labeled $^{15}NH_4Cl$ on current production of *S. mutans*.

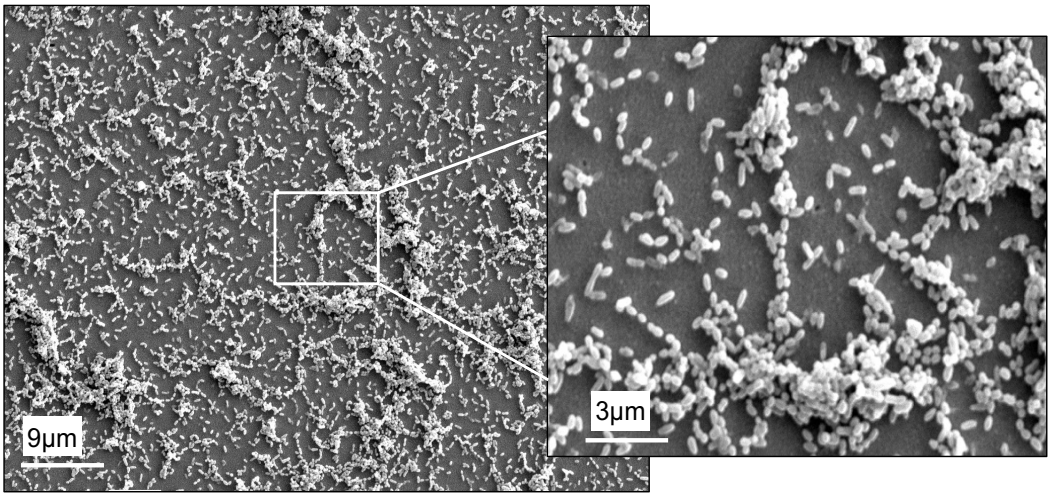

Figure. 2-8. Scanning electron microscope image of *S. mutans* cells attached on the electrode surface. After 24 hours of current production with 10 mM glucose at +0.4 V (versus SHE) *S. mutans* cells were intact on the electrode surface.

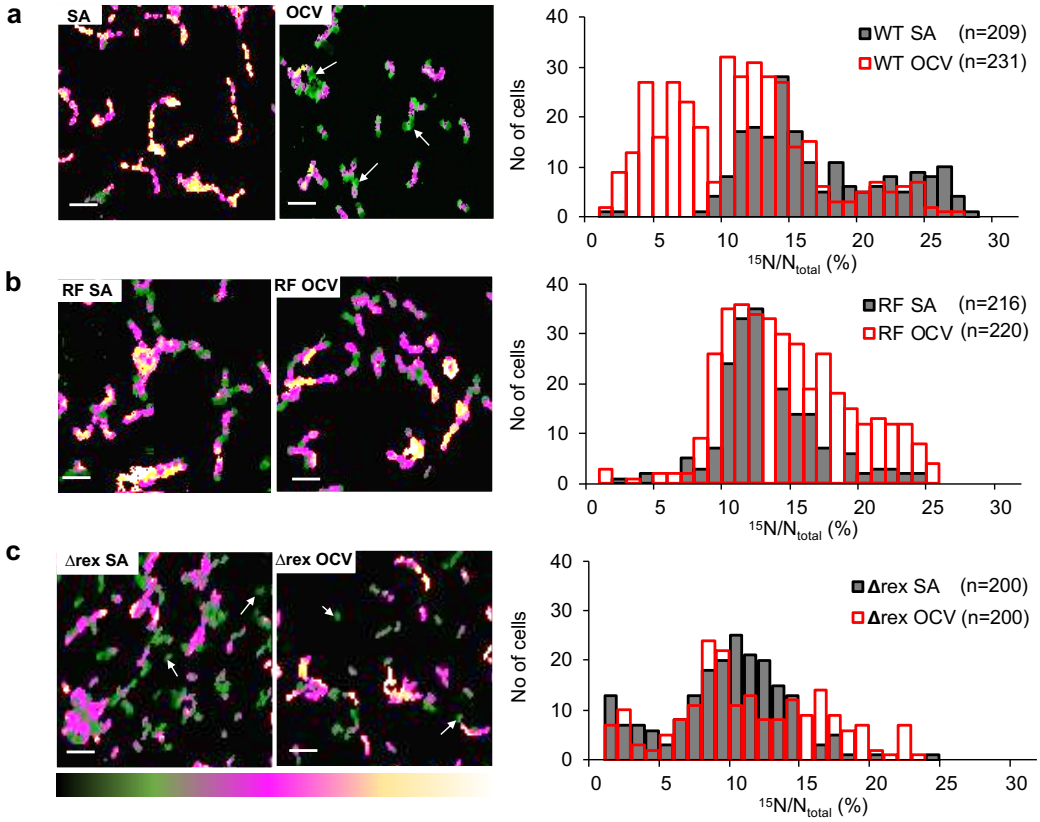

Figure. 2-9. Assimilation of ^{15}N expressed as the $^{15}N/N_{total}$ (%) ratio in *S. mutans* and a *rex* gene-deleted strain. a–c, nanoSIMS images of the electrode-attached *S. mutans* without riboflavin (a), with riboflavin (RF) (b), and in *rex*-deleted mutant (Δ*rex*) cells (c), under single-potential amperometry (SA) and open circuit voltage (OCV) conditions showing $^{15}N/N_{total}$ (%) assimilation (scale bars: 5 μm). Warmer-colored cells were more enriched in ^{15}N, which corresponded with higher levels of anabolic activity. Arrows indicate cells with relatively low anabolic activity. Histograms show the distribution of the ratio of assimilated ^{15}N to total nitrogen (N_{total}) in approximately 200 cells from two individual experiments.

Table. 2-1. Assimilation of ^{15}N% (ratio of ^{15}N to total nitrogen) in *S. mutans* wild type (WT) and Δ*rex* under single-potential amperometry (SA) and open circuit voltage (OCV) conditions with and without riboflavin (RF). The data shown are the concurrent results of two individual experiments with standard errors of means (SEMs).

$^{15}N/N_{total}$ (%)		
Condition (total number of cells)	Mean%	SEM%
WT-OCV (n=231)	13	0.46
WT-SA (n=209)	16.44	0.36
WT RF-OCV (n=220)	13.82	0.28
WT RF-SA (n=216)	13.01	0.24
Δ*rex*-OCV (n=200)	10.92	0.4
Δ*rex*-SA (n=200)	9.42	0.3

Table. 2-2. Percentage of cells with low ^{15}N% incorporation (<10%) in *S. mutans* wild type (WT) and Δ*rex* under single-potential amperometry (SA) and open circuit voltage (OCV) conditions without/with riboflavin (RF).

Condition (total number of cells)	No of low active cells <10%	% of low active cells to total no of cells
WT-OCV (n=231)	83	42%
WT-SA (n=209)	8	4%
WT RF-OCV (n=220)	45	23%
WT RF-SA (n=216)	25	13%
Δ*rex*-OCV (n=200)	95	47.5%
Δ*rex*-SA (n=200)	92	46%

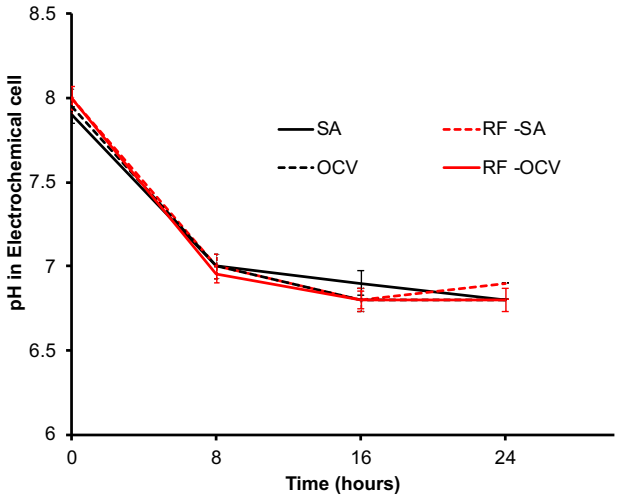

Figure. 2-10. Time course of the electrolyte pH during the electrochemical operations under single-potential amperometry (SA) and open circuit voltage (OCV) conditions in the presence and absence of riboflavin (RF).

Higher sensitivity of *S. mutans Rex* coupled Extracellular electron transfer

Although electron export strongly impacted the metabolic pathway and activity, the electron transfer ratio to the electrode surface from NADH was only 0.20‰–0.02‰ (Figure. 2-11a). Consistently, the redox active dye Redox Sensor Green could not differentiate between SA and OCV conditions, suggesting that the cytoplasmic NADH/NAD^+ ratio may change to a lesser extent (Figure. 2-12). To confirm that low electron export did in fact couple with the redox regulator Rex and shifted the metabolite and anabolic activities, we used a mutant strain lacking the gene *SMU_1053* encoding Rex (Δ*rex*) [41,66]. Δ*rex* showed 3-fold lower production of the current coupled with glucose oxidation in the absence of riboflavin, compared with that of the wild type (Figure. 2-2a and 2-2b). The coulombic efficiency was found to be higher than that of OCV with riboflavin (Figure. 2-11a). However, metabolite production and the ^{15}N fixation ratio were almost identical in SA and OCV conditions (Figure. 2-2b–2-2e, 2-2c). Lower anabolic activity than that of the wild type may be explained by the involvement of Rex in susceptibility to reactive oxygen species [73] (Table. 2-1 and Table.2-2). These data demonstrate that *S. mutans* uses the low electric current for regulating the Rex protein, rather than stoichiometrically exporting the excess reductive energy to maintain intracellular redox balance fermentative metabolism. Furthermore, the Rex in *S. mutans* is highly sensitive to NAD^+ production.

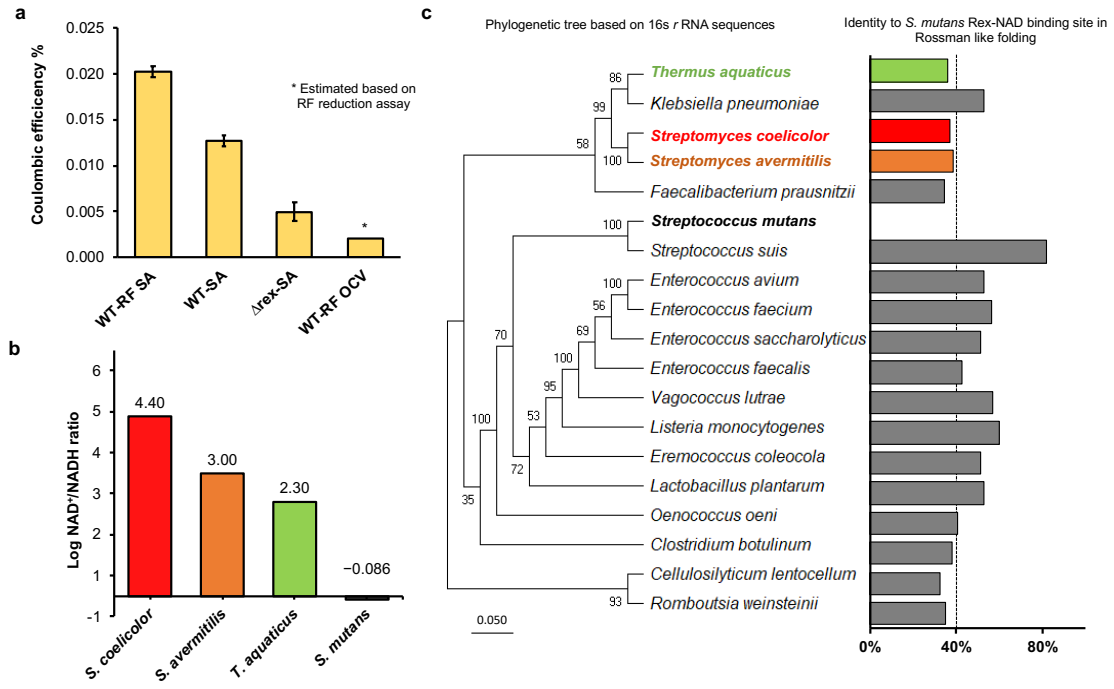

Figure 2-11. High sensitivity of Rex to NAD^+ generation in *S. mutans*. a, Coulombic efficiency of *S. mutans* (WT) in the presence/absence of riboflavin (RF) and in Rex-deleted mutant (Δ*rex*) as determined by consumed glucose, time vs. current profile, and RF reduction assay. b, The minimum logarithmic NAD^+/NADH ratio to form 100% Rex–DNA complexes in *S. mutans* determined by the amount of glucose consumed and lactate produced (See supplementary text). Data for *S. coelicolor, S. avermitilis,* and *T. aquaticus* were from references 15,16,20. c, Phylogenetic tree representing identity among Rex in microbes with EET potential and the environmental microbes *S. coelicolor, S. avermitilis,* and *T. aquaticus*. The tree was based on 16S rRNA sequence alignment, which was generated using MUSCLE; the neighbor-joining method was employed for phylogenetic tree construction (Scale bar: 0.05 substitutions per site). Bar graphs represent the % identity obtained by NCBI blastp searches of the predicted NAD binding site in the Rossman-like folding motifs of Rex sequences compared to that of *S. mutans*.

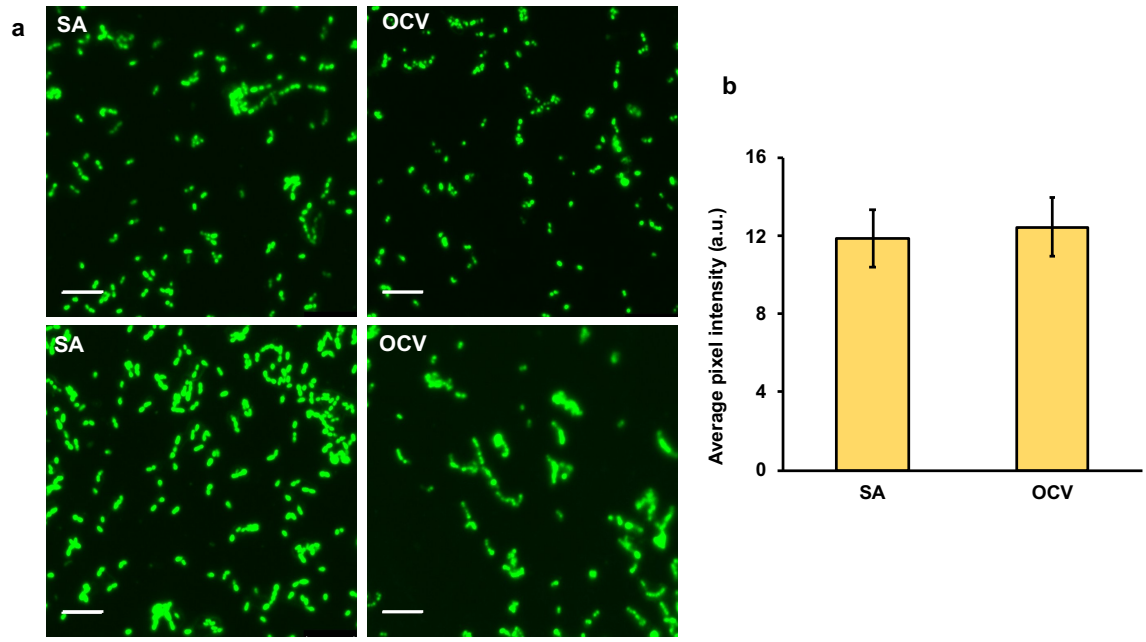

Figure. 2-12. Fluorescent microscopic analysis of *S. mutans* cells by Redox Sensor Green (RSG) dye. a, Fluorescence microscopic images of RSG-stained *S. mutans* cells attached on the electrode surface under single-potential amperometry (SA) and open circuit voltage (OCV) condition. b, Average pixel intensity per image was calculated for 27 images per condition. The average number of cells per image was 238 and 248 for SA and OCV, respectively. Error bars indicate standard error mean in average pixel intensities (per population) per image. Scale bar: 7μm

As members of the Rex family, which regulate the fermentative pathway, are widely conserved among fermentative gram-positive bacteria, we conducted amino acid alignment to check the generality of highly sensitive Rex to NAD^+ with *S. mutans* in EET-capable bacteria. The *rex* gene is widespread in other gram-positive bacteria with flavin-based EET mechanisms [32], in the fermentation-associated EET-capable gut pathogens [63], and in other cytochrome-mediated EET-capable microbes and archaea [60,71] (Table. 2-3). Our study found that Rex in *S. mutans* was more sensitive to NAD^+ compared to its homologues in environmental bacteria such as *Streptomyces coelicolor* [69], *Streptomyces avermitilis* [68], and *Thermus aquaticus* [72]. We hypothesized the complete suppression of *pdhAB* transcription in

SA conditions in the presence and absence of riboflavin (Figure. 2-2d) and approximated the *S. mutans* NAD^+/NADH ratio based on the amounts of NAD^+ generated and NADH consumed via lactate production as determined by lactate and glucose concentrations (Figure. 2-1, Figure. 2-2b and 2-2c,). As described in Figure 2-1, the NADH redox sensor Rex repressed the transcription of pyruvate dehydrogenase upon sensing a NAD^+/NADH ratio and Rex-DNA complex formation, that resulted in the suppression and enhancement of the ethanol and lactate production, respectively. In the SA conditions of our present study, we detected significant amounts of lactate but no amount of ethanol end product. Therefore, we considered 100% activation of Rex-DNA complex formation in the SA conditions of *S. mutans,* and approximated the intracellular NAD^+/NADH ratio that corresponded to 100% activation of Rex-DNA complex formation by using lactate and glucose concentration at 8 hours, 16 hours, and 24 hours in SA conditions of our present study in the presence of RF or absence of RF. Eight-hour data in the presence of riboflavin gave the minimum value of -0.09 among the calculated logarithmic NAD^+/NADH ratios (Figure. 2-11b). We then compared the ratio with those corresponding to 100% activation of Rex-DNA complex in the purified Rex proteins from *S. coelicolor, S. avermitilis*, and *T. aquaticus* (references 15,16,20) (Figure. 2-11b).

The logarithmic NAD^+/NADH ratio corresponding to 100% activation of Rex was at least smaller by two orders of magnitude in *S. mutans* than in other microbes [68,69,72] (Figure. 2-11b). The high NAD^+ sensitivity can be explained by the structure of the Rossman-like folding motif in Rex [72]. A sequence identity greater than 40% was observed in the EET-capable pathogens (Figure. 2-11c) whose the Rossman-like folding sequences were identified and NAD binding was predicted by the bioinformatics software Cofactory v.1.0 [54], with a minimum of 35 residues (Table. 2-4), satisfying the length-dependent threshold for significant structure homology [79,80]. Although amino acid sequence identity among the Rossman-like folding motif was low in environmental bacteria (~ 37%) compared to that in *S. mutans*, relatively high identity was confirmed in the analyses of EET pathogens such as *Listeria monocytogenes* [32], *Enterococcus faecalis* [62], *Klebsiella pneumoniae* [63], and other bacteria with iron reducing capability [32]. The discordance between the phylogenetic

relationships and the identity of Rossman-like folding sequences may be attributable to habitat variation; the environmental non-EET bacteria and EET-capable pathogens have significantly higher divergence than that of the 16S *r*RNA and the Rex-NAD binding sites in the Rossman-like folding (Figure. 2-11c). These results suggest that the critical impact of EET observed in *S. mutans* as shown in schematic figure 2-13 may be conserved among low-EET as well as high-EET bacteria, like *L. monocytogenes*.

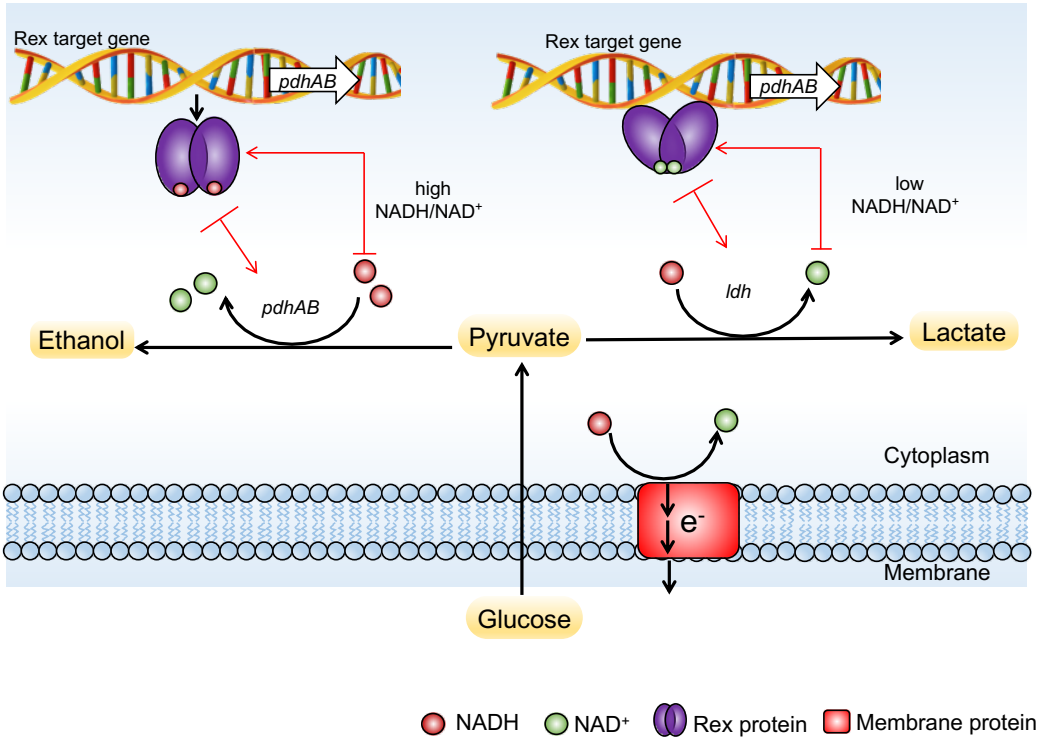

Figure 2-13. Schematic depiction of metabolic pathways coupled with Extracellular electron transport (EET) and *rex* in *Streptococcus mutans* UA159. Low electron export via EET creates a low NADH in cytoplasm, hence NADH redox sensor Rex represses the transcription of pyruvate dehydrogenase (*pdhAB*) upon sensing low NADH, thus lactate fermentation pathway is more active. While in case of high NADH accumulation, Rex cannot bind the pyruvate dehydrogenase target genes, thus ethanol production is more active in the absence of external electron acceptors in order to sustain the fermentation.

Table 2-3. List of EET-capable bacteria and *Archaea*, their potential EET mechanism and their gene names assigned as redox regulator Rex in the database of National Center for Biotechnology Information.

EET mechanism	Organism	*rex* Gene name
Flavin based complex	*Streptococcus dysgalactiae*	SDSE_0916
	Granulicatella elegans	HMPREF0446_01247
	Trichococcus pasteurii	TPAS_2663
	Pisciglobus halotolerans	SAMN04489868_12010
	Alkalibacterium gilvum	SAMN04488113_13626
	Lactococcus lactis	LL1060
	Lactococcus garvieae	LCGL_1020
	Bacillus circulans	C2I06_21170
	Caldanaerobius fijiensis	SAMN02746089_00712
	mahella australiensis	Mahau_0374
	Clostridium intestinale	CINTURNW_0232
	Romboutsia weinsteinii	CHL78_017725
	Cellulosilyticum lentocellum	Clole_3033
	Faecalibacterium prausnitzii	FPR_01980
	Streptococcus suis	SSGZ1_0943
	Clostridium botulinum	CBO3306
	Eremococcus coleocola	HMPREF9257_0586
	Oenococcus oeni	OEOE_1398
	Carnobacterium maltaromaticum	BN424_1284
	Lactobacillus plantarum	lp_0725
	Vagococcus lutrae	T233_01518
	Enterococcus saccharolyticus	OMQ_00682
	Enterococcus faecalis	EF_2638
	Enterococcus faecium	A5810_002288
	Listeria Monocytogenes	LMOf2365_2104
Cytochrome mediated EET	*Thermincola potens*	TherJR_2553
Fermentation associated EET	*Enterococcus avium*	OMU_04218
	Klebsiella pneumoniae	BU230_13650
Cytochrome mediated EET in *Archaea*	*Methanosarcinales archaeon*	DRN98_10615

Table 2-4. List of amino acid sequence of Rossman-like folding identified by Cofactory v.1.0 and their length.

Rossman like folding sequence identified by Cofactory v.1.0	Sequence length
>*Streptomyces coelicolor* QDWPVVIVGIGNLGAALANYGGFASRGFRVAALIDADPGMAGKP	44
>*Streptomyces avermitilis* QDWPVVIVGIGNLGAALANYGGFASRGFRVAALIDADPAMAGKPV	45
>*Thermus aquaticus* WGLCIVGMGRLGSALADYPGFGESFELRGFFDVDPEKVGR	37
>*Klebsiella pneumoniae* ITRVALIGVGNLGTAFLHYNFTKNNNTKIEMAFDVSEE	35
>*Faecalibacterium prausnitzii* TILIGCGRLGKAVSRFITTDTNGYKLIAAFDVAENEVGKEISGI	41
>*Streptococcus mutans* STTNVLLVGVGNIGRALLNYRFHERNKMKIAMAFDTDDNEQVGQ	41
>*Streptococcus suis* ITNVMLVGVGNMGRALLHYRFHERNKMKIVMAFEADDNPA	37
>*Enterococcus avium* QLTNVALVGVGNLGSALLKFKFHQSNSIRVSCAFDVKE	35
>*Enterococcus faecium* QLTNVALIGVGNLGSALLKYKFHQSNSIRISCAFDVNEEIVG	39
>*Enterococcus saccharolyticus* QMTNVALIGVGNLGSALLKYKFHQSNSIRVSAAFDVNPDI	37
>*Enterococcus faecalis* EEKRIALIGCGNLGKALLKNNFRRNENLNIVCAFDNDSALVGTT	41
>*Vagococcus lutrae* RLTNVALIGVGNLGNALLNYGFHQGNNIRISAAFDVKED	36
>*Listeria monocytogenes* KQTNVALIGVGNLGTALLHYNFMKNNNIKIVAAFDVDPAKVGSVQQ	43
>*Eremococcus coleocola* RLTSVGLVGVGNLGNALLNYNFRKNHNIRISAGFDINPEIVGTIHS	43
>*Lactobacillus plantarum* LTNVALIGVGNLGHALLNFNFHKNSNVRISAAFDVNEAIANTVQS	42
>*Oenococcus oeni* KLNKVAVVGTGNLGQALMKYNFVHSSNIQIVMGFDVDPKKKELKI	42
>*Clostridium botulinum* NPYNIIIIGAGNIGQALANYTRFSKLGFNVKAMFDTNPKLIGL	40
>*Cellulosilyticum lentocellum* QNYKMIIVGVGNLGQAIANSTSFSKRGFKLIGLFDVNPRLIGMS	41
>*Romboutsia weinsteinii* SYNAILVGAGNLGQAIANYSGFRKAGFEIKALFDANPKMIGL	39

The low requirement for the extent of EET may enable pathogens to sense even low concentrations of extracellular redox reagents such as oxygen, soluble and insoluble redox-active compounds, and cell-surface redox enzymes of other bacteria in the vicinity. Therefore, such mechanisms may support the colonization, biofilm, and syntrophy of these pathogens in addition to molecular-based sensing mechanisms such as quorum sensing [74]. Accordingly, the Δ*rex* mutant of *S. mutans* was found to be deficient in biofilm formation capability [73].

In conclusion, we have shown that low EET coupled with fermentation modified and activated the metabolism in *S. mutans* (Figure. 2-13), and this large impact was mediated by the sensing mechanism of Rex via the generation of NAD^+. Rex amplified the effect of small charges through gene regulation, which was distinct from the stoichiometric effect of EET on metabolism, which has been considered as a primary role of EET [75,78,81]. The identified gene and its motif for sensing NAD^+ were found to be present in a wide-ranging group of Gram-positive bacteria and archaea that have potential genes for EET. Although microbes with high EET capability have been the focal point for bioenergetic applications, our work implies the underestimated importance of low EET capability of microbes [76] that may have important but currently negligible effects on various processes including pathogenic biofilm formation [32,62,63], electro fermentation process [75,78] and symbiosis coupled with anaerobic methane oxidation [71].

Publications of chapter 2:

1. **Divya Naradasu**, Shu Zhang, Toshinori Okinaga, Tatsuji Nishihara, Akihiro Okamoto. Low Electron Transport Regulates Metabolic Pathways in *Streptococcus mutans* (under submission with *Nature microbiology*).

Chapter 3

Assessment of acid stress induced extracellular electron transport and its association with metabolic activity in *Streptococcus mutans*: A possible cariogenesis mechanism.

Introduction

The mouth is colonized by 200 to 300 bacterial species, but only a limited number of these species participate in dental decay (caries) or periodontal disease. Dental decay is due to the irreversible solubilization of tooth mineral by acid produced by certain bacteria that adhere to the tooth surface in bacterial communities known as dental plaque. The tooth surface normally loses some tooth mineral from the action of the acid formed by plaque bacteria after ingestion of foods containing fermentable carbohydrates. This mineral is normally replenished by the saliva between meals. However, when fermentable foods are eaten frequently, the low pH in the plaque is sustained and a net loss of mineral from the tooth occurs. This low pH selects for aciduric organisms, such as *S. mutans* and lactobacilli, which (especially *S. mutans*) store polysaccharide and continue to secrete acid long after the food has been swallowed. As *S. mutans* makes initial attachment on the tooth surface and initiates the biofilm formation with other microbes, the pH of the biofilm decreases to acidic (~ pH4) with microbial fermentation, yet *S. mutans* survives and proliferates the diseases by competing with niche microbes [82-85]. Discovered electron transport capability of *S. mutans* may, therefore, facilitate the survival in the low-pH and highly reductive condition. Hence, we hypnotized and examined whether low-pH could be a triggering aspect for the electron transfer capability or not. To this end, we performed bioelectrochemical analyses to test the pH dependency on EET capability, and quantified the cell-surface redox enzymes, which is crucial for the direct electron transfer mechanism in environmental bacteria [71,86,87]. *S. mutans* was precultured in buffered (pH7±0.2) and non-buffered (pH of growth medium decreases to 4.6±0.2) BHI medium and electrochemical measurements were conducted in the presence of 10 mM glucose to test the effect of acid stress on electron transport capability and expression of redox enzymes.

Biofilm formation is an essential part of the life cycle of many bacteria and protects bacteria against many environmental factors [88,89]. Bacterial biofilms are also a major cause of hospital-acquired infections and chronic infections [90]. The high tolerance and quick recovery of biofilm against conventional drugs and physical removal has resulted in a paradigm shift towards new types of drugs discovery, which require the establishment of direct assays to measure the metabolic activity of biofilm-forming bacteria. The traditional techniques for analyzing biofilms such as phase-contrast microscopy, confocal laser scanning microscopy, and biofilm disruption methods combined with staining assays require many time consuming steps, reagents and samples [91-93]. Moreover, platforms for developing and analyzing biofilms such as flow cells or microwell plates are quite complex and not very effective for early screening of new drugs [93]. Therefore, simple, fast and low-cost methods are largely in demand for the determination of biofilm's metabolic activity for new drugs assessment.

In this chapter, we conducted a whole-cell electrochemical assay using *Streptococcus mutans*, an oral pathogen and model bacterium for studying biofilm formation. We used single-potential amperometry (SA) to study the EET capability of *S. mutans* and the effect of different pH pregrown conditions on its current production, as *S. mutans* is known to be pathogenic at low-pH [94]. Based on the electrogenic activity, we tested cell wall and metabolic inhibitors for our preliminary electroactive pathogenic biofilm metabolism model. A single-cell activity assay using a cell-specific isotope fixation process was employed to find the link between electrochemical activity and biofilm metabolism. Furthermore, we characterized the energy level of potential electron transfer pathways by differential pulse voltammetry (DPV) and localized redox-active compounds in single cells under a transmission electron micrograph (TEM) using the redox-dependent staining method [71,86].

Results & Discussion

The frequent ingestion of sucrose has been shown to increase the lengths of time that sucrose could be detected in the saliva. This means that if this sucrose were available for microbial fermentation in the plaque, low plaque pHs would be present for long periods each day [82,95-97]. When the plaque pH value falls below 5.0-5.2, the salivary buffers are overwhelmed, and as lactic acid diffuses into the tooth, enamel begins to dissolve, releasing Ca and PO_4 ions from sites beneath the surface enamel (Figure 3-1). Normally, the bathing saliva replenishes these minerals, but if the length of the flux from the enamel is great, repair does not occur and cavitation results. Thus, sucrose consumption per se does not cause decay, but the frequent ingestion of sucrose by prolonging the time period by which the plaque is acidic, is cariogenic.

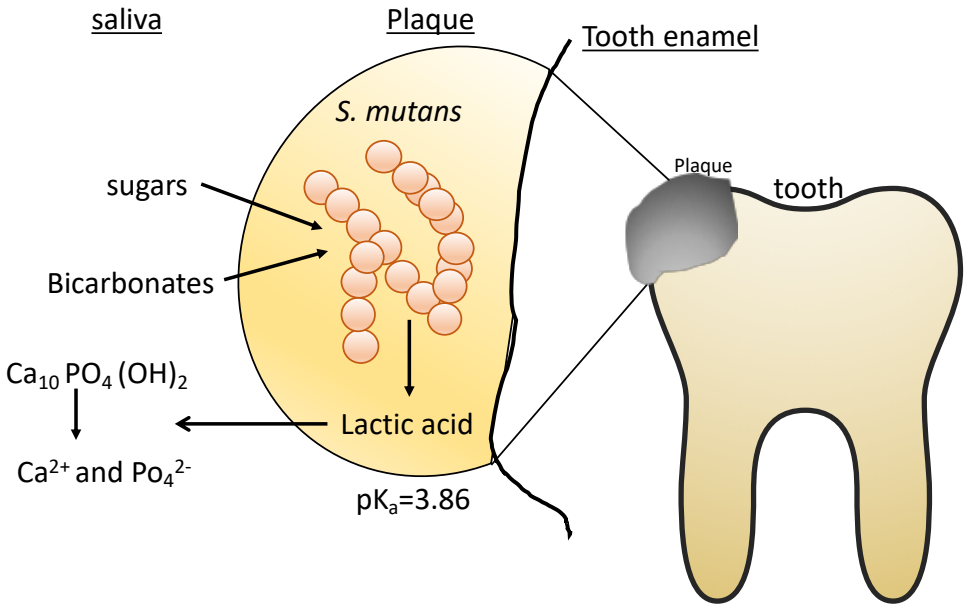

Figure 3-1. classical model for pathogenesis of dental decay. Plaque formed on the tooth surface contains *S. mutans* which ferments the sugars and produce lactic acid (pK_a: 3.86). Acids accumulation leads to the dissolution of tooth enamel.

The survival mechanism of *S. mutans* at low pH environments was not fully understood. In our study the effect of acid exposure was tested on *S. mutans* extracellular electron transport capability in order to understand the mechanism underlying the acid stress survival. As discussed in chapter 2. *S. mutans* extracellular electron transport has a role in maintaining the redox homeostasis by maintain the intracellular NADH/NAD^+ redox ratio. Thus, redox balance mediated by REX regulon effects the cell anabolic activity. Electron export to survive and maintain the activity under acidic reductive environments may have the link to its caries causing pathogenicity. Hence, we studied the effect of acid stress on electron transport capability of *S. mutans* grown at acid and neutral pHs in electrochemical set up.

S. mutans grown at pHs *i.e* neutral pH in buffered BHI and at lower pH (4) in non-buffered condition had shown similar growth rates during the pre-culture conditions as shown in figure 3-2. pH of the growth medium was dropped to 4.6 at the end of exponential growth phase in case of low pH cells whereas pH was maintained at approximately 6.8 in case of buffered medium.

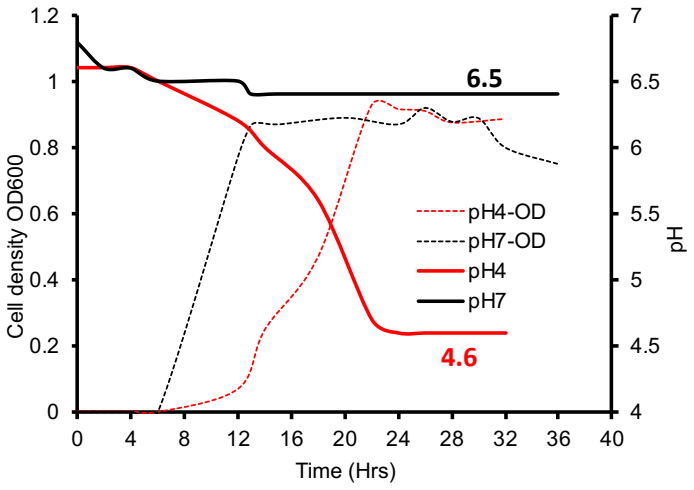

Figure 3-2. Time vs cell density and pH measurement of *S. mutans* during the pre-culture condition in buffered and non-buffered BHI medium. The dotted line showing the growth and solid lines are indicating the pH of the growth medium.

Growth and pH measurements during the pre-culture showing the similar trend in the growth except with a little late in the initiation of lag phase in case of pH7 (Figure 3-2 solid lines), while the maximum OD in both cases was reached to about 1 at late exponential phase

and continued to stationary phase by decreasing time dependently (Figure 2 dotted lines). The pH pf the BHI medium dropped to 4.6 in case of non-buffered medium suggesting the acidic environment created by the secretion of acids by *S. mutans* and yet continued to survive at such low pH until 32 to 36 hours in the stationary phase. pH of the buffered BHI growth condition has showed a little drop in pH and maintained at 6.5 (Figure 3-2 dotted lines). and cells were sustained during this phase in the stationary phase.

Acid stress induced Electron transfer capability of *S. mutans*

We initially examined the electron transfer capability of *S. mutans* in a three-electrode electrochemical reactor system with different pregrown culture cells. Given that *S. mutans* stays at low-pH in biofilm and has strong phenotype dependency on the pH, we hypothesized that the electron transfer capability of *S. mutans* changes under different pH conditions. To this end, *S. mutans* was precultured in buffered (pH 7.0 ± 0.2) and non-buffered (pH 4.6 ± 0.2, as in its natural niche) brain heart infusion (BHI) medium and electrochemical measurements were conducted in the presence of 10 mM glucose to test the electron transport capability. EET was observed in repeated experiments with low-pH-grown cells. Both current (to approximately 50 nA/cm^2) (Figure. 3-3a) and glucose consumption (Figure. 3-3b, black line) increased in the DM medium containing 10 mM glucose, indicating that current production was associated with glucose oxidation. However, no significant current generation was observed in repeated experiments with *S. mutans* grown at neutral-pH without electron donors (Figure. 3-3a), and the number of bacteria collected were the same as in the growth phase of the pregrown conditions, i.e., late exponential phase of OD_{600} 1.0. These results suggest that electron transfer was induced by acid stress exposure in *S. mutans.* SEM observations after 8 hours of incubation showed that low-pH precultured cells made multilayer biofilm on the electrode surface, which was not observed at neutral-pH (Figure. 3-3C). These results suggest that the high current production in low-pH-pregrown cells supported the growth in the electrochemical reactor (Figure. 3-3b, blue line), in accordance with previous studies observing that the pathogen is EET-capable [32,98]. These results strongly

suggest that *S. mutans* is capable of EET, and this may be associated with microbial energy production.

Next, to examine whether the cell metabolic activity on the electrode reflects current production, we used antibiotics to suppress metabolic reactions to the electrochemical system during current production after approximately 8 hours, because this incubation time would be sufficient for *S. mutans* to form biofilm (Figure. 3-3b, blue line). Ampicillin, which inhibits the cell wall formation, i.e., effects cell growth and Triclosan, a glycolysis inhibitor, were added at lethal concentrations [46,47]. Addition of ampicillin (Figure. 3-3d, red profile) yielded an instant ~10% decrease in current production; this may be linked to biofilm disturbance, as current production recovered soon after and then continued to increase at its initial pattern. Given that ampicillin effects growing cells only, its small impact on current production suggests that *S. mutans* cells had already made a biofilm and were no longer actively growing on the electrode. Adding the Triclosan yielded a significant negative effect on current production, i.e., an ~80% decrease in current production (Figure. 3-3d, green profile) and did not recover to the same levels as the ampicillin and control experiments (Figure. 3-3d, blue line) with DMSO (an organic solvent used to dissolve Triclosan), suggesting that metabolism is directly linked with current production in *S. mutans*.

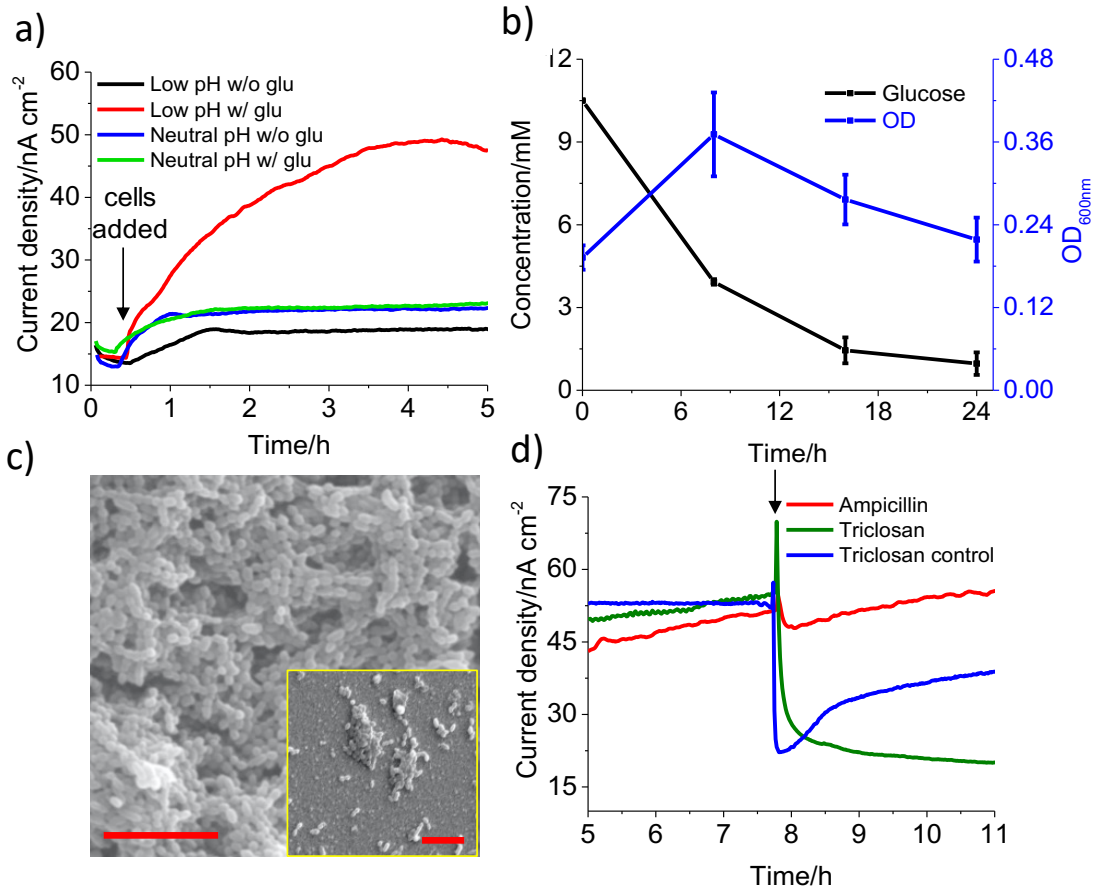

Figure 3-3. a) Current production versus time measurements conducted in anaerobic reactors equipped with ITO electrodes poised at +0.4 V (vs SHE). *S. mutans* adapted to low-pH (4.6±0.2) showed electron transport capabilities, whereas neutral-pH (7±0.2)-adapted cells showed significantly less electron transport, suggesting that pH affects EET capability. b) Time profile of glucose consumption (black line) and OD_{600nm} change (blue line) in an electrochemical reactor with low-pH-grown *S. mutans*. c) Scanning electron microscopy images, low-pH-grown cells on the ITO electrode after 8 h. Neutral-pH grown cells are shown in the inset. Scale bar = 5 µm. d) Effect of antibiotics on current generation. Ampicillin, an inhibitor of cell wall biosynthesis (red line) and Triclosan, a metabolism inhibitor (green line) were added at the points indicated by the arrow test their impacts on *S. mutans*

electrochemical activity. Triclosan control (blue line): DMSO (same volume as in Triclosan treatment) (green line) was added to test the impact of organic solvent on current generation.

S. mutans showed higher activity during EET and the behavior of direct electron transfer by to the electrode surface via cell surface bound redox enzymes as explained in chapter 2. The DAB staining resulted in the staining of the cell membrane of *S. mutans* which displayed the strong precipitation of DAB at cytoplasmic membrane (Figure. 3-4a) under transmission electron microscopy (TEM). The staining was not obvious in DAB negative (without H_2O_2) condition (Figure. 3-4b), supporting the presence of a metal redox enzyme, though it could be any transition metal, might be responsible for its direct electron transfer to outside of the cell. From the microscope images, cytoplasmic membrane is showing definite staining, however it's also showing the presence of thin surface layer above the peptidoglycan layer in both cases, which requires further analysis. As a control analysis, *S. mutans* grown at higher pH of 7 in buffered BHI preculture condition (pre-higher pH) was tested for membrane staining by DAB. This resulted in (Figure. 3-4c, 3-4d) neither significant staining in the cytoplasmic membrane region nor a difference in both DAB positive and negative cases. The absence of DAB staining is suggesting that redox active enzymes were not present on *S. mutans* membrane grown at pre-higher pH compared to the pre-lower pH cells.

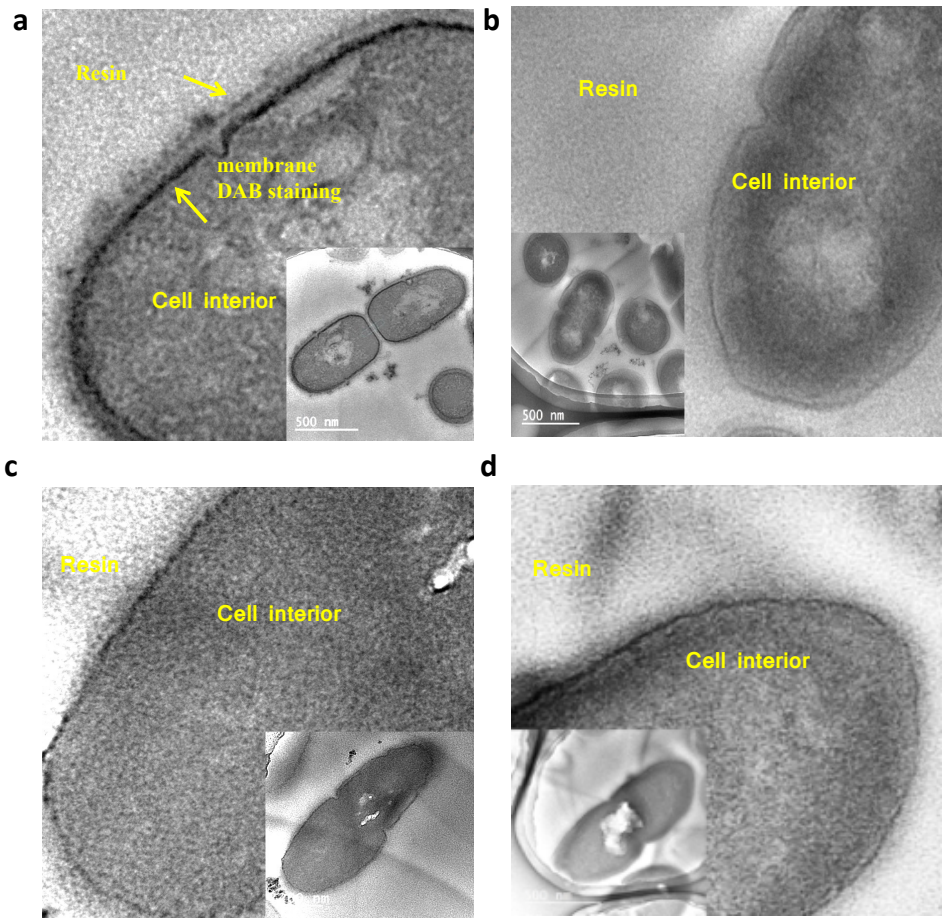

Figure 3-4. Transmission electron microscope images. Redox enzyme reactive DAB stained in the presence of H_2O_2 (DAB positive) and in the absence of H_2O_2 (DAB negative) of *S. mutans* grown at lower pH (a-b), and at neutral pH (c-d) indicating that the redox enzymes were expressed upon acid exposure only whereas neutral pH cells do not have redox enzymes thus didn't show the current production

Compared with the staining observed in the DAB-positive conditions. TEM-LINE profile analysis of the peptidoglycan region highlighted the presence of DAB-active agents, and the normalized absorption was comparable to that of outer-membrane c-type cytochrome in environmental EET microbes (Figure. 3-5) [33,71,99,100].

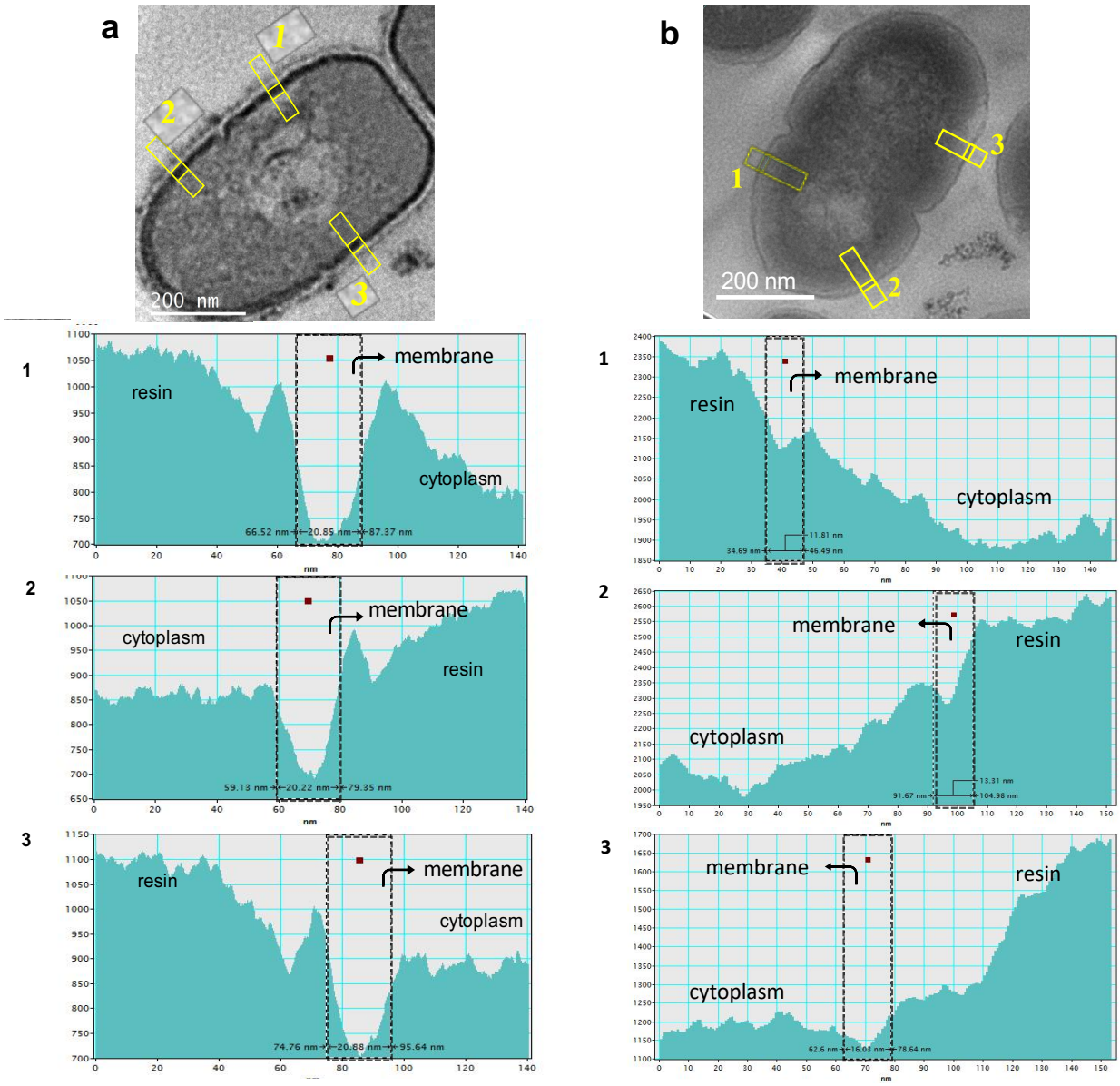

Figure 3-5. TEM-Line profiles of membrane regions of S. mutans pre-cultured in BHI broth and treated by DAB-H_2O_2 staining method. a, DAB positive stained S. mutans. b, DAB negative stained S. mutans. Y axis is electron transmission amount, X axis is the length (nm) of selected frame of analysis. Line profiles can be roughly divided into three regions. Region within the frame (yellow box) with the lowest values indicated cell membrane (black arrow),

while regions on each side of the dotted frame indicates LR white resin or cell interior. White arrows in panel a represent the DAB-active agents localized on the cell surface or the peptidoglycan layer. Average of normalized absorption from these three profiles was estimated to be 1.23 (see details below, Table. 3-1), which is close to the value of 1.88 in environmental bacteria.

Quantitative analysis of the membrane absorption of *S. mutans* was performed by comparing the electron transmission (ET) amounts of the LR white resin, cytoplasm, and membrane region acquired from LINE profiles of DAB-positive stained cells, as described elsewhere (79). Greater DAB-osmium distribution on the membrane lead to higher absorption of the electron beam (*i.e.*, a lower ET rate) (eq. 1), as shown in eq. 2.

Peptidoglycan ET rate (T) = ET amount of peptidoglycan/ET amount of resin, eq.1

Peptidoglycan absorption (A) = 1/ T, eq. 2

To calculate the ET amount of the membrane, we first normalized all LINE profiles with different ET amounts (resin - cytoplasm) to a fixed value as below:

1) The section (resin) thickness was maintained at 80 nm; therefore, as the electron beam intensity was kept the same for all observations, the ET value for the resin had to be constant and was fixed at 1540 (average ET amount for the resin of *S. mutans* cells).

2) For the *S. mutans* cytoplasm composition, the ET amount was set at 1194 (average ET amount for the cytoplasm of *S. mutans* cells).

The lowest ET value in the peptidoglycan region, the highest ET amount in the cytoplasm, and the ET values at a distance of 20 nm from the peptidoglycan in the resin were used for calculations. An example is shown in the table below. We used three LINE profiles for calculation of average absorption in *S. mutans* as explained in Figure. 5.

Table. 3-1. Example calculation of membrane absorption with normalization of ΔET (resin-cytoplasm).

Raw ET amounts acquired from the LINE profile						
			1	3		
Cytoplasm	Peptidoglycan	Resin	ΔET (resin-cytoplasm)	ΔET (cytoplasm-peptidoglycan)		
800	900	1050	1050-800 =250	800-900 =−100		
Calculation of membrane absorption with normalization of ΔET (resin-interior)						
	5		2	4	6	7
Fixed cytoplasm	Calculated peptidoglycan	Fixed resin	Fixed ΔET (resin-cytoplasm)	Normalized ΔET (cytoplasm-peptidoglycan)	Peptidoglycan ET rate	Peptidoglycan absorption
1194	1194− (−138.4) =1332.4	1540	1540-1194 =346	−100*(346/250) =−138.4	1332.4/1540 =0.8652	1.16

Note: The cells shaded in grey contain calculated values, and the calculation orders are indicated with numbers.

The induction of redox active enzymes in acidic pH adapted cells, which are capable EET is indicating that acid stress has an impact on the membrane topology. When higher pH cells were tested in electrochemical cell, they didn't show significant current generation and no redox signals were observed in DPV analysis of the biofilm (Figure 3-6).

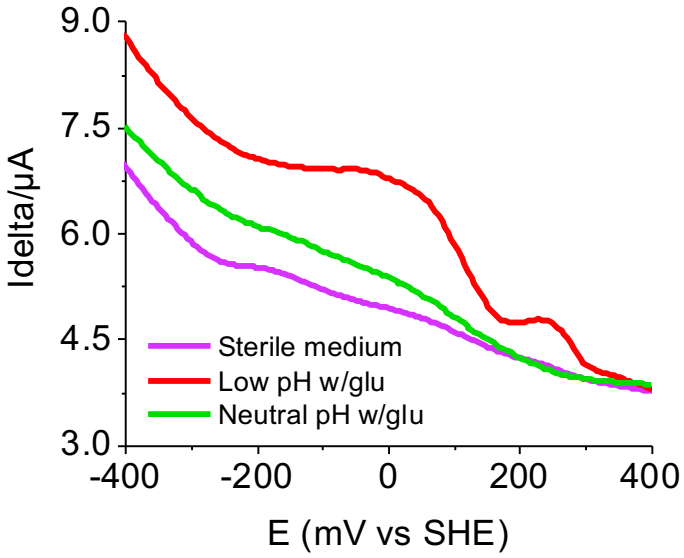

Figure 3-6. Differential pulse voltammograms of the lower pH adapted *S. mutans* (red line) and higher pH adapted *S. muatns* cells (black line) and sterile medium (blue line), suggesting that the redox enzyes were not present in pH7 cells.

These data are demonstrating that acid stress has induced redox enzymes in the membrane of *S. mutans*, which might be responsible for its EET. As enormous research conducted on acid tolerance mechanisms has revealed that *S. mutans* changes its membrane physiology and gene expression in order to adapt and survive at low pH environments, production of redox active enzymes during acid adaptation and ability of EET could be one of the acid survival mechanism of *S. mutans*. However, use of soluble redox mediator vitamin K3, which shuttle electron via diffusive process regardless. Vitamin K3 addition instantaneously increased the current production of cells precultured to pH 7 (Figure 3-7), indicating the less current production is assignable of limitation in electron transport pathway but not in the cellular metabolic activity.

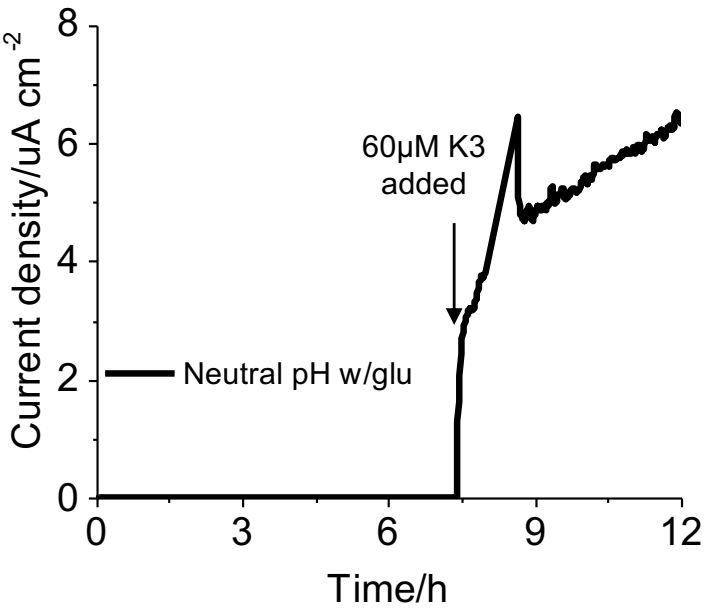

Figure 3-7. Addition of vitaminK3 has increased the current flow in neutral pH grown *S. mutans* cells indicating the rate limiting EET step, as mediators can aid in electron transfer despite the absence of redox enzymes.

To investigate of the contribution of EET to the energy production in *S. mutans,* we analyzed the activity of *S. mutans* grown at lower pH and higher pH conditions on the electrode surface with nanoSIMS by measuring the uptake of ^{15}N as solo nitrogen source in the EET and OCV conditions by individual cells. After 24 hours incubation at +0.4 V vs Ag/AgCl, we analysed anabolic activity by measuring assimilation of $^{15}NH_4Cl$, and results also showed the higher assimilation of pH4 *S. mutans* cells (15.86%) than pH7 cells (1.60%) (Figure 3-8a-d). The distribution of ^{15}N% measured in about 100 *S. mutans* cells displayed in histogram (Figure 3-8e) showed that the cells that are less active (low ^{15}N% assimilation) in pH7 grown condition higher incorporation of ^{15}N% in pH4 condition indicative of higher anabolism. NanoSIMS serves as a best tool to measure activity [71] as *S. mutans* activity on electrode surface by nanoSIMS analysis revealed that EET has a role to activate cells that are less active in absence of electron acceptor.

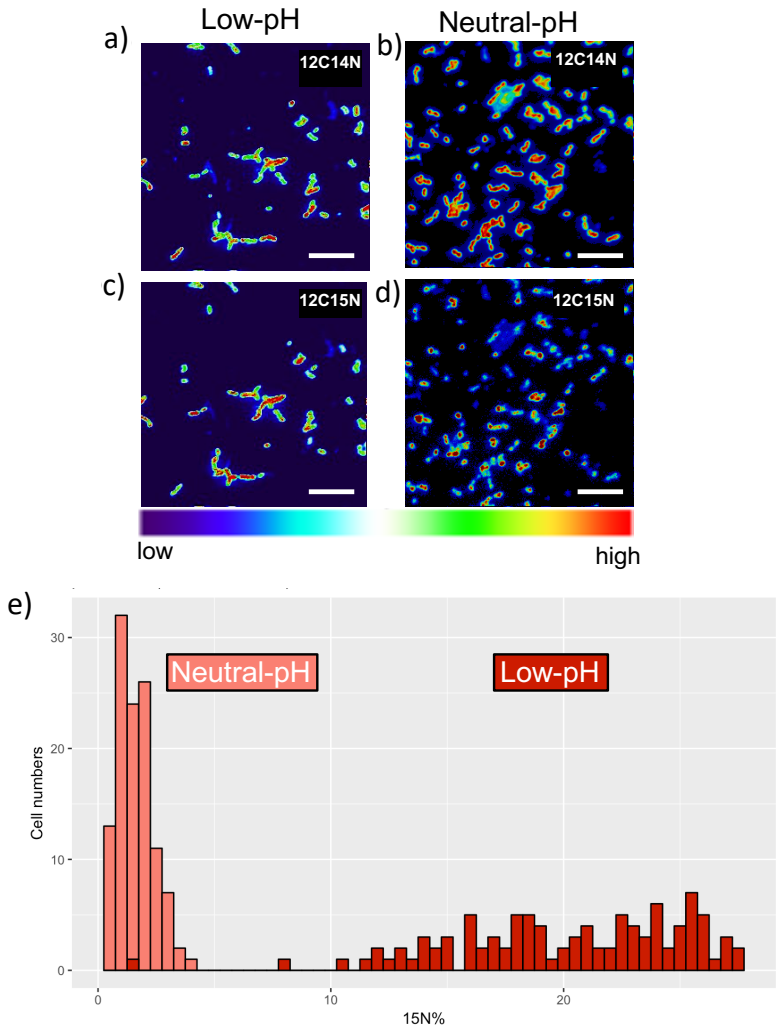

Figure 3-8. a-d) nanoSIMS analysis of *S. mutans* precultured at higher pH7 attached to electrode surface in pH4 cells (a, b) and pH7 cells (c, d), scale bar 5µm. e) Assimilation distribution of 15N% in number of cells in pH4 and pH7 grown conditions respectively, showing higher active cells in EET condition in case of pH4 cells. The nanoSIMS analyses were conducted more than 3 times and representative values were shown.

The direct electron transfer between *S. mutans* and the electrode could be attributed to any hypothetical membrane protein present in the cell membrane or on the cell surface. Our DAB staining analysis suggest the presence of a metal redox enzyme, though it could be any transition metal, might be responsible for its direct electron transfer to outside of the cell.

Given all the enzymes for EET in environmental bacteria are multi-heme protein, EET from *S. mutans* that lacks cytochrome gene [82] opens the possibility that unknown none-heme protein take an important role for EET in human microbiome.

However, enormous research was conducted on higher activity of *S. mutans* in acidic environments assuming it does only conventional fermentation, our novel finding of EET capability in oral pathogen *S. mutans* via acid stress induced membrane bound redox enzymes is a previously unexplored direction. Our NanoSIMS analysis is indicating that fermentation is not beneficial for cells in biofilm and long-range electron transfer via EET is supporting the fermentative cells to sustain in reductive condition by transferring the reductive energy to outside of cells. Expression of redox active enzymes in acidic reductive biofilms and ability of extracellular electron transfer to sustain redox energy, could be one of the acid stress survival mechanism of *S. mutans* in oral microbiomes.

The development of dental plaque biofilms follows a well-defined series of events where initial colonizers, predominantly streptococci, establish an environment conducive for later colonization by more overtly pathogenic species. Cytoplasmic membrane staining indicating that electrons can be transferred form cytoplasmic membrane enzyme to outside crossing peptidoglycan layer, which should act as conductive conduit to facilitate electron transfer, suggesting that the biofilm could be conductive to transfer electrons to electrode. Oral plaque is electrically conductive and forms nanowires [87], which might facilitate long electron transfer from the reducing environment within biofilms to electron acceptors located at more electropositive potentials near the biofilm surface and also aids to maintain redox balance at the bottom of biofilm. Reducing electron acceptors via long range electron transfer could establish charge separation and create thermodynamically unfavorable conditions in dense biofilms, with protons accumulating with in the biofilm and are absorbed by calcium phosphate in bone as it dissolves [71]. This would be an interesting theory to test in future lines of investigation in this field.

Our electrochemical characterization showed that the oral pathogen *S. mutans* is electroactive under biofilm conditions on an electrode and that current production was associated with metabolic activity, as indicated by the significant impact of the glycolysis

inhibitor. NanoSIMS analysis further confirmed that electrogenic activity is associated with metabolic activity in single cells. Preference for the EET electron pathway at low-pH further supports our idea that EET is good indicator for the activity of cells living. These preliminary data demonstrate that electrogenic activity can be used to incubate biofilm of fermentative pathogens and assess the impacts of drugs when screening for new drugs to deactivate cellular metabolism inside the biofilm. It is important to mention that, as decreased antibiotic susceptibility is also associated with reduced antibiotic penetration, new drugs are being designed to enhance biofilm penetration and reach its bottom. In this aspect, our proposed model could also be effective, because electroactive biofilms favor growth at the biofilm-electrode interface, and most active cells are found at the electrode surface [101]; hence, drug penetration can be combined with electroactivity. These results suggest that current producing capability of pathogens can be an effective assay for quantifying and qualifying the time-dependent impact of antibiotics with rapid analysis of cellular activity localized at the electrode surface, compared to conventional techniques involving microscopic observation of cells, complex sensor systems and longer cultivation time assays [102,103]. The shortcoming of this system is that the current volume of the reactors is large for high throughput screening; therefore, future studies should scale down the system, e.g., using screen-printed electrodes that require minimum amounts of sample and drugs. Overall, this platform provides an excellent basis for primary screening of antibiofilm compounds in electroactive pathogenic biofilms.

Publications of chapter 3:

Divya Naradasu, Alexis Guionet, Waheed Miran, and Akihiro Okamoto* Electrochemical Metabolic Activity Assessment for Biofilm Using Current Production Capability of *Streptococcus mutans.* (under review in *Biosensors and Bioelectronics*).

Chapter 4

Extracellular electron transport- mechanism and energetics in oral pathogens

Introduction

Low amount of extracellular electron transport associated with the fermentation has proved a physiological importance in facilitating the fermentation metabolism and maintain the activity of cells in case of *S. mutans.* The export of excess electrons to maintain the redox balance has an implication to oral biofilm physiology as redox homeostasis is major crisis for biofilm development in case of biofilm associated diseases. Human oral environment contains highly diverse microbial lifestyles. These microbial activities also contribute to the dental caries, the failure of dental implant restoration, severe inflammation and oral cancers. To further prevent and treat oral diseases, the characterization of oral pathogenic metabolism and the role in dental caries and periodontal diseases appears to be critical. The predominantly studied oral pathogens are *Capnocytophaga ochracea, Aggregatibacter, Porphyromonas gingivalis* along with the *Streptococcus mutans. Capnocytophaga ochracea* was a well-known subgingival oral pathogen, causing severe oral problems, such as oral inflammation and periodontitis [104-112]. It is an important microbial building block in the teeth biofilm with gliding motility [113], *Aggregatibacter* and *Porphyromonas gingivalis* [111,114] were well know pathogens involved in periodontics diseases. Since electrogenic activity of *S. mutans* has given insight into the importance of low electron export on cell sustainability, it is important to explore such electron export capability in other oral pathogens and understand their mechanism.

Long range inter cellular electron transport in oral biofilm

In the real environment of oral plaque bacteria are found to form a biofilm with thickness ranging from 10-100 micrometer length. In a recent study[115] a distinctive microbiome arrangement of supragingival dental plaque was observed. The consortium consists of a radially arranged, nine-taxon structure organized around cells of filamentous

corynebacteria. The consortium ranges in size from a few tens to a few hundreds of microns in radius and is spatially differentiated spanning from tooth surface to the aerobic space above the tooth surface. Within the structure, individual taxa are localized at the micron scale in a manner resembling their functional niche in the consortium. For example, anaerobic microbes were found to be in the interior of the biofilm near the tooth surface, whereas facultative or obligate aerobes tend to be at the surface the biofilm near the oxygen availability region. The poly microbial biofilm forms containing an oxygen gradient with in the biofilm *i.e* bottom of the biofilm have less oxygen or completely anaerobic whereas top of the biofilm is exposed to the aerobic space. In another study the plaque taken from a patient having microbes are found be connected by a conductive nanowire [87].

The activity of these microbes in the interior of the biofilm had found to be more in terms of gene expression compared to the cells at the aerobic surface[116] and being active these microbes play a critical role in oral diseases such as caries, periodontitis, gingivalis etc. Though many studied have been conducted for more than a decade in order to understand these pathogens behavior and their activity in infectious diseases, the clear mechanism was still ambiguous. Most of the pathogenic studies focus from host point view to understand how these microbes are affecting the human cells, but not on survival mechanisms of these cells. By observing these points of oxygen gradients with higher microbial activity in anaerobic region and conductive nanowires in oral biofilm, we hypothesized that there is a possibility of long-range intercellular electron transport in oral biofilms (Figure. 4-1).

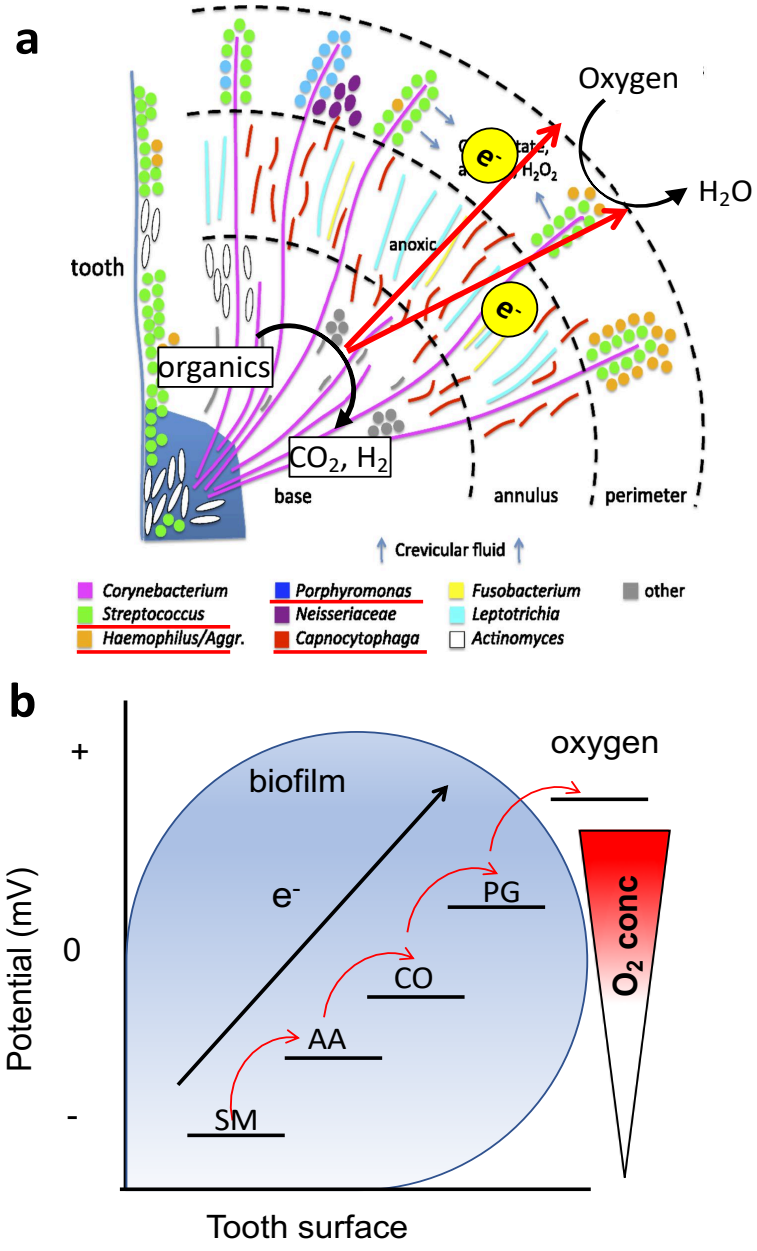

Figure 4-1. Consortia arrangement in oral plaque taken from Mark Welch, J.L, *et.al.* showing the schematic of long-range extracellular electron transport from inside to the put side of the biofilm (a), Schematic depicting the long-range electron transport via an energy gradient redox environment between cells ranging from anaerobic to aerobic space (b).

As reported in Mark Welch, J.L, *et.al* [115]. study, the spatial arrangement of oral microbes spanning from anaerobic to aerobic space as shown in figure.6a, *streptococcus* and *Aggregatibacter* are at the anaerobic surface inside the biofilm. *Capnocytophaga* and *Porphyromonas* are at the anoxic and aerobic space respectively. These four genera are widely studied and found to be abundant in oral infections. *Streptococcus mutans* is a well-known tooth cavity causing pathogen, *Aggregatibacter actinomycetemcomitans* is a major pathogen in aggressive periodontitis. *Capnocytophaga ochracea* and *Porphyromonas gingivalis* are found to be associated with the gingivalis and related gum diseases. The extracellular electron transport capability of *Streptococcus mutans* was identified in this study and found to have cell surface redox enzymes. As we hypothesis the possibility of long-range extracellular electron transport in the oral biofilm, it requires an intercellular electron transport with redox gradient from bottom to the surface of aerobic region to utilize the oxygen as a terminal electron acceptor (Figure 4-1b). For inter cellular electron transport the cells must possess the EET capability with cell surface redox enzymes or via a redox mediator.

In this chapter we tested the extracellular electron transport capability and mechanism of oral pathogens with their energetics and presented in three parts. Extracellular electron transport mechanism of chapter 4-1: *Capnocytophaga ochracea,* Chapter 4-2: *Aggregatibacter actinomycetemcomitnas* and *Porphyromonas gingivalis,* Chapter 4-3: Energetics of oral plaque pathogens extracellular electron transfer and implication to interspecies long-range electron transfer in oral plaque.

Chapter 4-1: Extracellular electron transport mechanism of *Capnocytophaga ochracea:*

Population induced extracellular electron transport mechanisms and Membrane vesicle involves in rate enhancement of EET in *Capnocytophaga ochracea*

Introduction:

Extracellular electron transport (EET) mechanism has been studied in environmental bacterial strains, such as *Shewanella oneidensis* MR-1 and *Geobacter sulfurreducens* PCA [14,99]. Direct electron transport by outer-membrane cytochrome, and indirect electron shuttling processes are known as a major mechanism for EET in these iron-reducing strain. Recently new enzymes have identified in marine sulfate-reducing bacteria *Desulfovibrio ferrophilus* IS5 [86] and food-borne pathogen *Listeria monocytogenes*[32] . Especially, the flavin-based enzyme is a distinct enzyme involved in EET for various strains. These new clades of EET mechanism suggest that novel environment has unknown EET mechanism.

Human oral environment contains highly diverse microbial lifestyles and has been extensively characterized by cultivation and culture-independent molecular methods The oral microbial activities contribute to the dental caries, the failure of dental implant restoration, severe inflammation, and oral cancers [112,117]. To further prevent and treat oral diseases, the characterization of oral pathogenic metabolism and the role in dental caries and periodontal diseases appears to be critical. *Capnocytophaga ochracea* (a gram-negative bacteria) is a well-known subgingival oral pathogen, causing severe oral problems, such as oral inflammation and periodontitis [117-119]. It is an important microbial building block in the teeth biofilm with gliding motility [118-121]. However, extensive studies on *Capnocytophaga* were not as much as other oral pathogens, such as *Streptococcus mutans*, *Porphyromonas gingivalis* and *Aggregatibacter actinomycetemcomitans*. Thus, there is an urgent need to investigate its growth condition, metabolism and electrochemical traits.

Pathogenic bacteria are known to release membrane vesicles (MVs) that influence diverse biological processes, such as virulence, horizontal gene transfer, export of cellular metabolites, phage infection and cell- to-cell communication [122-124]. Especially, gram-

negative bacteria associated with chronic periodontitis has also been witnessed to express vesicles on their cell surface as well as release them to its environments [122]. A study based on proteomics analyses has reported the similarity between protein profiles of oral pathogen associated vesicles and major outer membrane proteins [122-124]. This suggests that these vesicles may serve as a vehicle for some important virulence factors and proteolytic enzymes of oral pathogens. The potential role of these components (MVs) in the metabolic activity of. *C. ochracea* with reference to EET also called for investigation as no information is available in literature in this regard.

Overall, this study is the first to present valuable insights into electroactive microbiome in human oral cavity using a periodontitis-causing oral pathogen. Although human oral pathogens were well studied in the medical field, their microbial electrical activities, in particular the capability of extracellular electron transportation that we discovered in this study, were scarcely reported. The divergent metabolic features and microbial lifestyle elucidated in this study would be a tremendous expansion in human microbiome research and provide practical references of disease treatment in medical field.

Results & Discussion

Cell-density dependent EET capability in *Capnocytophaga ochracea*

To address the possibility of current production and to evaluate cell-density behavior during current generation of *C. ochracea,* a three-electrode electrochemical system was used with tin-doped indium oxide (ITO)-coated glass substrate as a working electrode (WE), platinum wire as a counter electrode (CE), and Ag/AgCl (saturated KCl) as a reference electrode (RE). Single-potential amperometry (SA) was performed at +0.2 V (vs Ag/AgCl) using the defined medium (DM) as an electrolyte in the presence of 10 mM glucose. Upon the addition of bacterial cells into the reactor to a final OD_{600} of 0.5, an immediate current increase was observed, reaching approximately 60 $nAcm^{-2}$ after 5 h (Figure 4-1-1a). This current production is much lower in comparison to environmental bacteria like *Geobacter* and *Shewanella* likely due to different electron transfer pathway. Such low current is also observed in other weak electricigens[125]. A significantly less extent, but a similar time course

of current production was observed even in the absence of glucose, indicating that approximately 50% of current production was derived from glucose oxidation and the remaining current from nutrients such as yeast extract present in the medium (Figure 4-1-1a). Accordingly, we confirmed a significant decrease in glucose concentration during current production (Figure 4-1-1b). These results strongly suggest that *C. ochracea* is an EET-capable bacterium with current production associated with glucose oxidation.

We next examined the cell-density dependency on current production in *C. ochracea* at different OD_{600} from 0.1 to 1.0 under the same electrochemical condition as mentioned above. At ODs of 0.1 and 0.2, current production did not significantly differ from the background current (Figure 4-1-1a), while cellular attachment on the electrode surface was confirmed. In contrast, when the cell-density was at an OD_{600} of 0.5, current production was ~10-fold higher than 0.1. Furthermore, although the cell-density was sufficient to cover the whole electrode surface at an OD_{600} of 0.5, a higher current was produced at an OD_{600} of 1.0. Also, a significant increase in charge transfer to the anode at higher ODs was observed, which was calculated by subtracting the charge generated in the absence of glucose from that generated in the presence of glucose by *C. ochracea* at their respective cell-densities (Figure 4-1-1b).

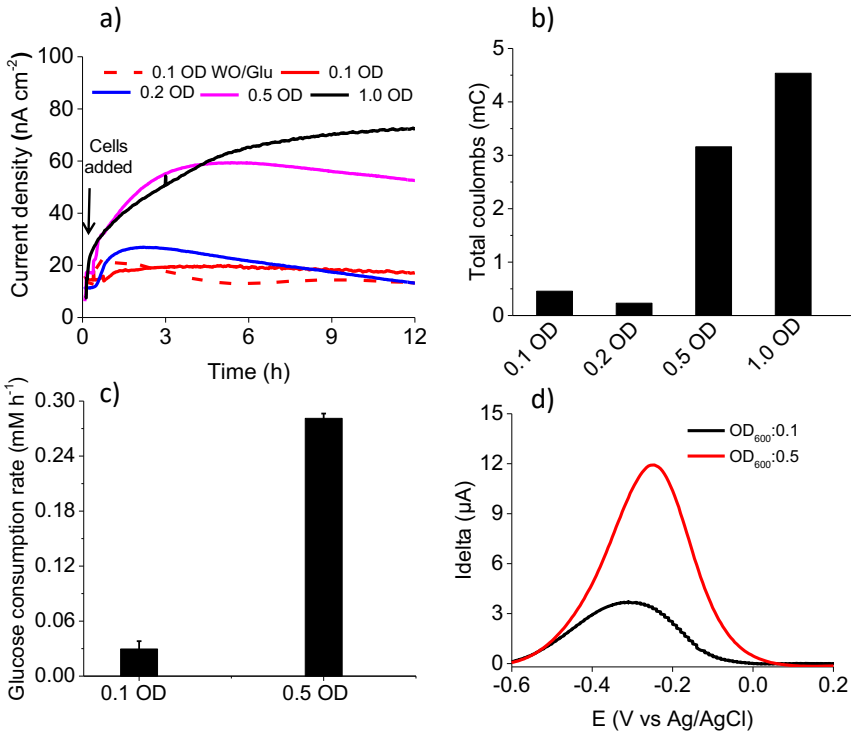

Figure 4-1-1. Population-induced EET capability and metabolism activation of *C. ochracea*. (a) Current production versus time measurements conducted in anaerobic reactors equipped with ITO electrodes (surface area: 3.14 cm^2) poised at +0.2 V vs Ag/AgCl in the absence (red dashed line) and presence of 10 mM glucose and the OD_{600} of 0.1, 0.2, 0.5 and 1.0 represent the initial cell densities in the reactors. Arrow position indicates the time of cell addition in the electrochemical reactor. (b) Total coulombs generated by *C. ochracea* with different initial cell densities as in Figure 4-1-1a, calculated by subtracting the charge generated in the absence of glucose from that generated in the presence of glucose. (c) Glucose consumption rate based on 8 h sampling from anaerobic reactors of *C. ochracea* measured at OD_{600} of 0.1 and 0.5 with initial glucose concentration of 10 mM. Data values represent the mean ± standard deviations from two independent experiments. (d) Baseline subtracted differential pulse voltammogram (DPV) of *C. ochracea* measured for anaerobic reactors at OD_{600} of 0.1 and 0.5.

C. ochracea followed a non-proportional OD-dependent current production unlike, *Shewanella*, a model EET-capable microbe in the environment. The current production of *Shewanella* came from the electrode-attached single cell using a direct electron transport mechanism via outer-membrane *c*-type cytochromes.[126] However, electron transport of *C. ochracea* was enhanced at a certain threshold of cell-density, not following the same mechanism of direct electron transport to the electrode as in *Shewanella.* A possible explanation is that *Shewanella* uses non-fermentable carbon sources and so the metabolic activity of *Shewanella* might be low when it cannot use an electron acceptor. Therefore, cells that are not in direct contact with the electrode (or able to avail themselves of a shuttle) would be expected to be relatively metabolically inactive. In contrast, *C. ochracea* can ferment glucose and so the cells that are not in direct contact with the electrode should also have considerable metabolic activity and impact the current production.

Glucose concentration was measured at 8^{th} h for OD_{600} of 0.1 and 0.5 during current production under the same condition as Figure 4-1-1a. A 10-fold higher glucose consumption rate at OD_{600} of 0.5 compared to 0.1 showed that the metabolism of *C. ochracea* was substantially activated at high cell-density (Figure 4-1-1c). The electrochemically detected

quantity of redox substrate on the electrode by differential pulse voltammograms (DPV) also showed a significant increase with OD (Figure 4-1-1d). However, the magnitude of difference in DPV peaks for low OD and high OD is not same as the current production and glucose consumptions, because DPV analysis reflects the information about redox-active molecules present only at the electrode surface, either coming from bacterial surface electron transfer agent and/or soluble mediators. DPV measured at OD_{600} of 0.1 and 0.5 showed a slight difference in the peak potential (E_p) shift approximately from –0.35 (OD_{600} of 0.1) to –0.3 (OD_{600} of 0.5) V vs Ag/AgCl (Figure 4-1-1d). These data suggest that current enhancement at high cell-density results from both metabolic activation and the increase in redox substrates having redox potential of approximately –0.3 V vs Ag/AgCl.

Population-induced EET mechanism via cell secreted redox-substrate shuttling in *C. ochracea*

To examine whether *C. ochracea* could use the redox substrate detected in DPV in its current production, we performed supernatant swapping with fresh medium in the reactor at an OD_{600} of 0.5, after current production was saturated. The removal of planktonic cells decreased the current production (Figure 4-1-2a), suggesting that electron shuttling substrate contribute to the current production at an OD_{600} of 0.5. We confirmed the presence of an electron shuttle substrate at low and high OD_{600} by voltammetric analysis of the cell-free supernatant (cells were removed by centrifugation) collected from the reactor. The DPV of the cell-free supernatant solution from OD_{600} of 0.5 showed a 7-times higher peak current (ΔI) compared to OD_{600} of 0.2. Furthermore, while an OD_{600} of 0.2 showed a single peak at E_p of –0.2 V vs Ag/AgCl, an oxidative signal in the case of OD_{600} of 0.5 contained multiple peaks at different E_p values (Figure 4-1-2b). These significant differences in oxidative signals suggest that the accumulated redox substrate at OD_{600} of 0.5 is critical for current enhancement.

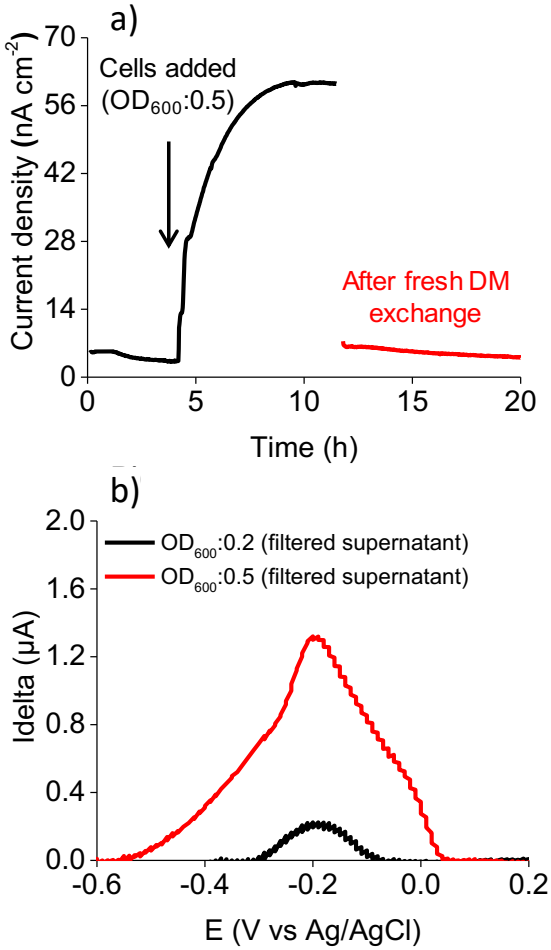

Figure 4-1-2. Electron shuttling capability of *C. ochracea* and free redox agent accumulation. (a) Supernatant replacement during the current production of *C. ochracea* at poised potential of +0.2 V vs Ag/AgCl. At indicated times, the medium was removed and replaced with fresh defined medium (DM) containing 10 mM glucose lead to a decrease in current production. (b) Baseline subtracted differential pulse voltammogram (DPV) showing the redox peaks of cell-free supernatants collected from OD_{600} of 0.2 and OD_{600} of 0.5 reactors.

We next examined the effect of external electron shuttles (which are also essential nutrients in many dietary products), such as menadione (Vitamin K3, VK3) and riboflavin (Vitamin B2, VB2), on current production. The addition of VK3 and VB2 to the reactor with high OD significantly increased current production over 10-fold (Figure 4-1-3a) compared to the absence of electron shuttles. In addition to E_p of –0.2 V vs Ag/AgCl assignable to the

cell surface protein, sharp oxidative peaks were observed with E_p at –0.4 V and +0.3 V vs Ag/AgCl in the presence of VB2 and VK3 in DPV, respectively (Figure 4-1-3b). Each peak represents a free oxidized redox shuttle in the reactor as half peak-width of these redox peaks is about 60 mV, indicating a $2e^-$ consumption by fully oxidized flavins rather than a $1e^-$ semiquinone.[127] Therefore, the population-induced EET mechanism was dominated by the electron shuttling mechanism, and *C. ochracea* likely accumulated cell-secreted electron shuttles as shown in the schematics (Figure. 4-1-4). Further, because *Capnocytophaga* is a flavobacterium[121] that secretes flavins, we measured the fluorescence spectrum of the collected cell-free supernatant from the electrochemical reactor during EET to detect the secreted flavins (Figure 4-1-5). However, no difference was observed between fresh DM and cell-free supernatant, indicating that *C. ochracea* produced insignificant amounts of flavins in the electrochemical reactor, confirming that flavin was not involved in the current generation by *C. ochracea* and there is likely an involvement of other redox molecules.

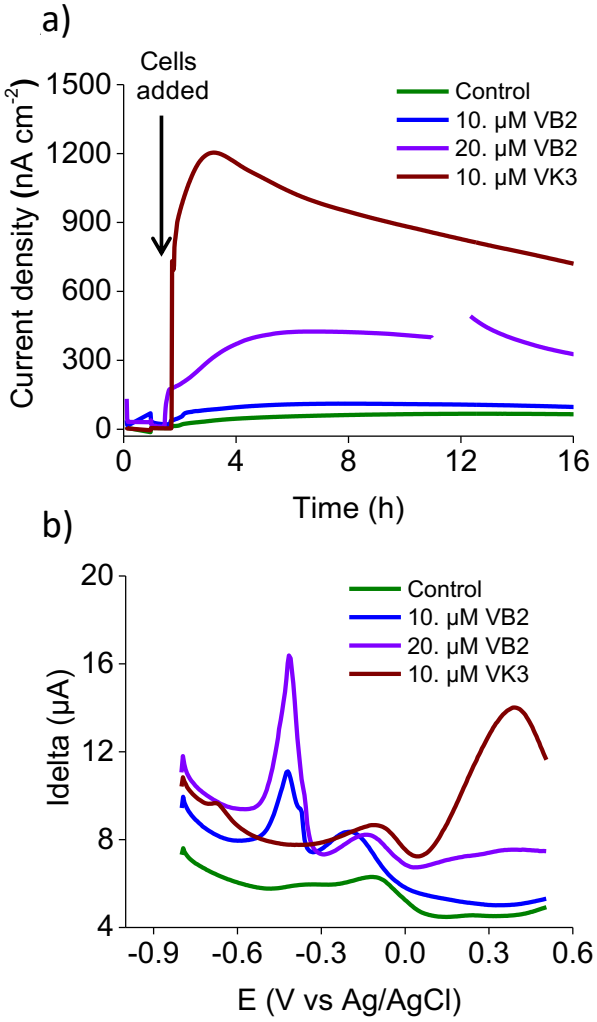

Figure 4-1-3. Impact of electron shuttles on electrochemical measurements of *C. ochracea* cells.

(a) Time vs Current production by *C. ochracea* in the absence (control) and the presence of electron shuttles *i.e.*, Vitamin K3 (VK3) and Vitamin B2 (VB2). Line break in 20 µM VB2 profile is due to DPV measurements at that point. (b) Differential pulse voltammogram (DPV) of *C. ochracea* in the presence and absence (control) of electron shuttles (VB2, VK3).

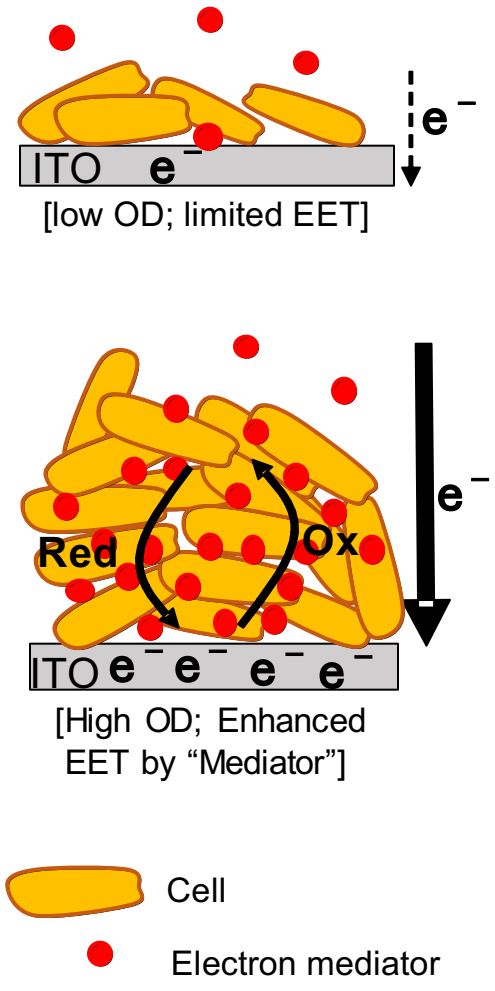

Figure 4-1-4. Schematic of possible electron transport mechanism by *C. Ochracea* cells. At low OD the EET is limited by the amount of cell-secreted redox-substrate whereas at higher ODs the concentration of redox-substrate is increased which acts as an electron mediator. Cell-secreted mediator attaches to the cell and shuttles the electrons to ITO via redox (Red) and oxidation (Ox) state cycling.

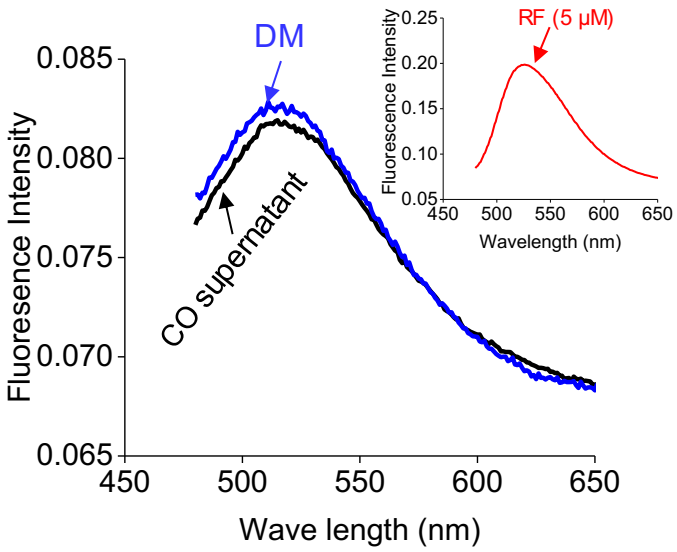

Figure 4-1-5. The Fluorescence emission spectrum of *C. ochracea* (CO) free supernatant measured in an anaerobic cuvette. Fluorescence emission spectrum of oxidized riboflavin (RF) by excitation at 450 nm measured in 3 mL of defined medium (DM) and cell-free supernatant (CO-supernatant) after 24-h of electrochemical operation at OD_{600} of 0.5. Inset showing the large peak intensity of externally added riboflavin (5 µM) in DM.

The larger current production at high OD_{600} 0.5 was associated with both higher metabolic activity (Figure 4-1-1c) and the higher concentration of redox substrate secretion compared to low OD (Figure 4-1-1c, 4-1-2b). To this end, we analyzed the metabolic activity of bacterial cells in the electrochemical cell by nanoscale secondary ion mass spectrometry (NanoSIMS). NanoSIMS is a robust tool to visualize and quantify the incorporation of labeled substrates in a single cell.[128,129] Therefore, we used ^{13}C labeled glucose and ^{15}N labeled ammonium chloride ($^{15}NH_4Cl$) to investigate the anabolic activity coupled to glucose metabolism in *C. ochracea*. In the single-potential amperometry condition, *C. ochracea* harvested from the electrode surface presented less ^{13}C and ^{15}N anabolic activity than non-attached cells in the supernatant (Figure 4-1-6a and 4-1-6b). The lower activity of the attached cells may be derived from the low nutrient or glucose concentration at the bottom

of the cell accumulation. Subsequently, the $^{13}C/C_{total}$ (%) and $^{15}N/N_{total}$ (%) in the non-electrode attached *C. ochracea* were compared in the presence of electron shuttles, VB2 and VK3 (Figure 4-1-6c). It can be seen that high activity was more abundant in electrode non-attached cells in comparison to electrode attached cells, supporting the significance of non-attached cells on metabolic activity and ultimately enhanced the EET.

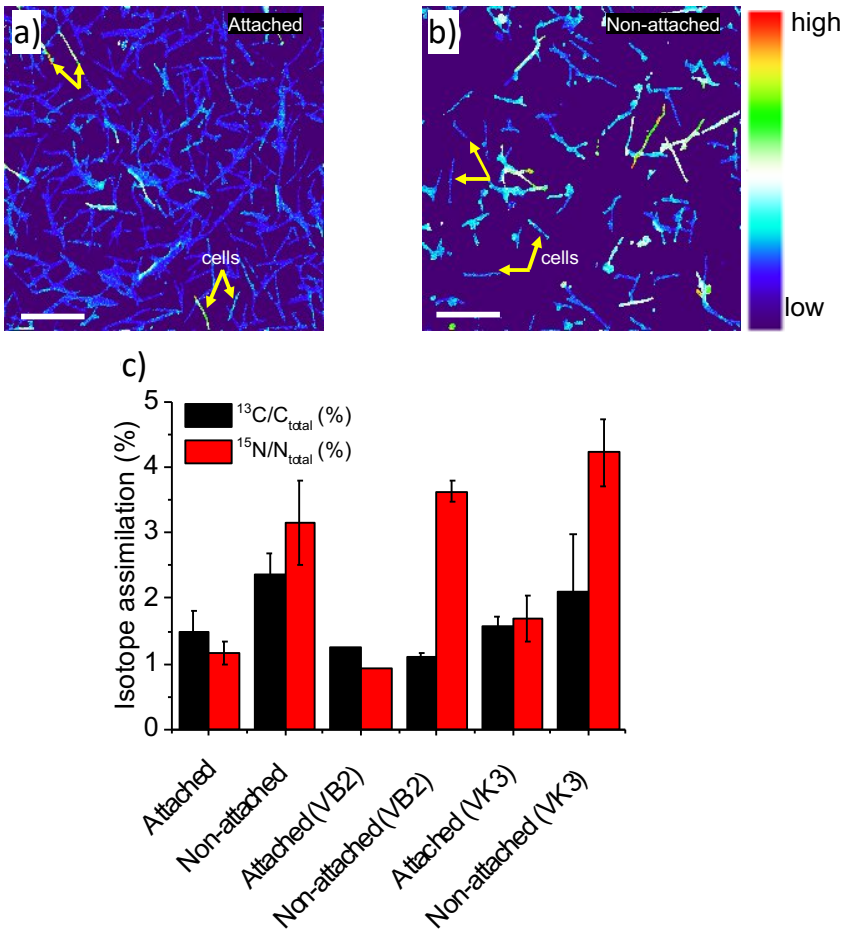

Figure 4-1-6. NanoSIMS analysis of *C. ochracea* in the presence and absence of shuttling molecules. NanoSIMS images of electrode attached cells (a) and non-attached cells (b) showing the $^{15}N/N_{total}$ (%) assimilation. Arrows indicating the rod-shaped *C. ochracea* cells (scale bars: 5μm). Warmer colored cells are more enriched in $^{15}N/N_{total}$ (%), which corresponds with higher levels of anabolic activity. (c) Bar graph showing the isotopic

assimilation of $^{13}C/C_{total}$ (%) and $^{15}N/N_{total}$ (%) in electrode surface attached and non-attached cells analyzed via NanoSIMS analysis. Given *C. ochracea* cells tend to form web-like morphology, to fully recover the isotope signals, the signals for each NanoSIMS image were averaged. Data values representing the mean ± standard deviations from two independent experiments and a similar tendency was observed in more than four individual experiments.

It is important to mention that electron shuttles affect interactions with the bacterial surface and eventually enhance the electron transfer rate to maintain the intracellular redox environments, i.e., redox homeostasis.[130] Metabolism-associated electron transfer of *C. ochracea* could act in concert to promote pathogenicity and biofilm development. Moreover, EET linked to population-level phenotypes can be critical during microbial colonization and biofilm formation. Therefore, EET would be an important population-level strategy against environmental stresses in addition to the QS mechanism.

Localization of redox-active biomolecule at cellular surface and membrane vesicles

The DAB staining was applied to probe the presence of heme-containing proteins [71]. As described previously, DAB can be oxidized by hydrogen peroxide coupled with redox enzymes and display a dark brown precipitation as indicated in Figure 4-1-7c. The active *Capnocytophaga* cells were harvested in the DSMZ 340 medium supplied with 1g/L sodium bicarbonate at 37 °C, presented a dark stain circling on the membrane after the staining treatment (Figure 4-1-7). This observation also supported the existence and activity of primary dehydrogenases- cytochromes, reported by[131] Surprisingly, abundant outer membrane vesicles (OMVs) were visualized in the DAB positive TEM images

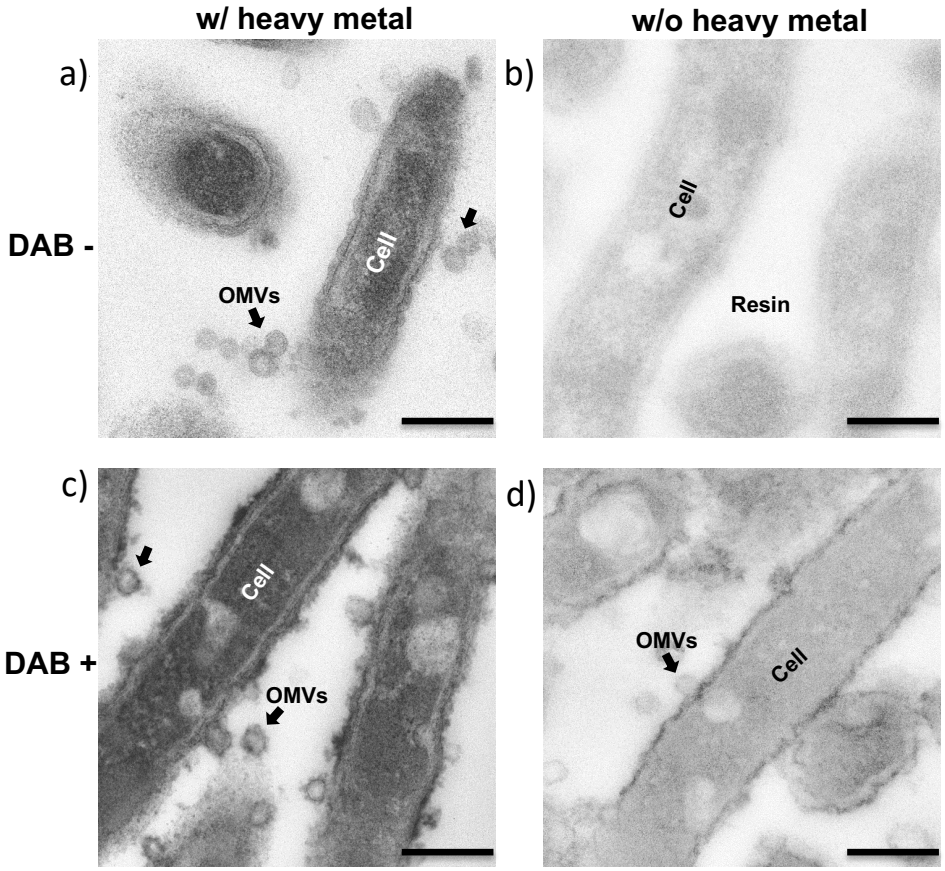

Figure 4-1-7. Transmission electron microscopy observation of thin sections of C. ochracea cells. (a to d) Transmission electron microscopy images of cells stained with or without heavy metals and redox-reactive DAB-H_2O_2. (a) Negative DAB staining in the absence of H2O2 and presence of heavy metals. (b) Negative DAB staining in the absence of both H_2O_2 and heavy metals. (c) Positive DAB staining in the presence of both H_2O_2 and heavy metals. (d) Positive DAB staining in the presence of H_2O_2 and absence of heavy metals. Scale bars, 200 nm. Note that heavy dark structures were clearly visible only with positive DAB staining in the presence of heavy metals revealing presence of redox species.

The impact of isolated MV addition on current production

The role of MVs in current production was corroborated in series of experiments. Firstly, the medium was removed from 0.5 OD EC at the time of maximum current generation and planktonic cells were removed by slow centrifugation while keeping MVs in medium under anaerobic conditions. This medium was exchanged in EC containing 0.1 OD, which led to a significant increase in current generation in a short span of time (Figure 4-1-8a). This result supported the MVs possible interaction with ITO attached cells for current generation and backed the likelihood of increase in electron transfer capability is linked to the dynamics of MVs. This was further confirmed with separate experiments with and without MVs. When more concentrated MVs isolated from large *C. ochracea* culture (500 ml) were added after washing in 0.1 OD EC and well shaken for mixing to examine the impact on current generation, a large increase i.e., approximately five times higher current than the original was observed (Figure 4-1-8b), elucidating the collaboration of MVs with cells at electrode surface for enhanced electron transfer rate. In another experiment, MVs were isolated from the EC medium at the time of maximum current generation and exchange of MVs' removed medium in 0.1 OD EC did not result in any increase in current generation (Figure 4-1-8c). This clearly showed that no soluble mediators were involved in electron transfer mechanism and MVs direct interaction with the ITO attached cells were responsible for higher current production.

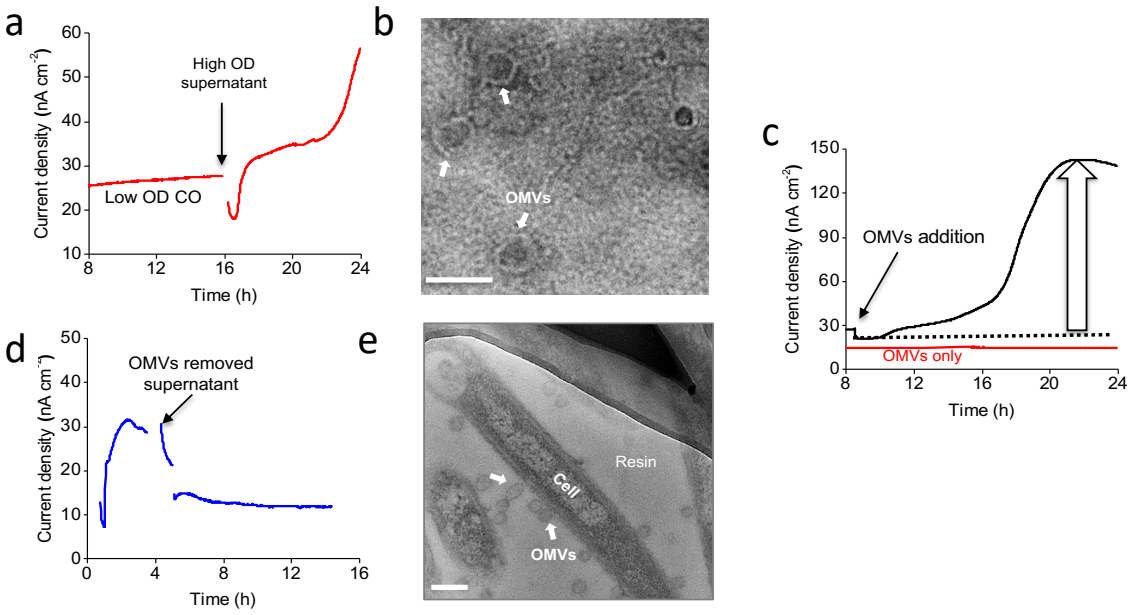

Figure 4-1-8. Role of OMVs in enhancement of electron transfer rate. (a) Effect on current profile when cell free supernatant added from high OD reactor to low OD reactor. (b) Transmission electron microscopy image of OMVs stained with ammonium molybdate. Scale bar,100 nm. (c) Effect on current generation of OMVs addition alone without cells (red line) and OMVs addition (500 ug) in low OD reactor (black line). (d) Effect of OMVs free electrolyte on current profile in low OD reactor. (e) Transmission electron microscopy image of cells stained with redox-reactive DAB- H_2O_2 where OMVs can be clearly seen. Scale bar, 200 nm. All current versus time measurements were conducted in anaerobic reactors equipped with ITO electrodes poised at +0.4 V (versus SHE)

We also performed LSV and DPV analysis to evidence the occurrence of redox agents that mediate current generation. Low scan LSV showed the offset potential of approximately -220 mV for MVs only while the offset potential shifted to more negative in case of *C. ochracea* and *C. ochracea* plus MVs (Figure 4-1-9a). Redox peaks were further determined by DPV for all these conditions. The distinct peak with potential at E= -160 mV emerged for MVs only, whereas a much broader peak was observed with max I delta at approximately -

250 mV for *C. ochracea* and *C. ochracea* plus MVs (Figure 4-1-9b), indicating the existence of redox enzyme(s)/species enabling the electron transfer. High cell density releases larger amount of OMVs, delivering electrons to the electrode, than low cell density. Moreover, in the absence of glucose, limited detectable currents could be resulted from the intuitive budding of OMVs. When we replace the planktonic cells with fresh medium to eliminate the source of OMVs, no significant currents can be detected (Figure 4-1-8). Collectively, these findings uncover the important role of redox-capable proteins in the EET of *C. Ochracea* and suggest the interplay of EET and glucose metabolism.

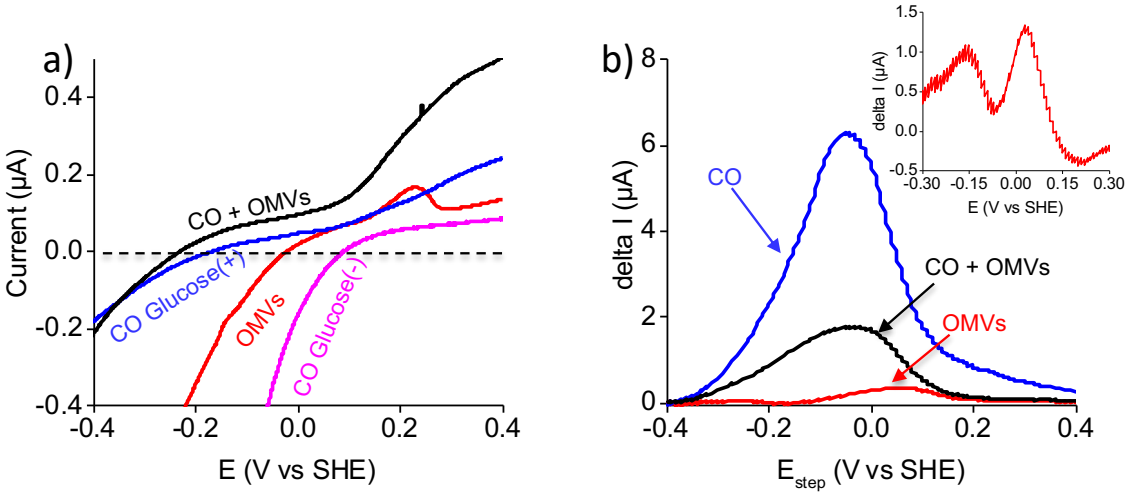

Figure 4-1-9. In vivo electrochemical measurements with C. ochracea cells and OMVs. (a) LS voltammograms measured at a scan rate of 0.1 mV/s for C. ochracea with and without glucose, OMVs only and C. ochracea after OMVs addition. (b) SOAS processed DPVs for C. ochracea, OMVs only and C. ochracea after OMVs addition. Inset is showing differential peak obtained by subtracting C. ochracea DPV from C. ochracea plus OMVs addition after matching their peak intensity.

The effect of mutant strain lacking gene for quorum sensing or biofilm formation

To further investigate the involvement of QS regulation in the EET rate enhancement of *C. ochracea* at high cell-density, we compared the current production of C. *ochracea* (WT) and its mutant strain (LKT7). LKT7, lacking the *luxS* gene, is a QS-deficient strain, which produces significantly fewer auto-inducers (AI-2) and less biofilm formation than WT, but with a similar growth rate.[132] Current generation measurements using the same conditions (OD_{600} of 0.5) revealed that LKT7 was also capable of producing significant anodic current, comparable to WT (Figure 4-1-10a). Hence, these deletion factors hardly pertained to the EET capability of *C. ochracea.* DPV results showed the possible involvement of the same redox enzyme in electron transfer, as notable redox peaks at almost the same E_p were observed in both WT and LKT7 (Figure 4-1-10b). These results suggest that the known *luxS* gene-based QS in *C. ochracea* was unlikely to contribute to EET enhancement at high cell-density. However, the possible involvement of another QS mechanism cannot be ruled out.

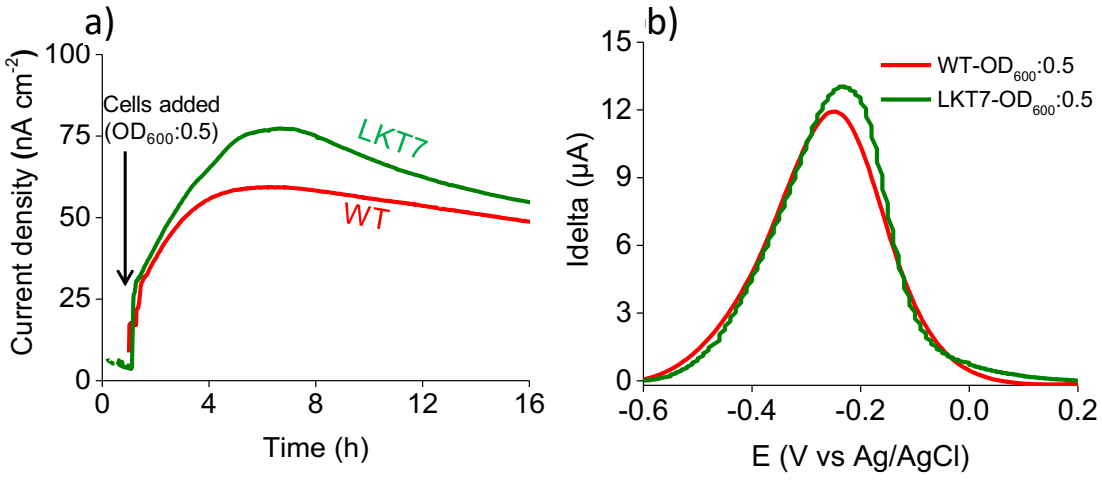

Figure 4-1-10. Effect of *luxS* gene deletion on EET of *C. ochracea.* (a) Current production profiles of *C. ochracea* WT and mutant strain- LKT7 (lacking quorum sensing gene l*uxS*) at OD_{600} of 0.5 at poised potential of +0.2 V vs Ag/AgCl. (b) Baseline subtracted differential pulse voltammogram (DPV) of *C. ochracea* WT and mutant strain- LKT7 at OD_{600} of 0.5.

The maximum metabolic current generated in case of LKT7 was even larger than wild type. TEM images of LKT7 also revealed the presence of MVs at its outer membrane. Although the production of MVs is a ubiquitous physiological process, the factors involving different stresses are also believed to trigger MVs production [122,133]. MVs production by EET capable environmental bacterial strain *S. oneidensis* is known to be promoted by the lack of DegQ as a result of an increase in envelope stress [134]. The stress of LuxS deficiency in *C. ochracea* mutant strain LKT7 might also have played a significant role in enhanced MVs production and ultimately playing an important role in current generation and enhanced electron transfer rate. DPV results also showed the possibility of same redox enzyme involved in electron transfer as noticeable redox peak at nearly similar positions with potential at E= -0.2 to -0.3 (Figure 4-1-10b) were observed in wild-type and mutant strain. Overall, these results further support the EET dependency on MVs as there was no negative impact on EET by deletion mutant strain (with less biofilm capability) was observed.

Although *C. ochracea* is able to transport electrons extracellularly, the current production was not comparable to well-known EET microorganisms, such as *Shewanella spp*. and *Geobacter spp*. [99,113] As previously described, there are direct and indirect EET deployed by EET-capable microorganisms [33]. Therefore, The DPV analysis revealed an outstanding redox peak with potential at E= -0.4 in the VB2 condition and at E=+0.3 in the VK3 condition (Figure 4-1-3b). Findings from these experiments implicate the different redox reactions and electron shuttling mechanisms between VK3 and VB2. Previous studies reported that VK3, as an electron shuttle, can penetrate cell membrane and carry electrons out from bacteria, whereas VB2 collaborated with the redox proteins, embedded on the cell membrane, to pass electron extracellularly [135]. The strikingly increase of current production in the presence of VK3 evidenced the capability of electron generation of *C. Ochracea*, and the promotion of EET in the presence of VB2 unveils the reductive energy export is the rate limiting step of *C. Ochracea* EET.

This study provides the insights into the MV mediated EET mechanism in *C. ochracea*, an oral pathogen. Two known distinct pathways of MV formation in gram negative

bacteria are blebbing of the outer membrane and endolysin-triggered cell lysis [122]. In case of *C. ochracea* it can be clearly seen in TEM images (Figure 4-1-7) that MVs were associated with blebbing of the outer membrane and no cell lysis based MVs were observed. Therefore, cytoplasmic components cannot be the part of these blebbing MVs as inner membrane remains intact. Hence, contrary to other secretion systems, MVs can carry insoluble membrane proteins, proteolytically unstable enzymes, and other nonprotein molecules all within particles that may stabilize and concentrate them until they can interact with host cell receptors. The surface of OMVs is thought to reflect the outer membrane composition of the bacterial cells whereas the lumen is predicted to contain mainly periplasmic components. Because some of these proteins have critical roles in host colonization, immune evasion, nutrient uptake, and tissue damage, it is thought that MV production may be a property that is important to pathogenesis [124]. OMVs are also promising immunogenic platforms and may play important roles in bacterial survival and pathogenesis. Because some of these proteins have critical roles in host colonization, immune evasion, nutrient uptake, and tissue damage, it is thought that OMV production may be a property that is important to pathogenesis [122-124,133]. Once these vesicles separate from the cell, and without a continuous source of electrons from the cytoplasm, they will be incapable of extracellular electron transfer. These vesicles would be expected, therefore, to contain outer membrane redox enzymes that are capable of extracellular electron transfer. Possible mechanism of MVs interaction with bacterial cells and electron transfer to exterior surface is shown in figure 4-1-11.

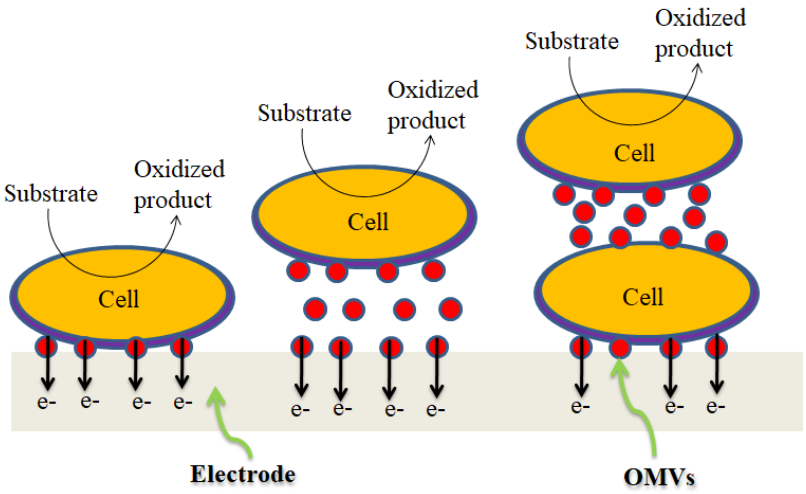

Figure 4-1-11. Schematic of possible OMV mediated EET in *Capnocytophaga ochracea*

This study is the first to present valuable insights into electroactive microbiome in human oral cavity using a periodontitis-causing oral pathogen. Although human oral pathogens were well studied in the medical field, their microbial electrical activities, in particular the capability of extracellular electron transportation that we discovered in this study, were scarcely reported. The divergent metabolic features and microbial lifestyle elucidated in this study would be a tremendous expansion in human microbiome research and provide practical references of disease treatment in medical field.

Publications of chapter 4-1:

1. Shu Zhang*, Miran Waheed*, **Divya Naradasu***, Siyi Guo and Akihiro Okamoto. A Human Pathogen *Capnocytophaga Ochracea* Exhibits Current Producing Capability. *Electrochemistry* (2020). *equal authors

2. **Divya Naradasu***, Shu Zhang*, Miran Waheed*, Shruti Sharma and Akihiro Okamoto† Membrane Vesicle Involves in Rate Enhancement of Extracellular Electron Transport in *Capnocytophaga ochracea*. (under preparation). *equal authors

Chapter 4-2: Extracellular electron transport mechanism of *Aggregatibacter actinomycetemcomitans* and *Porphyromonas gingivalis*

Introduction

In contrast with environmental bacteria, a few bacterial strains in the human microbiome are known to harbor EET capability via transmembrane redox proteins. Strains of *Enterococcus faecalis,* [98,136] *Listeria monocytogenes,* [32] and two other isolates from the human gut share homology with *Klebsiella pneumoniae* and *Enterococcus avium* with respect to the 16S rRNA gene, displayed a significant current production or metal oxide reduction.[63] These strains are associated with infectious diseases in humans, and it was suggested that their EET potential may facilitate their colonization in the host environment under anaerobic conditions. EET facilitates long-range and interspecific electron transport, and supports energy production in cell aggregates or biofilms.[137,138] Therefore, while the pathogens are fermentative in nature, their EET is potentially associated with anaerobic bacterial metabolism. Thus, the colonization of pathogens in the human microbiome would be supported by their EET potential and is important to explore such capability.

Extracellular electron transfer (EET) in human gut pathogens has gained increasing attention. However, the possible EET-capable bacterial niche such as oral plaque has not been explored yet. Here, we examined the EET capability of two predominant biofilm pathogens of the oral environment, *Aggregatibacter actinomycetemcomitans* and *Porphyromonas gingivalis*, which principally colonize in polymicrobial biofilms.[139,140] Both strains are Gram-negative, anaerobic, non-motile and are often found in oral biofilms associated with gingivitis and localized aggressive periodontitis.[141,142] Single-potential amperometry combined with metabolite analysis or use of metabolic inhibitor is a simple and direct method to examine the association of current production with metabolism.[143] Additionally, methodology for the characterization of EET mechanism has advanced in the past decade.[86,138] As well as conventional membrane extraction or gene deletions to identify the proteins involved in EET,[86,144] whole-cell electrochemical voltammetry and redox-

dependent cell staining methods utilize intact cells to characterize the cell surface redox protein. Upon confirming the direct attachment of cells to the electrode surface, the electrode-potential-dependent current profile represents the protein-specific redox kinetics to distinguish them from soluble redox mediators.[44,145] The 3,3'-diaminobenzidine (DAB) staining method has been applied to probe the localization of redox proteins. This is because transition-metal enzymes catalyze DAB oxidation through hydrogen peroxide (H_2O_2) to generate highly osmiophilic DAB polymers, which can be visualized under transmission electron micrograph (TEM).[138,146] These methods are applicable to any strain and are thus suitable to characterize new EET-capable bacteria.

In this study, we electrochemically characterized *A. actinomycetemcomitans* and *P. gingivalis*, using three-electrode electrochemical system. Microbial electrochemical catalytic activity was analyzed via single-potential amperometry by current production and metabolite analysis. Furthermore, the impact of cell wall and protein synthesis inhibitors on the current production was examined. The potential electron pathways via cell-surface compound redox reaction were also examined through cyclic voltammetry (CV) and differential pulse voltammetry (DPV). The presence of membrane redox compounds was assessed via TEM with DAB-stained bacterial cells.

Results and Discussion

Microbial electrode catalysis associated with metabolisms of oral pathogens.

Microbial electrode catalysis i.e., current production (i_c) in *Aggregatibacter actinomycetemcomitans,* as measured by single-potential amperometry (SA) with a working electrode of indium tin-doped oxide (ITO) at +0.4 V vs a standard hydrogen electrode (SHE). Bacterial cells were collected and washed with defined medium (DM, the electrolyte) to remove the cell secreted metabolites of the preculture medium. On transferring bacterial cells into the reactor to a final optical density of 0.1 at 600 nm (OD_{600nm}), a significant increase in i_c was immediately observed in the presence of 10 mM lactate (~80 $nAcm^{-2}$) rather than in the absence of electron donors (~15 $nAcm^{-2}$) (Figure 4-2-1a), indicating that the electrons are transferred from cell to electrode surface coupled with lactate oxidation. The net i_c increased

gradually and approached 65 $nAcm^{-2}$ in 24 h (Figure 4-2-1a), which is 100 times smaller as compared to environmental EET bacteria (1–100 μAcm^{-2}).[44] Accordingly, the lactate concentration gradually decreased within 16 hrs (Figure 4-2-1c), indicating that i_c generation is coupled with lactate oxidation. Time-course analysis of metabolite concentration revealed acetate production during current generation (Figure 4-2-1c). However, formate, succinate or propionate were not detected in ion-chromatography analysis, indicating that lactate fermentation occurred.[147] Lactate consumption was lower than acetate production in the first 8 h, thereby indicating that organic substrate retained in the cell from preculture may have sourced the acetate production. After 8 h, lactate consumption and acetate production were stabilized. Meanwhile, glucose supplementation showed less i_c of 10 $nAcm^{-2}$ relatives to that in the presence of lactate, consistent with a substrate preference in *A. actinomycetemcomitans* under fermentative conditions.[147,148] These results demonstrate the current producing capability by *A. actinomycetemcomitans* associated with the lactate fermentation reaction. Similarly, current producing capability was observed in *P. gingivalis* under the same experimental conditions. The *P. gingivalis* cells were introduced into the electrochemical reactor containing 10 mM glucose. Consequently, current flow increased slightly in the first 2 h and then steeply up to 16 $nAcm^{-2}$ in 8 h than in the absence of glucose. This increase can be associated with glucose consumption (Figure 4-2-1b, d). While *P. gingivalis* can utilize complex carbohydrates and amino acids,[149] no significant current production was observed in the presence of lactate distinct from *A. actinomycetemcomitans* (Figure 4-2-2). Together, in accordance with our hypothesis, both the pathogenic model bacteria displayed EET potential. The present study demonstrated EET potential in *A. actinomycetemcomitans* and *P. gingivalis,* in association with their fermentative metabolism of lactate and glucose, respectively. However, while the consumption of these electron donors stopped at 8 or 16 hours (Figure 4-2-1c and d), a continuous i_c was observed until 24 hours in both the systems. Given that the accumulation of reductive energy suppresses fermentation metabolism,[150,151] the metabolism is suppressed, but reductive energy retained within cells may be a source for continuous current generation even after the consumption of electron donors has stopped. This premise is consistent with a low coulombic efficiency value estimated on the basis of

current production and electron donor substrate consumption, *i.e.,* 1000-fold lesser than the number of electrons generated from glucose and lactate (considering glycolysis of glucose and lactate oxidation to pyruvate) in *P. gingivalis* and *A. actinomycetemcomitans* respectively (Figure 4-2-3). Compared to environmental EET-capable bacteria such as *Shewanella* MR1, *Geobacter sulfurreducens*, these current densities are lower as observed in our study and in a few other reported pathogens termed as weak electricigens. [76,152] The export of electrons would facilitate the fermentation reactions instead of accumulating the reductive energy inside the cells. [150]

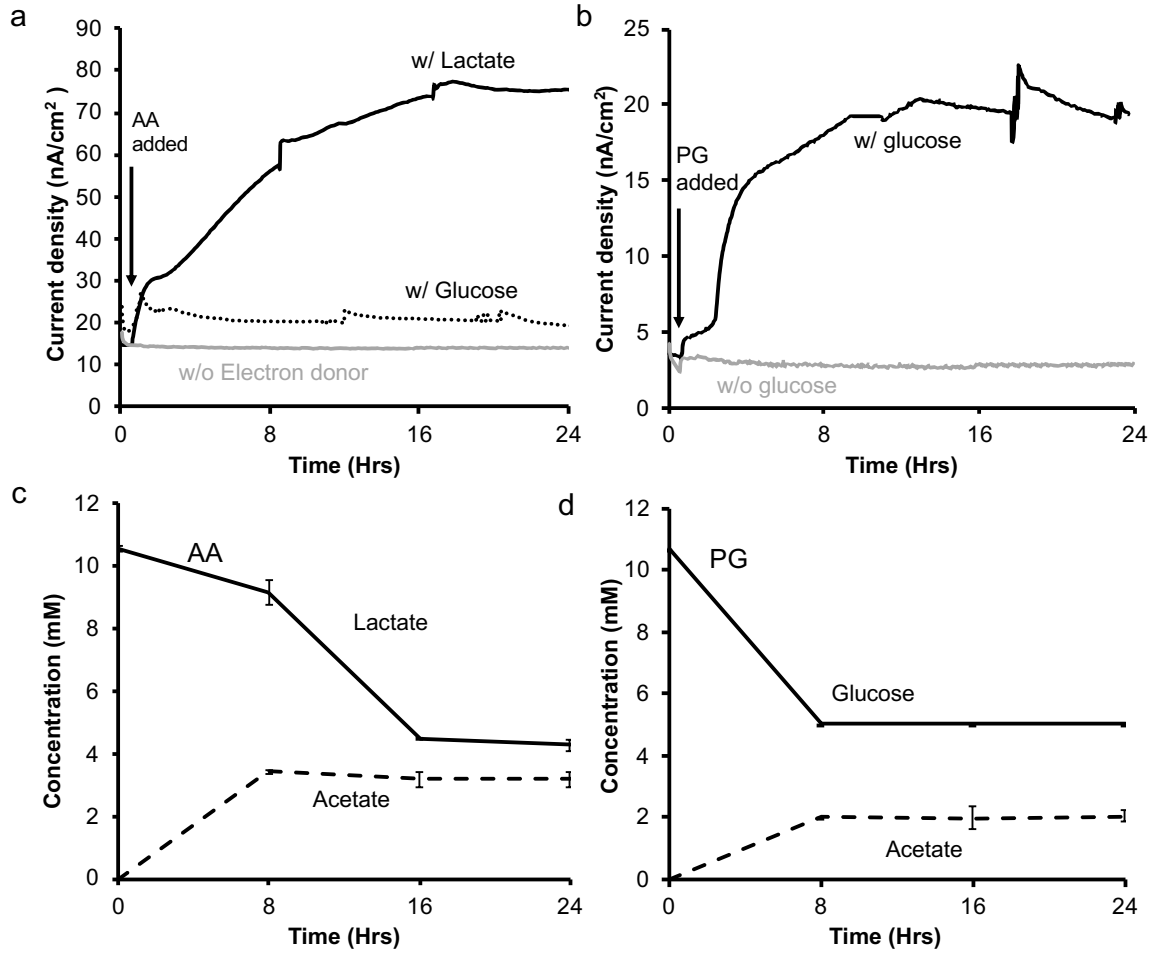

Figure 4-2-1. Microbial electrode catalysis i.e., current production (i_c) and metabolite profiles of *Aggregatibacter actinomycetemcomitans* (AA) and *Porphyromonas gingivalis* (PG) (a, b) Representative current production versus time measurements conducted in an anaerobic

reactor equipped with indium tin-doped oxide (ITO) electrodes (surface area: 3.14 cm^2) poised at +0.4 V (versus SHE) in the presence and absence of lactate and glucose. Similar tendency was observed in more than four individual experiments. (c, d) Time-course analysis of metabolite concentration in *A. actinomycetemcomitans* and *P. gingivalis* during current generation in the presence of lactate and glucose respectively. Data representing the mean ± standard deviations of two individual experiments

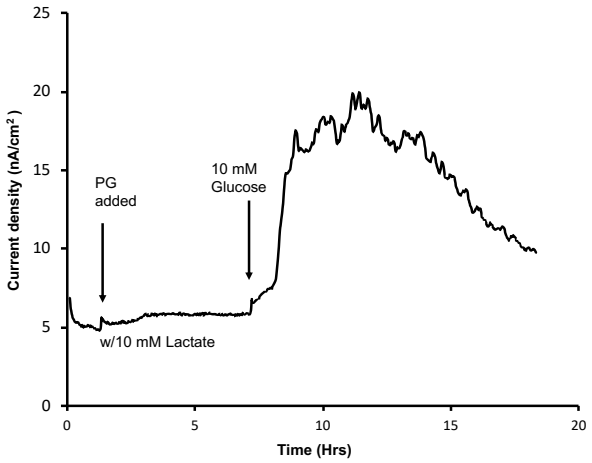

Figure 4-2-2. Representative current production versus time measurements of *P. gingivalis* (PG) conducted in an anaerobic reactor equipped with indium tin-doped oxide (ITO) electrodes (surface area: 3.14 cm^2) poised at +0.4 V (versus SHE), in the presence of lactate and glucose. No significant current was observed in the presence of lactate in case of PG, but glucose enhanced the electron transport. Similar tendency was observed in more than four individual experiments.

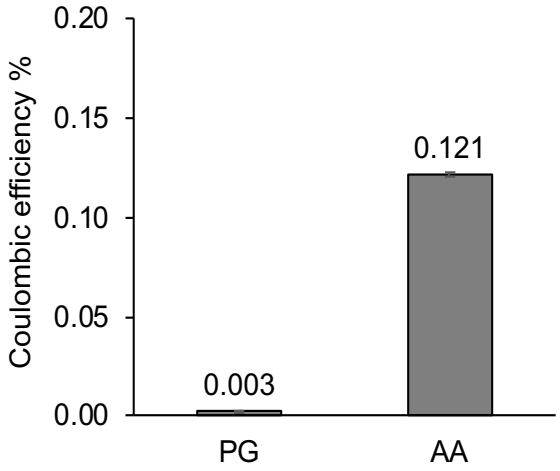

Figure 4-2-3. Coulombic efficiency of *P. gingivalis* (PG) and *A. actinomycetemcomitans* (AA) estimated from the consumed glucose and lactate and Time vs Current profile (Figure 1a, b) during the electrochemical measurement, respectively.

The effect of antibiotics on microbial current production.

Next, to further confirm the association of i_c with cellular metabolic activity, we examined the impact of major antibiotics on the current production of the two strains in the electrochemical system. We used Ampicillin, which inhibits cell wall formation i.e., suppresses the growth of cells and Kanamycin - a protein synthesis inhibitor, at lethal concentrations [46] for both *A. actinomycetemcomitans* and *P. gingivalis*. Addition of Ampicillin to *A. actinomycetemcomitans* electrochemical system during current production approximately after 8 hours (when current production was maximum), showed no significant impact at 1 mg/mL concentration. However, it showed a decrease of ~50% compared to maximum current production at 3 mg/mL concentration (Figure 4-2-4a), and then continued to decrease further. A similar current decrease was observed in the case of *P. gingivalis* instantly after the addition of 1 mg/mL ampicillin (Figure 4-2-4c). These gradual decreases in current production suggest that the cells were growing on the electrode surface during current production. Meanwhile, the addition of Kanamycin (1 mg/mL) steeply decreased the current within 5 - 10 minutes, and then the current recovered in 7 hours in the case of *A.*

actinomycetemcomitans (Figure 4-2-4b), suggesting that the effect of Kanamycin decreased with time.[153] Similarly, Kanamycin decreased the current production of *P. gingivalis* in the same time range, and gradually the current recovered (Figure 4-2-4d). Because protein synthesis occurs more frequently than cell growth, the relative time range for the impact of each antibiotic seems to be reasonable. These data therefore strongly suggest that the current production of these two strains reflects cell activities such as growth and protein synthesis. Hence, SA could be a unique assay applicable to any EET capable pathogens for qualifying their cellular metabolic activity, and physiological response to antibiofilm compounds compared to conventional techniques involving microscopic observation of cells, complex sensor systems and longer cultivation time assays. [102,154]

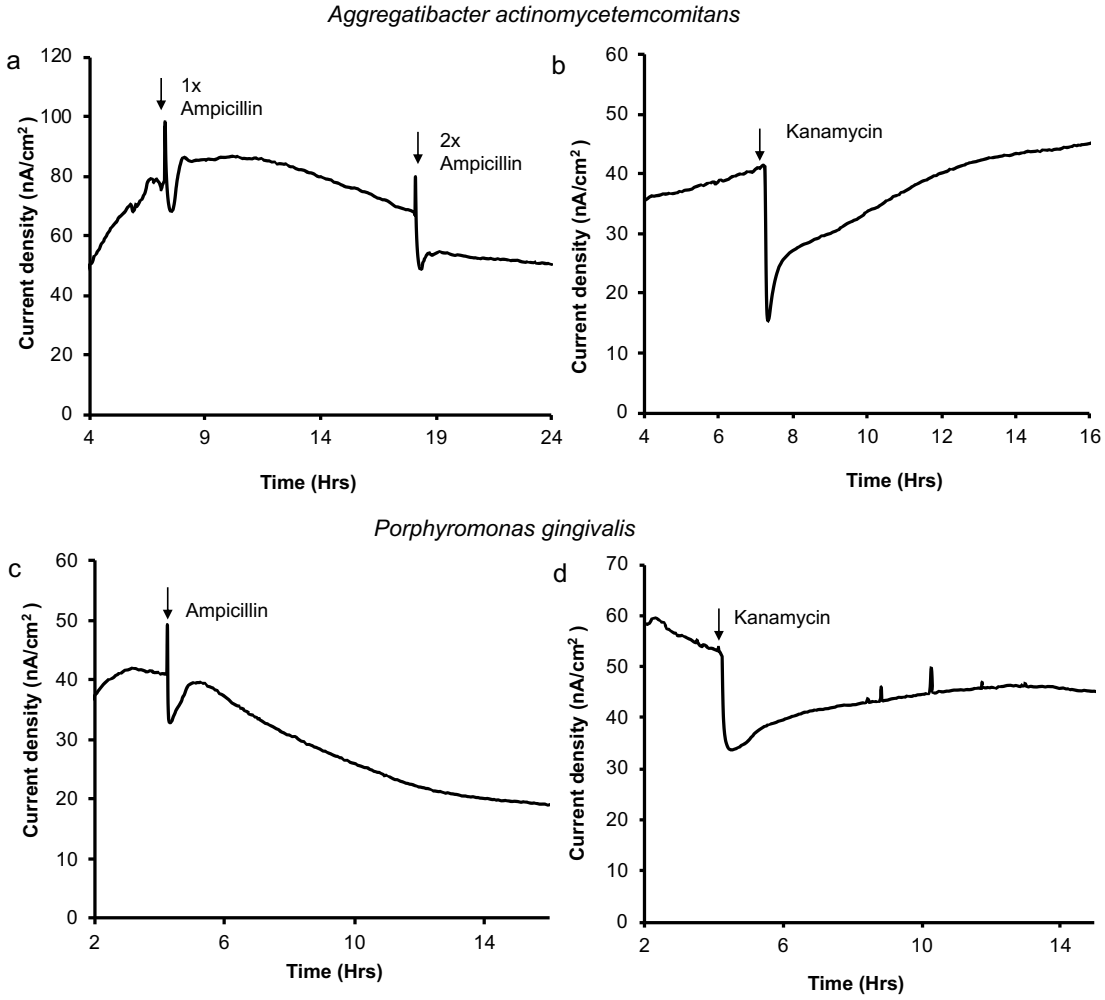

Figure 4-2-4. Representative current production versus time measurements of *A. actinomycetemcomitans* (**a, b)** and *P. gingivalis* **(c, d)** conducted in an anaerobic reactor equipped with indium tin-doped oxide (ITO) electrodes (surface area: 3.14 cm^2) poised at +0.4 V (versus SHE), at indicated times with arrows, antibiotics were added to the reactor to assess the effect on electron transport.

Voltammetric analysis during current production

To examine the potential electron pathways that mediate i_c in *A. actinomycetemcomitans* and *P. gingivalis*, we used a voltammetric approach. Differential pulse voltammetry (DPV) was measured. The presence of *A. actinomycetemcomitans* yielded an oxidative peak (E_p) in baseline subtracted DPV at approximately –60 mV vs SHE (Figure 2a). This indicates that *A. actinomycetemcomitans* contains redox agents that potentially mediate electron transport to the electrode surface. Also, baseline subtracted DP voltammetry revealed a redox peak current with two peak potentials at approximately +6 mV (E_{p1}) and +150 mV (E_{p2}) vs SHE in *P. gingivalis* (Figure 4-2-5a). Scanning electron microscopy displayed cellular attachment on the ITO electrode surface for both strains after several washes and dehydration (Figure 4-2-6). Consistently, even after supernatant replacement to fresh medium, a similar peak current was observed in DP voltammograms of both strains (Figure 4-2-7a, b). This can be attributed to the cell-surface bound redox enzymes or redox shuttles but not hydrogen, where exogenous or endogenous soluble, redox-active compounds may not be the primary components of the redox signal observed. Furthermore, the large half peak width, which indicates the number of electron transfers [155] of more than 200 mV for both strains, is consistent with earlier reported multi-heme outer-membrane cytochromes, but not with soluble electron mediators such as riboflavin with that of 60 mV (vs SHE).[44]

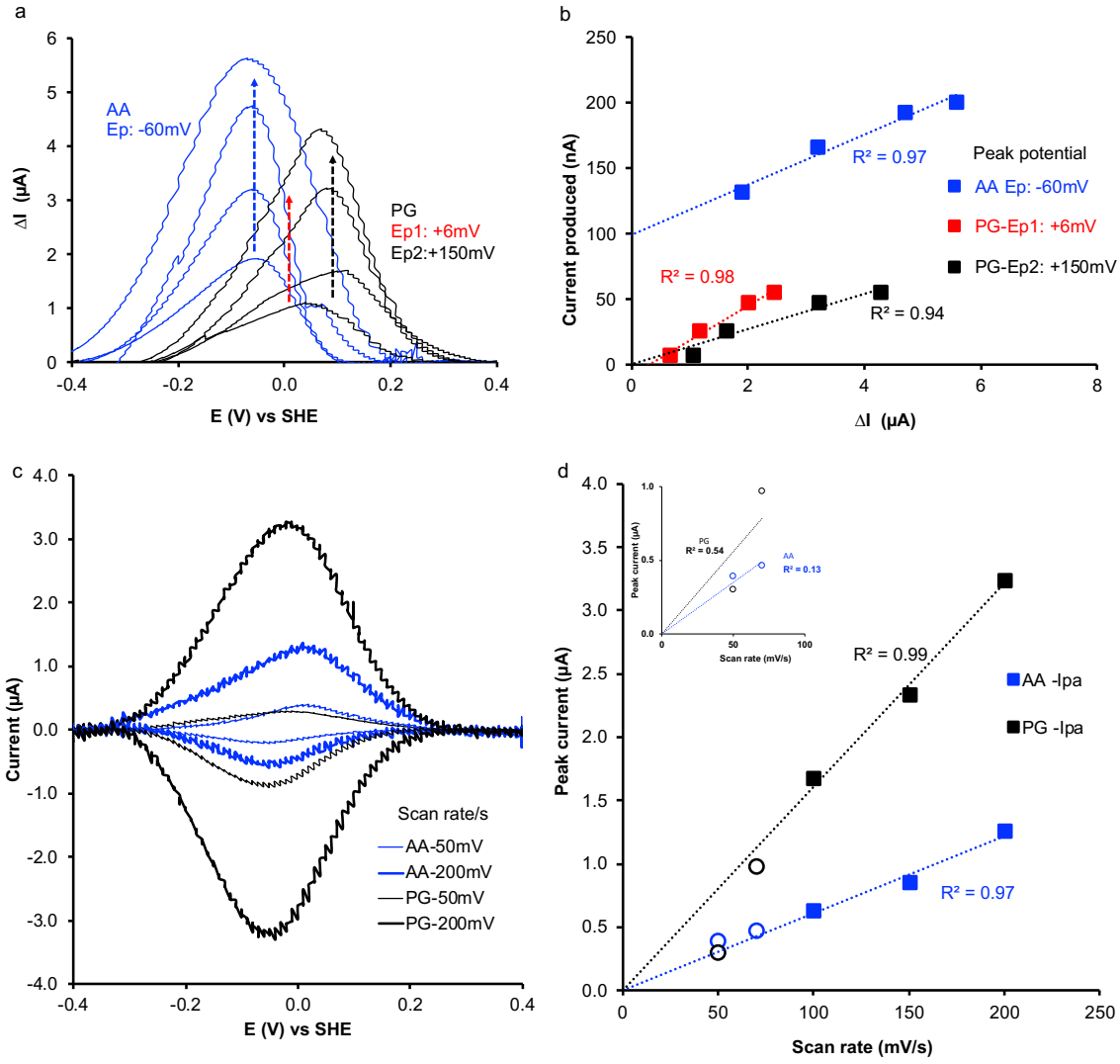

Figure 4-2-5. Contribution of cell-surface redox substrate for current production in *Aggregatibacter actinomycetemcomitans* (AA) and *Porphyromonas gingivalis* (PG). (a) Baseline subtracted Differential pulse (DP) voltammograms at different time points during current production measured with ITO electrodes (surface area: 3.14 cm^2) poised at +0.4 V (versus SHE). Arrow indicating the increasing order of DP voltammograms. (b) Bacterial current production (i_c) plotted against baseline-subtracted oxidative peak (E_p). (c) Baseline subtracted Cyclic voltammogram (CV) of *A. actinomycetemcomitans* and *P. gingivalis* measured at scan rates 50 mV/s and 200 mV/s. (d) Peak currents observed in CV of *A.*

actinomycetemcomitans and *P. gingivalis* were plotted against scan rates measured (50 mV/s to 200 mV/s), circle markers are the data points of 50 mV/s and 70 mV/s. inset showing the peak currents observed in baseline subtracted cyclic voltammogram of *A. actinomycetemcomitans* and *P. gingivalis* were plotted against scan rates measured at 50 mV/s and 70 mV/s. The squares of correlation coefficients were estimated by fitting the obtained data points linearly. Similar tendency was observed in two individual experiments.

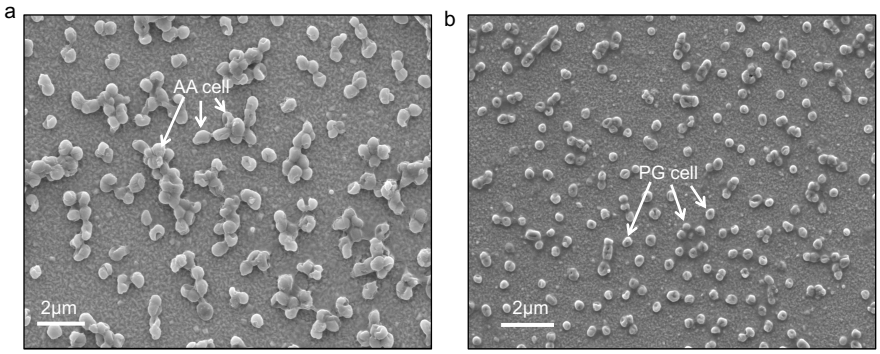

Figure 4-2-6. Scanning electron micrographs showing direct attachment (indicated with arrows) of (a) *A. actinomycetemcomitans* (AA) and (b) *P. gingivalis* (PG) on the ITO electrode surface.

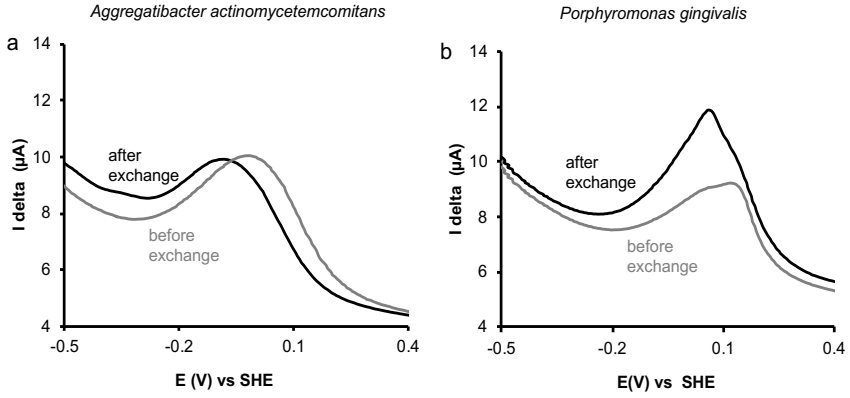

Figure 4-2-7. Differential pulse voltammogram of *A. actinomycetemcomitans* (a) and *P. gingivalis* (b) before and after the transfer of supernatant to fresh media, conducted in an anaerobic reactor equipped with indium tin-doped oxide (ITO) electrodes.

We next examined the contribution of the cell-surface redox agents for i_c by DPV. We performed DP voltammetry analysis at different time points during current production. Given that the peak current denotes the relative amount of the cell-surface redox protein, linear correlation indicates the extent of the cell-surface protein's role in current production.[44] The plots of i_c against the baseline subtracted peak current of DPV are shown in Figure 4-2-5b. Given that the peak current indicates the relative amount of the cell-surface redox protein, positive linear correlation passing near the origin in *P. gingivalis* (peak E_{p1}: +6 mV and peak E_{p2}: +150 mV) suggests a significant involvement of cell-surface compounds in current production. In contrast, while a similar linear correlation was observed in *A. actinomycetemcomitans*, approximately 120 nA of i_c is potentially generated even in the absence of the peak current originated from the cell surface compounds (Figure. 4-2-5b). These data suggest that both a direct electron transport and a diffusion dependent (redox shuttle mediated) electron transport are involved in the EET mechanism in *A. actinomycetemcomitans*.

Next, we performed cyclic voltammograms at different scan rates ranging from 50 mV/s to 200 mV/s to identify the diffusion-dependent or independent electron transfer by *A. actinomycetemcomitans* and *P. gingivalis* (Figure 4-2-5c). The presence of *A. actinomycetemcomitans* yielded an oxidative and reductive redox peak with a mid-point potential in baseline subtracted CV at approximately –4 mV vs SHE. Also, baseline subtracted CV redox peak with mid-point potential at approximately +2 mV vs SHE was observed in *P. gingivalis* (Figure 4-2-5c (50 mV/s scan)). Figure 4-2-5d showing the scan rates plotted against the oxidative peak currents observed in the CV to analyze the linearity. The redox peaks of *A. actinomycetemcomitans* and *P. gingivalis* have higher linearity at faster scan rates from 100 mV/s to 200 mV/s, suggesting that diffusion non-limited electron transfer process is associated with current production by *A. actinomycetemcomitans* and *P. gingivalis* (Figure 4-2-5d). At slower scan rates *i.e.,* 50 mV/s and 70 mV/s the CV anodic peak potentials were less linear (Figure 4-2-5d, inset) compared to fast scan rates, indicating that a diffusion-limited (possible redox shuttling) electron transport was also associated with the

current production. A Single peak was observed in CV analysis of *P. gingivalis,* while two peaks were observed in redox-sensitive DPV analysis (Figure 4-2-5a) suggesting that the DPV redox peak at approximately +150 mV (E_{p2}) is likely attributable to the diffusive molecule or redox agents on the surface of planktonic cell. On the other hand, the DPV redox peak at approximately +6 mV, (E_{p1}) having more linearity with the i_c dominates electron transport as observed in high scan rate CVs. This was further supported by the presence of redox molecules at approximately similar peak potentials of intact cell DPVs in cell-free supernatant solution collected during current production (cells were removed by centrifugation) of *A. actinomycetemcomitans* and *P. gingivalis* (Figure 4-2-8) measured via DPV analysis. This indicates that the redox shuttle secretion by these pathogens was involved in the diffusion limited EET process. Albeit, similar redox potentials were observed in the presence (cells on the ITO surface after supernatant replacement to fresh medium) and absence of cells (cell-free supernatant) (Figure 2a and Figure 4-2-8), identification of the cell surface proteins and redox shuttles would be an important direction of future study. Collectively these data indicate a significant cell surface bound redox protein in association with a redox shuttling EET mechanism in these pathogens.

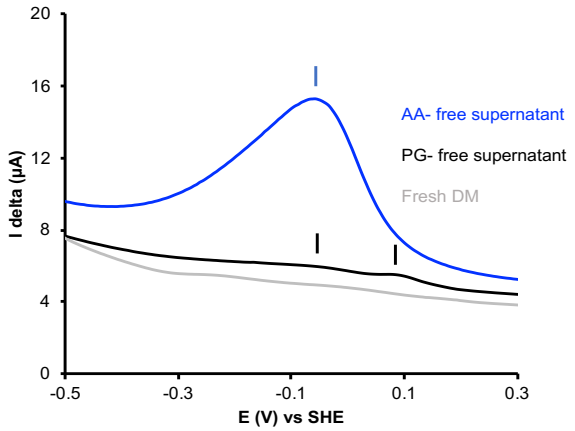

Figure 4-2-8. Differential pulse voltammogram of cell free supernatants of *Aggregatibacter actinomycetemcomitans* (AA- blue line) and *Porphyromonas gingivalis* (PG- black line) showing the presence of redox molecules, DPV of fresh medium (grey line) is also showed as a reference

***in-vitro* analysis of cell-surface compounds**

We employed an *in-vitro* analysis to detect the presence of cell-surface redox compounds by redox-dependent DAB chemical staining assay. Both the bacterial strains were cultured under the same conditions that we used for the electrochemical experiments and subjected to DAB staining. Cross-sectional images of DAB-stained *A. actinomycetemcomitans* cells displayed strong contrast and thicker cellular edges in the presence of H_2O_2 (DAB-positive) as compared to those in the absence of H_2O_2, shown herein as the DAB-negative condition (Figure 4-2-9a, b,). In contrast, the DAB-negative and -positive images of *P. gingivalis* showed almost identical thickness and absorption for the stained membrane analyzed via TEM-LINE profile analysis (Figure 4-2-9c, d, e, f, and Figure 4-2-10). Because *A. actinomycetemcomitans* and *P. gingivalis* have EET capability and oxidative current peak in CV and DP voltammograms, a comparable amount of cell-surface redox protein should be expressed. Therefore, the negligible difference in DAB staining of cellular membrane demonstrates that *P. gingivalis* carry out EET with cell-surface proteins containing a redox center with significantly lower reactivity for H_2O_2 oxidation.

In *A. actinomycetemcomitans*, the thickness of dark edge and absorption measured showed an approximately two-fold thicker stained membrane and comparable membrane absorption amounts to that of environmental EET bacteria [86] (Figure 4-2-9e, f) suggesting the presence of not only cytoplasmic membrane but also outer membrane and extracellular redox proteins with reactivity for H_2O_2 oxidation. Given DAB reaction occurs with reaction centers containing transition metals,[146] our data indicate that *A. actinomycetemcomitans* harbor outer membrane or extracellular proteins containing metal centers that catalyze H_2O_2 oxidation and are distinct from those in *P. gingivalis*. From these analyses it is strongly suggested that *A. actinomycetemcomitans* and *P. gingivalis* carry out EET with cell-surface proteins coupled with lactate and glucose fermentation reactions. Hence, a sophisticated cell surface protein analysis needs to be carried out to identify the membrane proteins in these pathogens and would be a future part of our research.

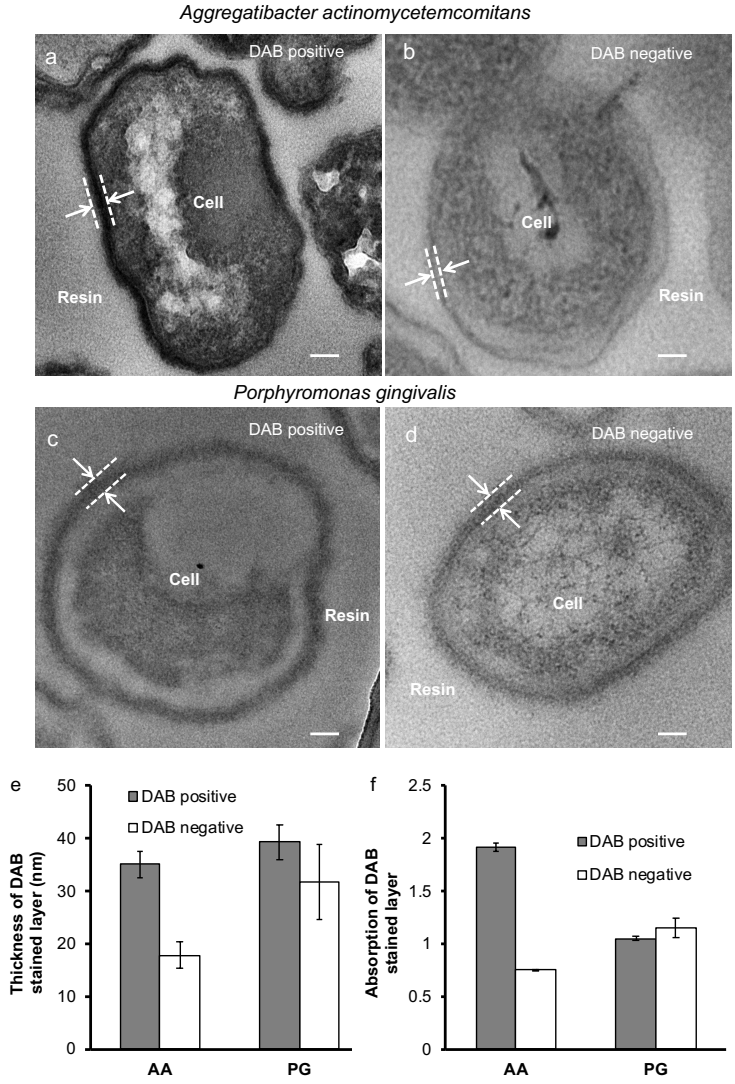

Figure 4-2-9. Transmission electron micrograph (TEM) of 3,3'-diaminobenzidene (DAB) -stained cells of *Aggregatibacter actinomycetemcomitans* (AA) and *Porphyromonas gingivalis* (PG). Positive DAB staining with the addition of H_2O_2 (a, c), and Negative DAB staining in the absence of H_2O_2 (b and d). Scale bars, 50 nm. (e) DAB-stained layer thickness, and (f) absorption of *A. actinomycetemcomitans* and *P. gingivalis* measured from (n=10) line profiles of TEM images under DAB-positive and -negative conditions.

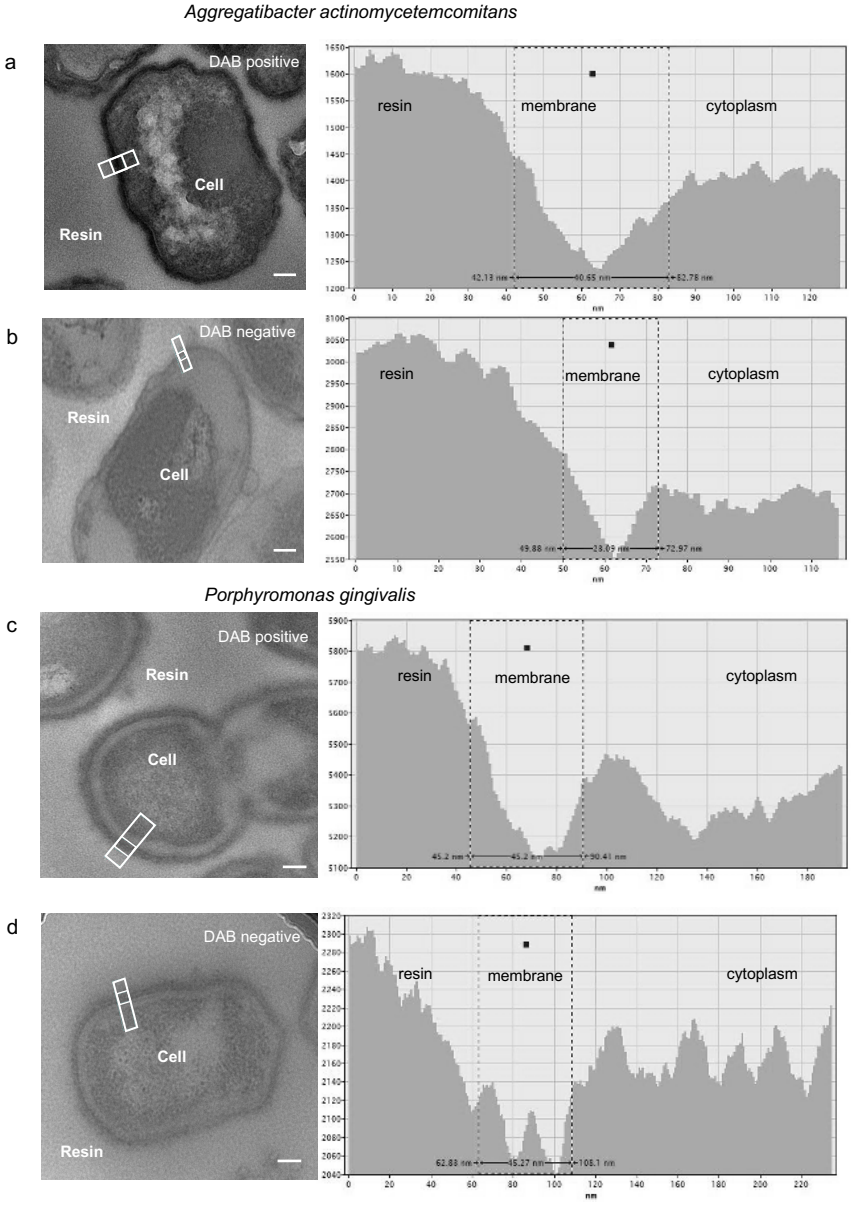

Figure 4-2-10. Example TEM-LINE profiles, of membrane regions of *Aggregatibacter actinomycetemcomitans* (a, b) and *Porphyromonas gingivalis* (c, d) in 3,3'-diaminobenzidine (DAB) positive and DAB negative respectively, used to estimate the membrane thickness and membrane absorption. Scale bar: 50 nm. White box drawn on TEM image indicates the respective LINE profile showing the location of membrane region. The amount of membrane absorption of estimated as reported earlier.

Although human oral pathogens have been extensively characterized in dental studies, their EET capability has remained uninvestigated. Such metabolic characteristics of *A. actinomycetemcomitans* and *P. gingivalis* showed herein may provide a basis to reevaluate pathogens in the human microbiome from the viewpoint of electrogenic activity and its EET mechanism. Since EET provides a conservative energy mechanism for survival in anaerobic environments such as biofilms where pathogens are thriving and causing diseases, identified current generation capability associated with cellular metabolism can be used as a time-dependent quantitative approach to assess the effect of the drugs or antibiocides on the pathogenic bacteria on the electrode.

Publications of chapter 4-2:

1. **Divya Naradasu,** Alexis Guionet, Toshinori Okinaga, Tatsuji Nishihara, Akihiro Okamoto. "Electrochemical Characterization of Current Producing Human Oral-pathogens by Whole-Cell Electrochemistry". *ChemElectroChem*, (2020). https://doi.org/10.1002/celc.202000117.

Chapter 4-3: Energetics of extracellular electron transfer by oral plaque pathogens: Redox gradient driven intercellular long-range electron transfer in oral plaque

Extracellular electron transport can occur over distances at molecular- scale in biological systems via electron hopping among a small number of immobilized redox molecules [156,157]. However, of the possibility of electron transport over length scales much longer than previously thought possible by using immobilized redox cofactors organized into electron transport conduits in biological systems. This is most apparent in microorganisms, such as *Shewanella* spp. and *Geobacter* spp., that can use electron acceptors residing outside the cell for anaerobic respiration [14,33,99] . For example, in the case of Shewanella, it is proposed that the MtrCAB complex *i.e* CymA-MtrA-MtrC complex spanning from inner membrane to outer membrane comprised of 3 multiheme c-type cytochromes in total 24 hemes acts as a multistep conduit that conducts respired electrons originating in the cytoplasm from the inner membrane through the periplasm and outer membrane to the cell outer surface [158-160]. Outside the cell, both *Shewanella* and *Geobacter* secretes, referred to as pili and microbial nanowires which are nanometer scale diameter, micrometer scale long proteinaceous filaments [161-163], that extend from their outer membrane surfaces into the extracellular matrix (ECM) thought to be involved in extracellular electron transport processes, including cell-to-cell electron transfer [164,165] and reduction of insoluble and soluble oxidants like iron oxides and flavins respectively.

Microbial long-distance electron transfer [166] could perform direct electron transport or via redox mediators by coupling the microbial metabolism processes across such redox gradients and would allow for a unique ecological niche in polymicrobial biofilms like human oral and gut environments where bacteria coexist with the human cells being a friend of foe[115]. Such long-distance electron transport was observed in marine sediments by cable bacteria which are filamentous, multicellular bacteria that efficiently transport electrons from one end to the other ranging from anaerobic space to oxygen environments [165,167,168].

According to Mark Welch, J.L*, et.al* [115] the oral microbiome is arranged in a manner to support the anaerobes and aerobes proliferation in the oral plaque which contains oxygen and nutrient gradients, but the mechanism or how the anaerobes are being survived under anaerobic conditions and being active by causing infectious diseases on tooth is ambiguous. In analogy to this reported observation extracellular electron transport from anaerobic to aerobic region would help these pathogens to survive under energy limited conditions and can harvest energy by inter species electron transport between the microbes. Extracellular electron transfer capability was observed in predominant oral pathogens *Streptococcus mutans, Capnocytophaga ochracea, Aggregatibacter actinomycetemcomitans,* and *Porphyromonas gingivalis* as described in chapter 2, 4-1 and 4-2 respectively.

To support our hypothesis, we studied the individual bacteria's extracellular electron transport capability in four predominant pathogens, and they found to have redox enzymes/molecules mediating their electron transport.

Results & Discussion

Extracellular electron transport mechanisms and associated metabolism are identified in the keystone oral pathogens *Streptococcus mutans*, *Capnocytophaga ochracea, Aggregatibacter actinomycetemcomitans,* and *Porphyromonas gingivalis* (Figure 4-3-1) and differential pulse voltammograms revealed the presence of cell surface redox enzymes as shown in figure 4-3-2. *Streptococcus mutans* (SM) has redox molecules responsible for its electron transport at +250 mV vs SHE which is comparatively more positive than reported redox molecules of environmental bacteria for example cytochromes of *Shewanella* MR1 [14,32,135]. Since *S. mutans* can utilize oxygen or survive with fermentative-EET under anaerobic conditions to reduce oxygen which has positive redox potential and its presence is observed at the surface of the oral biofilm as well [115,169] .

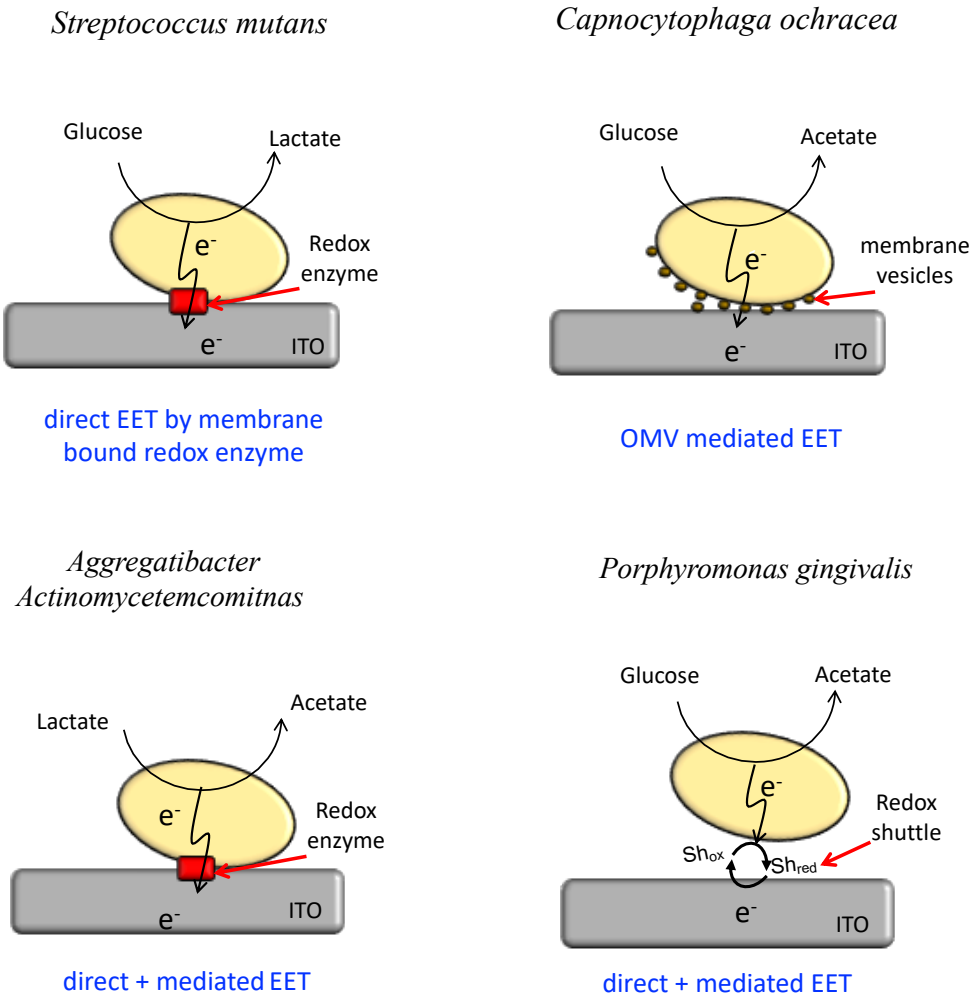

Figure 4-3-1. Schematics showing the summary of extracellular electron transport mechanisms associated with the metabolism of oral pathogens *Streptococcus mutans*- direct electron export via membrane bound redox enzymes, *Capnocytophaga ochracea*- OMVs associated electron export, membrane bound redox enzyme and mediated electron transport in *Aggregatibacter actinomycetemcomitans* and *Porphyromonas gingivalis.*

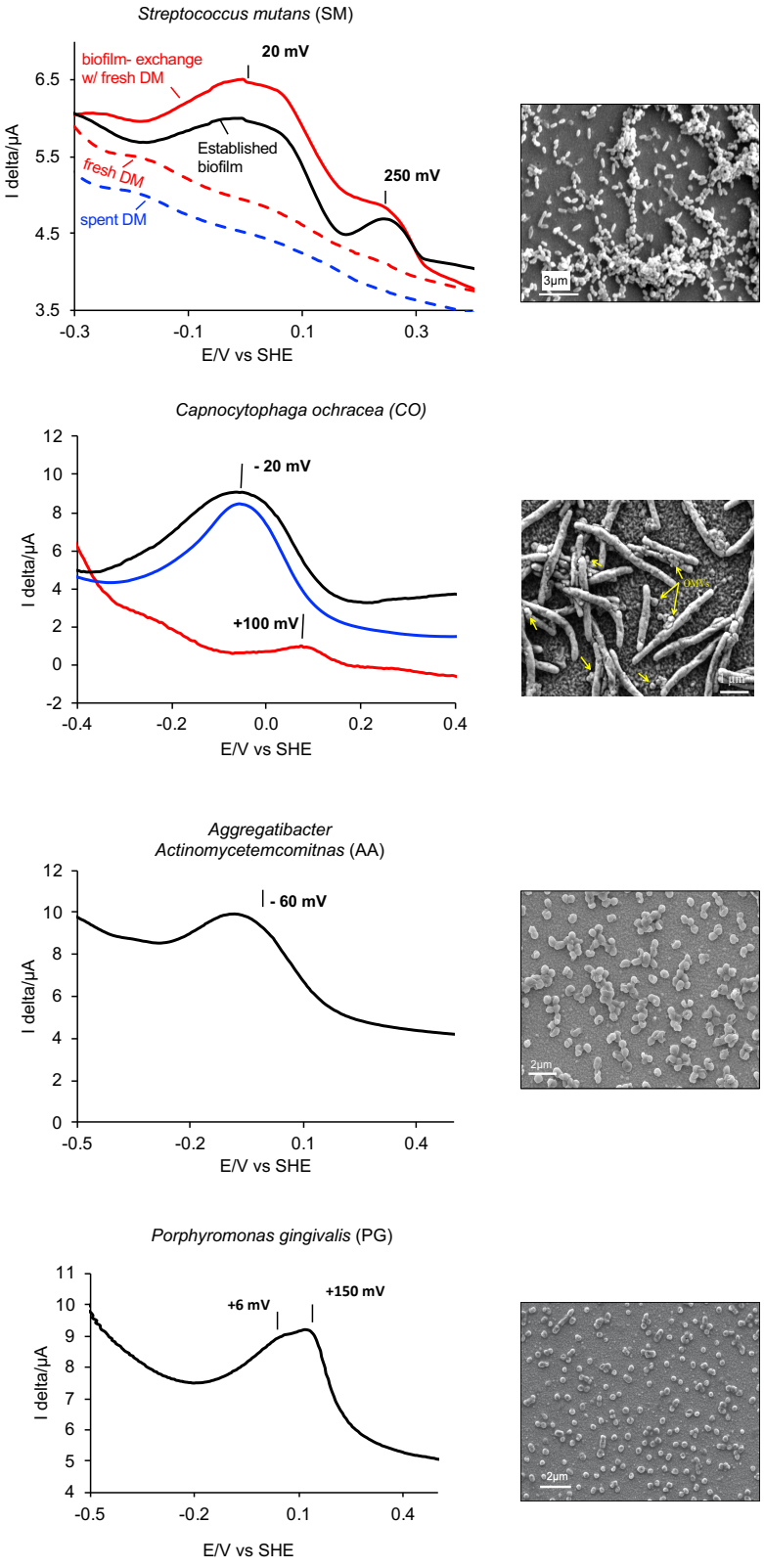

Figure 4-3-2. Differential pulse voltammograms of oral pathogens *Streptococcus mutans*, *Capnocytophaga ochracea*, *Aggregatibacter actinomycetemcomitans* and *Porphyromonas gingivalis* showing the redox molecule peaks and their SEM images.

Capnocytophaga ochracea (CO) has a distinct extracellular electron transport mechanism via outer membrane vesicles (OMV) which enhanced its electron transport. As outer membrane vesicles are well studied for their role in pathogenicity in human infections as they attack the human cells by transferring virulent factors. Secreted OMVs can be a source for electrons as well which can travel to distances to reduce the external electron acceptors like oxygen in oral environment or can be inter transferred between microbes in close niche. In our study OMVs have showed the attachment to the CO surface as shown in figure 4-3-3.

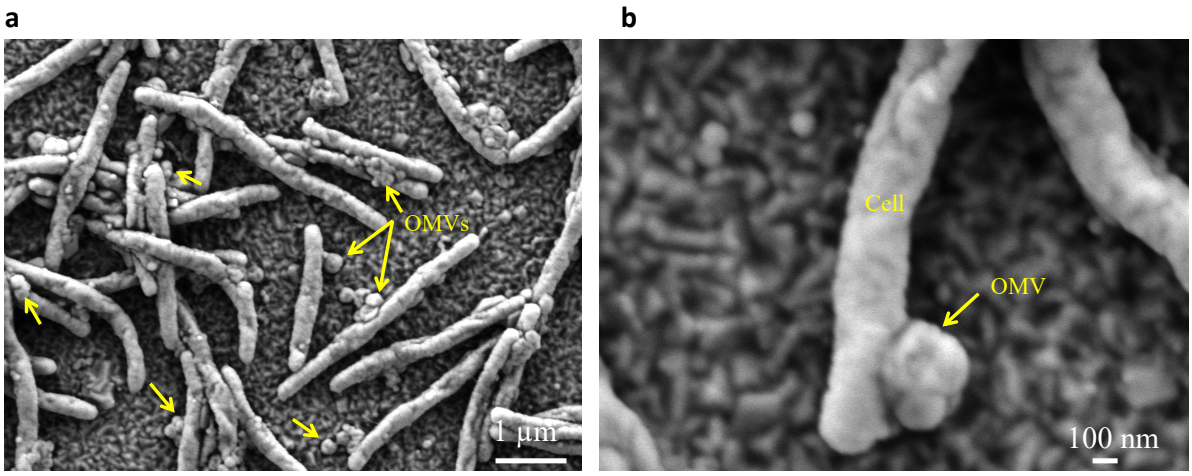

Figure 4-3-3. Scanning electron microscope images of *Capnocytophaga ochracea* and outer membrane vesicles (OMVs) attached to the cell surface as indicated by the arrows.

Capnocytophaga ochracea is a facultative anaerobe which can tolerate and survive in the presence of oxygen, hence their existence in the biofilm is found to be at the anoxic spaces where low oxygen and high CO_2 are available. But in our analysis *Capnocytophaga ochracea* seems to utilize outer membrane vesicles along with the membrane bound redox enzymes. *Capnocytophaga ochracea* has showed a redox peak at -20mVvs SHE on the electrode surface which is distinct from the redox signal of OMVs +100 mV vs SHE (Figure 4-3-2). The rate enhancement of electron transport is associated with the attachment of OMVs to the

cell surface, thus the redox signals of cell and OMVs might be distinct to allow the electron transport from negative potential to positive potential. The energy level of *Capnocytophaga ochracea* and its OMVs is less positive compared to the redox signal of *S. mutans* (Figure 4-3-1). Different redox signals of *S. mutans* and *Capnocytophaga ochracea* indicating the presence of different redox enzymes pertaining to their EET capability. Since *S. mutans* lacks cytochromes [82] and the redox peak appeared at positive potential of +250mV vs SHE is distinct from any reported cytochromes redox potential [32,135], it might have a novel enzyme helping its electron export and redox homeostasis. Cytochrome b or copper containing enzymes have reported to exhibit the redox potentials in the range of +200 to 300 mV vs SHE which in the near range of *S. mutans* redox signals [33,170]. Thus, there is a possibility of the presence of cytochrome b or copper enzymes in *S. mutans,* which is supported by the redox enzyme DAB staining of its cell surface because DAB reacts with transition metal ions which reduce the hydrogen peroxide to form black precipitation as observed under TEM analysis (chapter 2). However, the redox signal of -20mV vs SHE of *Capnocytophaga ochracea* is also distinct from reported *Shewanella*'s cytochromes, it has a number of cytochromes in its genome [158-160] . Apart from the redox enzymes present on the cell surface the DAB staining has showed the redox active species on the surface of membrane vesicle secreted by *Capnocytophaga ochracea.* Though the redox potentials are observed to be distinct between *Capnocytophaga ochracea* cell surface and OMVs, proteins that are expressed in the OMVs might be different or likely to have same protein t that of cell surface but might have highly expressed.

Aggregatibacter actinomycetemcomitans is a facultative anaerobe which has a tri heme cytochrome on its membrane and found to be involved in virulence mechanisms observed in periodontics diseases [107,171]. The redox signal observed at a potential of -60mVvs SHE in the differential pulse voltammogram (Figure 4-3-2) is a negative potential compared to that of *S. mutans* and *Capnocytophaga ochracea. Aggregatibacter actinomycetemcomitans* resides in the deep pockets of teeth causing aggressive periodontitis by dissolve the bone surrounding the tooth surface and has a relatively more negative redox potential on its cell surface compared to the microbes resides in anoxic and aerobic spaces of

the oral biofilm. In analogy to the arrangement of oral microbes in oral biofilm [115] the negative redox potential cell surface enzymes are seems to be confined to the microbes residing in the deep anaerobic environments where as *S. mutans* and *Capnocytophaga ochracea* have a relatively positive redox potentials and reside in the anoxic and aerobic environments.

Porphyromonas gingivalis is a gram-negative facultative anaerobe which is abundant in aggressive periodontitis and gingivalis diseases leading to tooth loss. DAB redox staining has showed no difference between DAB positive and negative conditions supporting the absence of a direct extracellular electron transport in *Porphyromonas gingivalis.* Supernatant swapping of the medium during extracellular electron transfer suggesting a mediated electron transport. However, we observed the redox signals from *Porphyromonas gingivalis* biofilm attached on the electrode surface after medium exchanges at potentials of 6mV vs SHE and 150 mV vs SHE (Figure 4-3-2). The complete abolishment of current production after supernatant removal (chapter 4-2) and presence of redox enzymes on the biofilm suggesting a different EET mechanism in *Porphyromonas gingivalis* compared to *Aggregatibacter actinomycetemcomitans, S. mutans* and *Capnocytophaga ochracea* which showed a direct EET mechanism. The removal planktonic cells from surrounding biofilm may have the impact on electron transport rather than the removal of redox shuttles because intact cells on the electrode surface have exhibited the redox potential peaks aroused from *Porphyromonas gingivalis* cell surface.

Based on the energy levels *i.e.* redox potential of cell surface enzymes and redox molecules involved in their electron export observed in the differential pulse voltammograms of oral plaque pathogens energy level was determined as shown in schematic of *Streptococcus* (figure 4-3-4) and an energy diagram was plotted as shown in figure 4-3-5 to implicate the long-range electron transport in oral biofilm.

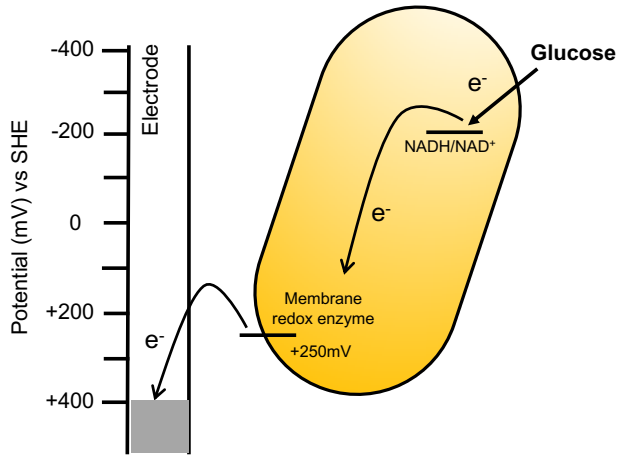

Figure 4-3-4. Energy level of *Streptococcus mutans* estimated based on its EET mechanism and differential pulse voltammogram.

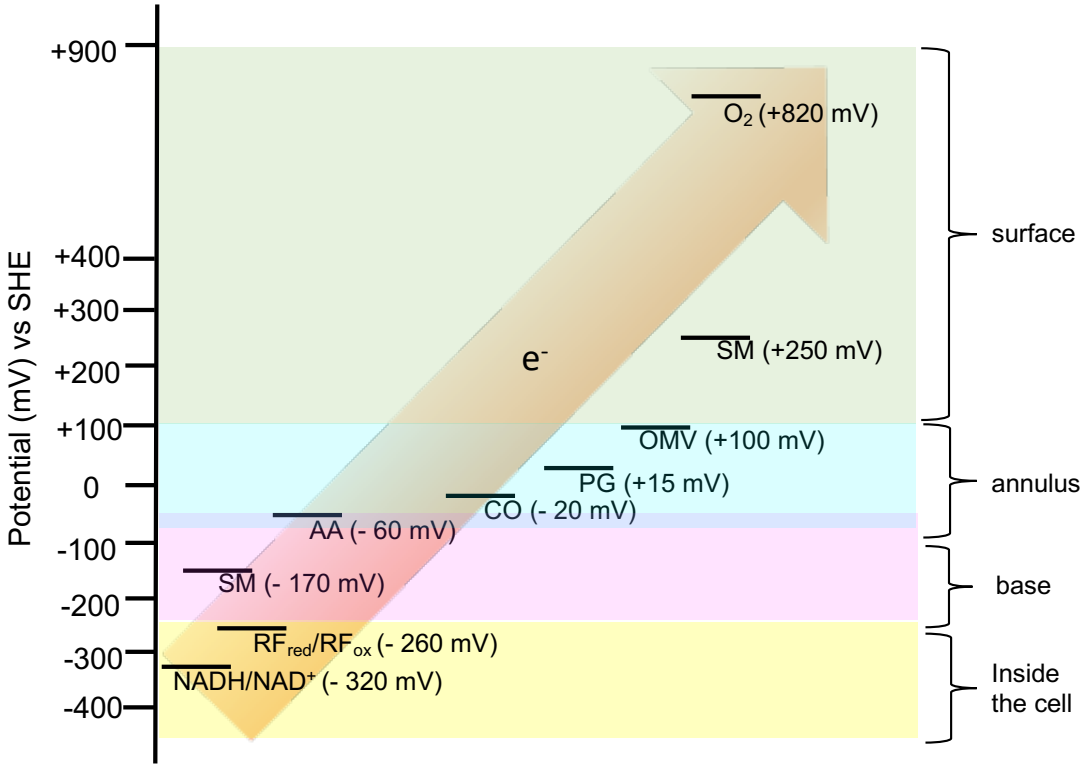

Figure 4-3-5. Energy diagram of oral pathogens used in this study SM: *Streptococcus mutans*, CO: *Capnocytophaga Ochracea* PG: *Porphyromonas gingivalis*, AA: *Aggregatibacter Actinomycetemcomitnas*, RF: Riboflavin, OMV: Outer Membrane Vesicles. The redox potentials of pathogens are in accordance with the arrangement in real environment of oral plaque suggesting an interspecies long-range electron transfer.

Fermentation associated extracellular electron transport was observed in the oral pathogens which we used in this study as glucose consumption leaded to the production of fermentative products like lactate, acetate, formate, ethanol. Glucose consumption could generate the NADH during the glycolysis which can serve as a source of electrons and further consumed during electron export or fermentative metabolites production to regenerate the NAD^+. NADH/NAD^+ conversion have a redox potential of -320mV vs SHE which more negative compared to the redox signals of oral microbes' cell surface redox enzymes (Figure 4-3-5). Electrons from NADH can get transferred to an electron acceptor in the biofilm which have a positive redox potential than -320mV for example riboflavin whose redox potential is at -260mV vs SHE at neutral pH. Though the oral plaque reported to have a slightly acidic pH which may influence the redox potential of riboflavin. Oral microbes have the pathways to synthesize and secrete such flavin molecules hence flavin can act as an electron shuttle from anaerobic space to aerobic environment or can transfer electrons to surrounding microbes in the niche.

S. mutans and *Aggregatibacter actinomycetemcomitans* are present inside of the biofilm in low oxygen environments with redox potentials of -170mV vs SHE and -60mV vs SHE respectively. Nearby cells may uptake the electrons released by *S. mutans* and *Aggregatibacter actinomycetemcomitans* because they have a direct electron export mechanism and such electron exchange would be possible if the redox potential is gradient for example negative to positive. *Capnocytophaga ochracea* have a mechanism of utilizing OMVs along with redox enzymes having potential of -20mV vs SHE which is little positive than that of *S. mutans* and *Aggregatibacter actinomycetemcomitans,* surrounded by *Porphyromonas gingivalis* a key pathogen near anoxic and aerobic regions. +150 mV vs SHE redox potential of *Porphyromonas gingivalis* cell surface is nearer that of oxygen reduction potential +0.82mV vs SHE, as *S. mutans* has another redox peak at +250mV vs SHE which can be utilized to transfer electron and reduce the oxygen. The single strain electrochemical analysis of oral pathogens which develop an organized biofilm on the tooth surface has showed a reductive environment with different redox potentials spanning from negative

potential inside of the biofilm to positive potential at the surface of the biofilm, supporting our hypothesis of interspecies long-range electron transport.

The biofilm development and sustainability are the key factors of pathogenicity in oral diseases, such sustainability depends on the metabolism and interspecies polymicrobial interaction to avoid the competitiveness. Interspecies extracellular electron transport mediated symbiosis reduces the reductive stress in biofilms to enhance energy conservation. To our knowledge this is the first study to present valuable insights into electroactive microbiome in human oral cavity causes chronic oral diseases. Although human oral pathogens were well studied in the medical field, their microbial electrical activities, in particular the capability of extracellular electron transportation that we discovered in this study, were scarcely reported. We anticipate that the role of EET has broad applicability beyond these strains as redox homeostasis is a universal issue in various types of biofilms and provide a potential explanation for higher activity of fermentative pathogen in highly reduced space of thick biofilms. Thus, our findings of novel energy maintenance mechanism could enable the generation of new therapeutic targets for drug-based or electrical control of pathogenicity in polymicrobial biofilms. Electrochemical analysis can be used as a tool to study pathogens energetics in human environments like gut other than oral environments.

Publications of chapter 4-3:

Divya Naradasu, Waheed Miran, Kazuhito Hashimoto and Akihiro Okamoto. Electroactive pathogens of oral plaque – possibility of long range inter species extracellular electron transport: a review (under preparation).

Chapter 5

Isolation and Characterization of Human Gut Bacteria Capable of Extracellular Electron Transport by Electrochemical Techniques.

Introduction

Extracellular electron transfer (EET) mechanisms have evolved in microorganisms as an anaerobic metabolic strategy coupled with the reduction of extracellular solid materials [58,172]. EET mechanisms have been proposed to be mediated by cell-surface transmembrane cytochromes, exogenous or endogenous soluble redox-active compounds, or electrically conductive nanowires. The significance of EET for their energy conservation in anaerobic respiration has provided a reasonable explanation for not only microbial energy conservation and physiology but also interaction with the environments. While EET have been well characterized in terms of mechanistic bases in mainly two model bacterial strains, *Geobacter sulfurreducens PCA* and *Shewanella oneidensis MR-1* [58,173], electrochemical enrichments combined with 16S rRNA-based assessments from a variety of environments, advocate that more physiologically and phylogenetically diverse microorganisms may be capable of using exterior surfaces as electron acceptors. However, it is vital to mention that the survival or enrichment of a microbe on an electrode is not the ultimate evidence of EET ability, and hence further electrochemical characterization is essential for probing EET processes after the isolation of microbes. A number of enrichments have resulted in the isolation of pure cultures that accomplish EET with electrodes, indicating that microbial electrochemical activity at redox-active surfaces may be advantageous in a wide variety of habitats [174-177]. Moreover, many bacteria with either respiration or fermentation as their main metabolic pathway have also been isolated and characterized for EET capability [178-180].

In anaerobic environments with substantially lower redox potentials (-500 to -200 mV) such as the human gut [181], fermentation is the primary microbial metabolism in which the redox cycling of biological electron carriers such as nicotinamide adenine dinucleotide (NADH) drives the intracellular oxidation and reduction of organic substrates. Because

fermentation does not require extracellular electron acceptors to terminate the metabolism, energy gain under such conditions is potentially lower than respiratory metabolisms; therefore, EET capability to increase the rate of NAD^+ regeneration and fermentative metabolism may be important for them to increase net energy gain and compete with other respiratory bacteria [182]. In fact, a few studies have shown that the fermentative gut microbes are capable of EET using soluble electron carrier molecules [62,98,180]. However, it is impossible by simply studying the isolated bacterial cultures to examine which bacteria highly rely on the EET-coupled metabolism in the human gut and to study the ecophysiological importance of EET coupled with fermentation against that with anaerobic respiration which is also abundant in the gut environments [34]. Here, we examined the enrichment competition between fermentative and respiratory bacteria on the electrode surface that enriches the EET-capable bacteria. Specifically, we performed the electrochemical enrichment initiated with a diluted gut microbial community by employing two different medium conditions biasing for fermentation or anaerobic respiration. Isolated bacterial strains were characterized by electrochemical assay for their metabolism associated with the current production and the EET mechanism.

Results & Discussion

Electrochemical enrichment and isolation of EET capable human gut microbes

Toward the isolation of fermentative bacteria capable of EET, we initiated electrochemical enrichment in rich GAM medium with microbial consortium sample collected from human gut and diluted to the concentration of 10^{-7} (v/v) at 37°C. Current production (I_c) went to about $0.3 - 0.4$ μAcm^{-2} in each cycle at around 48 h, and gradually decreased. After 1 week of incubation, we refreshed spent medium with new GAM medium, and after another week of electrochemical incubation, electrode surface was washed to collect enriched bacterial cells. Although subsequent plating resulted in many colony formations, none of colony showed the transparent spot on the black δ-MnO_2-agar plate i.e., MnO_2 was not reduced and hence colonies of EET-capable bacteria were not isolated. This unsuccessful result was probably because GAM medium grew too much fermentative bacterial cells uncapable of

EET in bulk, and the EET-capable bacteria potentially enriched on the electrode became minority.

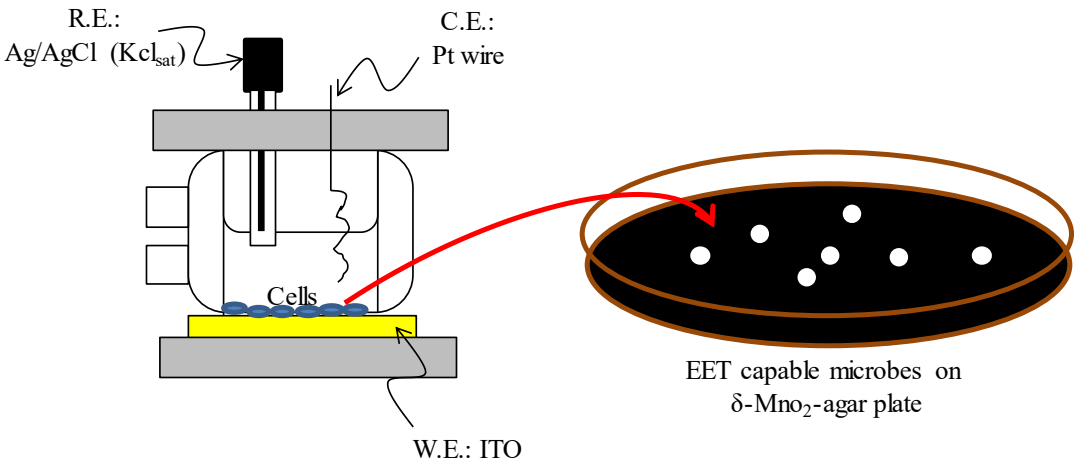

Figure 5-1. Schematic illustration of enrichment procedures initiating from a human fecal sample.

Next, we used DM1 containing either 30 mM acetate or 30 mM lactate as an electron donor to enrich bacteria that couple EET with anaerobic respiration for the same time duration with the enrichment using GAM medium. Although I_c reached to only 15-20 nAcm^{-2} during DM1 cycles as shown in Figure. 5-2a & b, transparent spots in δ-MnO_2 agar plates (Figure 5-1) were observed after the incubation of cells collected from the reactors enriched with either lactate or acetate. All the colonies with transparent spots looked identical, and one of the colonies from each plate were analyzed for 16S rRNA gene sequence.

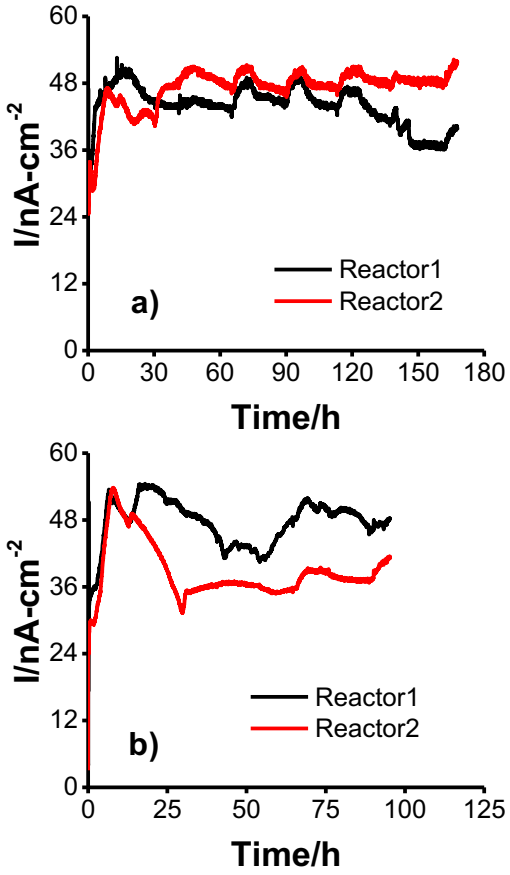

Figure 5-2. Electrochemical activity of gut microbes during enrichment phase a) first cycle and b) second cycle (the replacement of medium) with minimum medium. Reactor 1 and Reactor 2 were operated with acetate and lactate as electron donor, respectively.

The sequence alignment in NCBI showed that the strain isolated from acetate fed reactor belongs to genus *Enterococcus* and the strain isolated from lactate fed reactor belongs to genus *Klebsiella*. The 16S rRNA gene sequences of strain *Gut-S1* in the GenBank database showed that it has more than 99% identity with *Enterococcus avium* and the 16S rRNA gene sequences of the lactate enriched strain *Gut-S2* showed that it has more than 99% identity with *Klebsiella pneumoniae*. Ribosomal RNA gene sequences of these isolated strains were aligned with representative microbial community sequences previously reported for EET capability in gut microbes (*Enterococcus faecalis* and *Faecalibacterium prausnitzii)* and phylogenetic analyses is shown in Fig. 5-3. *E. avium* and *K. pneumoniae* which are similar to *Gut-S1* and *Gut-S2* are Gram-positive and Gram-negative strains, respectively, and both are fermentative under anaerobic conditions.

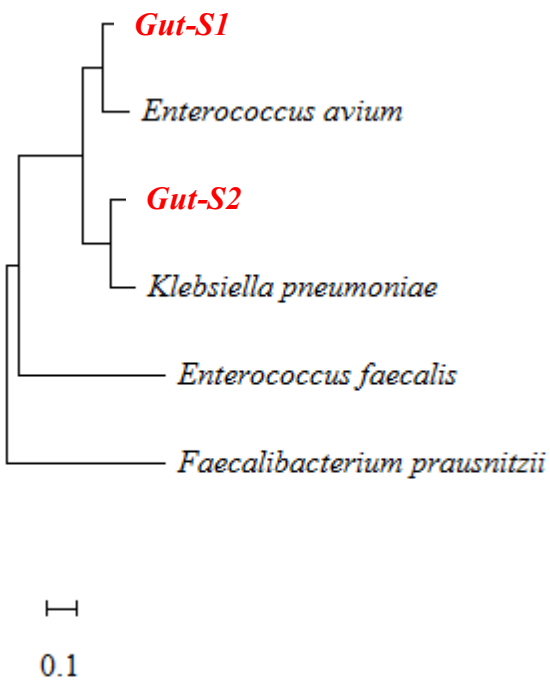

Figure 5-3. Ribosomal RNA gene sequences from electrogenic microbes isolated (isolated in bold red) and aligned with representative microbial sequences previously reported for EET capability in gut microbes. Alignment was carried out using MUSCLE and neigh joining method was employed for phylogenetic tree construction.

Electrochemical characterization of metabolism in isolated strains

SA experiment with isolated strains was performed with DM1 media without adding acetate or lactate at the start (Figure 5-4). Anodic current initiated to increase once *Gut-S1* was added to reactor with sterile media (Figure 5-4a), suggesting the microbial capability of EET to the anode in *Gut-S1*. However, this medium did not contain acetate, and hence the current production was most likely due to the oxidation of yeast extract as no other organic source was present. To our surprise, upon the addition of acetate (30 mM), current production immediately decreased 10% and gradually decreased followed by short-time current recovery, suggesting 30 mM of acetate might damage *Gut-S1*, although we used acetate to enrich *Gut-S1* strain. Current increased to 120 $nAcm^{-2}$ with later glucose addition, demonstrating microbial viability of *Gut-S1* and its capability to couple glucose oxidation with current production. These data strongly suggest that *Gut-S1* was enriched by complex organic substrates in yeast extract rather than acetate, implying there was no microbial strain that use abundant acetate and outcompete the bacteria that utilize yeast extract.

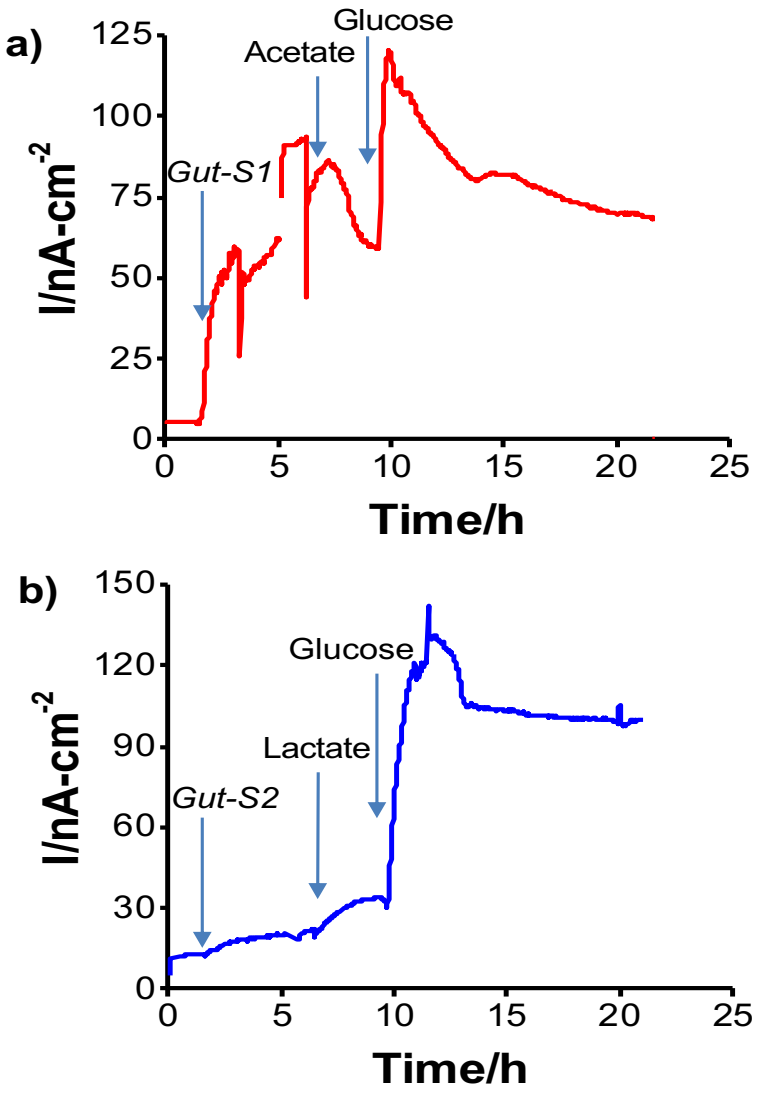

Figure 5-4. Representative current production data versus time in isolated a) *Gut-S1* and b) *Gut-S2* with electrode poised at 0.4 V vs. SHE initiated with sterile DM1 medium with yeast extract at t =0.

In contrast, gradual current increase of 15 $nAcm^{-2}$ was observed upon the lactate addition in case of *Gut-S2* (Figure. 5-4b), suggesting that lactate oxidation contribute to the current production. Because glucose addition resulted in immediate current increase in *Gut-S1 and Gut-S2*, current production may be limited by the rate of metabolic reaction in both strains. These results indicate that lactate-oxidation metabolism takes the key role for enrichment of *Gut-S2* cells on the surface of electrode.

We further characterized the metabolism of two strains and the EET mechanism in these strains by electrochemistry and metabolite assay in different minimum medium DM2, which we usually use to characterize current production capability and EET mechanism of *Shewanella oneidensis* MR-1 [183], with lower yeast concentration than DM1 and without trace minerals and vitamin solution. Also, acetate and lactate concentration were reduced to 10 mM for eliminating the possibility of toxicity to bacterial cell at high organics concentration. No significant change was observed in current generation with and without acetate (in yeast extract containing media) in *Gut-S1*, signifying that EET did not couple with acetate oxidation (Figure. 5-5).

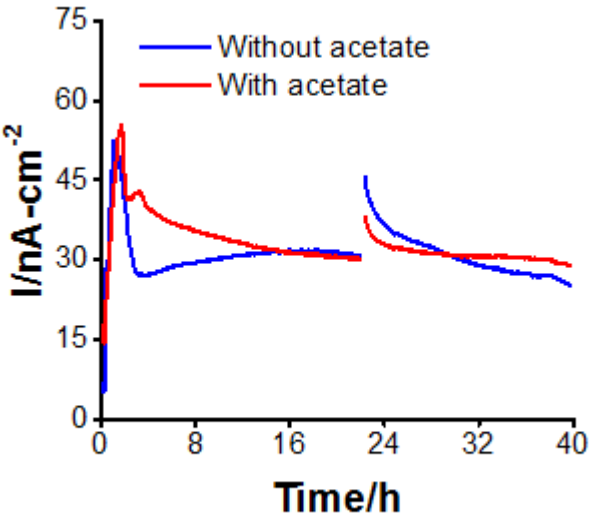

Figure 5-5. Representative current production data versus time in isolated *Gut-S1* with electrode poised at +0.2 V vs. Ag/AgCl (sat. KCl) initiated with (10 mM) and without acetate in DM2 medium.

Furthermore, metabolites quantification in IC showed that acetate concentration increased and was not consumed, which was most likely due to the acetate production from the oxidation of yeast extract (Figure. 5-6a). In case of *Gut-S2*, we observed lactate oxidation and acetate production associated with current production (Figure. 5-6b), indicating lactate was not fermented but anaerobically respired. Slightly less consumption of lactate compared with the production of acetate indicates the oxidation of yeast extract to produce acetate in *Gut-S2*. These results demonstrated that *Gut-S2* have EET capability associated with lactate oxidation, which is the similar with the anaerobic respiration of model EET microbial strain, *S. oneidensis* MR-1.

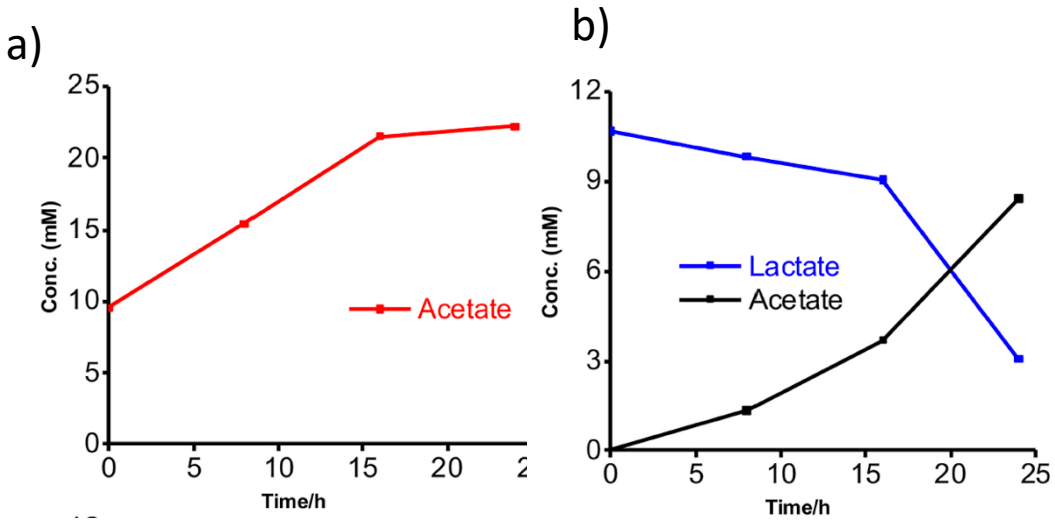

Figure 5-6. Metabolites concentration versus time during current production from isolated strains in the presence of acetate or lactate. a) acetate concentration in the presence of Gut-S1 using DM2 with acetate (and yeast extract). b) lactate and acetate concentration in case of Gut-S2 using DM2 with lactate (and yeast extract).

To examine their capability of coupling EET with fermentation, metabolites were further explored with glucose in the electrochemical system. The consumption and production rate of glucose and the metabolites, respectively, were identified with *Gut-S1* and *Gut-S2* in DM2. Ten mM of glucose was completely consumed with both strains in 24 h, which is 50 to 80 % faster than the consumption rate of lactate in *S. oneidensis* MR-1, indicating considerable microbial activity (Figure 5-7a). *Gut-S1* produced lactate and acetate (Figure. 5-7b), and acetate and formate were the main metabolites in case of *Gut-S2* (Figure 5-7c). Lactate and formate are known as the common end product of bacterial fermentation, and formate can be further oxidized to CO_2 and H_2 under anoxic conditions [184]. The hydrogen produced in electrochemical cells may be oxidized at the ITO electrode surface and contributed to the current generation in *Gut-S2*. A very low coulombic efficiency *i.e.*, less than 0.02 % was observed with both strains based on glucose consumption and coulombs generated. Given this value is much less than that of the environmental bacteria like *S. oneidensis* MR-1 [185], the role of EET in fermentation may be distinct from that of well-studied microbe that associates EET with the anaerobic respiration.

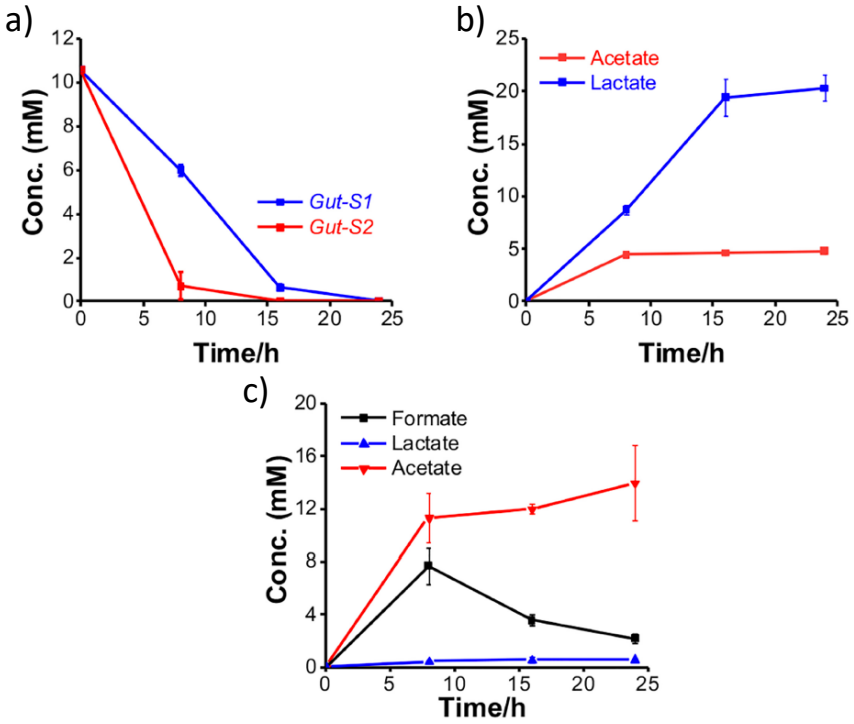

Figure 5-7. Time course of glucose consumption and its metabolites concentration with. b) Gut-S1 and. c) Gut-S2 using DM2 during current production. Glucose consumption was 100% and metabolites produced were lactate and acetate in case of *Gut*S1 whereas formate was additional product observed in case of *Gut*S2 along with lactate and acetate.

EET mechanism in the two isolates

S. oneidensis MR-1 has two potential EET mechanisms, direct electron transfer, and an indirect electron transport mediated by a cell-surface enzyme and soluble electron carriers, respectively[135]. To distinguish the two mechanisms for current production, medium exchange experiments have been performed to elucidate the contribution of soluble electron carrier to net current production [186]. After we exchanged spent medium to fresh one, there was 20% decrease in current for short period and it recovered to the current level before the medium exchange (Figure. 5-8a), suggesting low contribution of soluble electron carrier in current production. Accordingly, differential pulse (DP) voltammogram measured before and after exchange of electrolyte did not show significant change, showing oxidative peak current were

observed at around -0.35 and 0 V (Figure. 5-8b). In contrast, current production decreased approximately 50%, and did not recovered to the level before the medium exchange in *Gut-S2* (Figure. 5-8c) and oxidative peak potential significantly shifted to the positive region in DP voltammogram (Figure. 5-8d), indicating larger contribution of soluble electron shuttle for the current production.

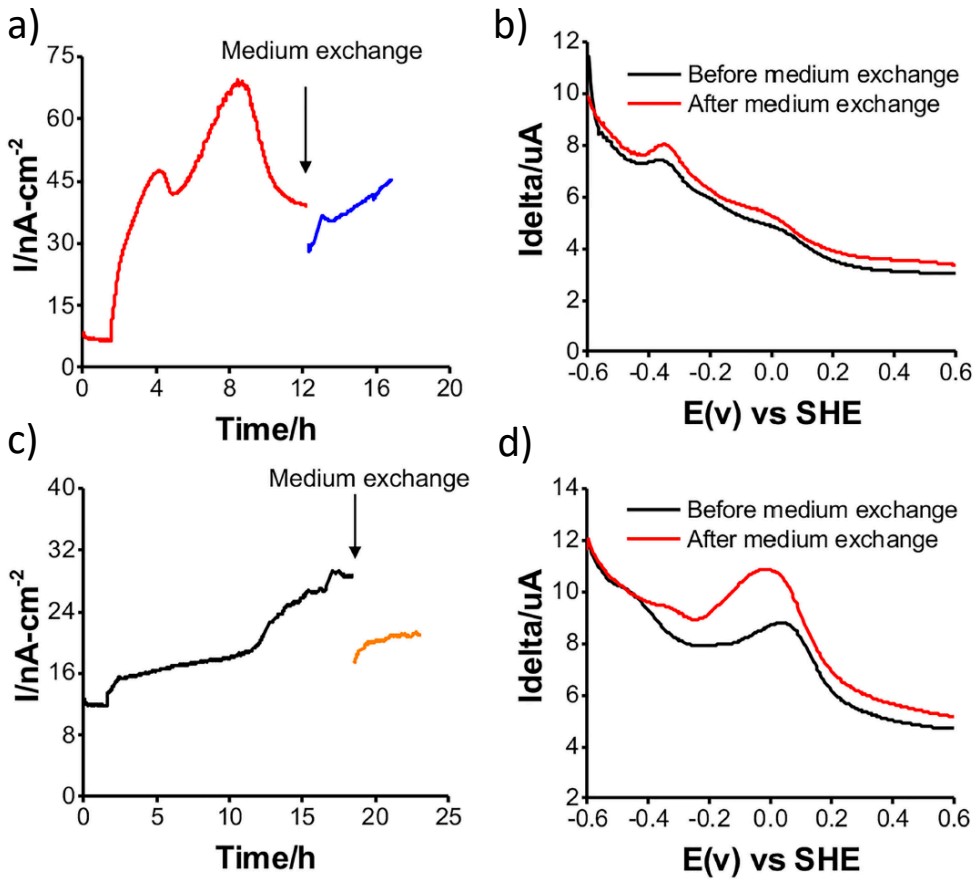

Figure 5-8. Medium exchange experiments for examining the contribution of soluble electron carrier to the current production, and differential pulse voltammograms before and after medium exchange in reactors with Gut-S1 (a and b) and Gut-S2 (c and d)

Given Gut-S2 cells most likely generated hydrogen, their current production could be assignable to the oxidation of fermentatively generated hydrogen. However, because clear peak was still observed at -0.05 V even after the medium exchange, *Gut-S2* may also have cell-surface redox enzyme. Accordingly, for both *Gut-S1* and *S2*, cellular attachment on the electrode surface was confirmed by SEM after the current production in the presence of glucose (Figure. 5-9). Taken together, different peak position and intensity of oxidative peak in DP voltammograms suggest that different redox proteins involved in these two strains.

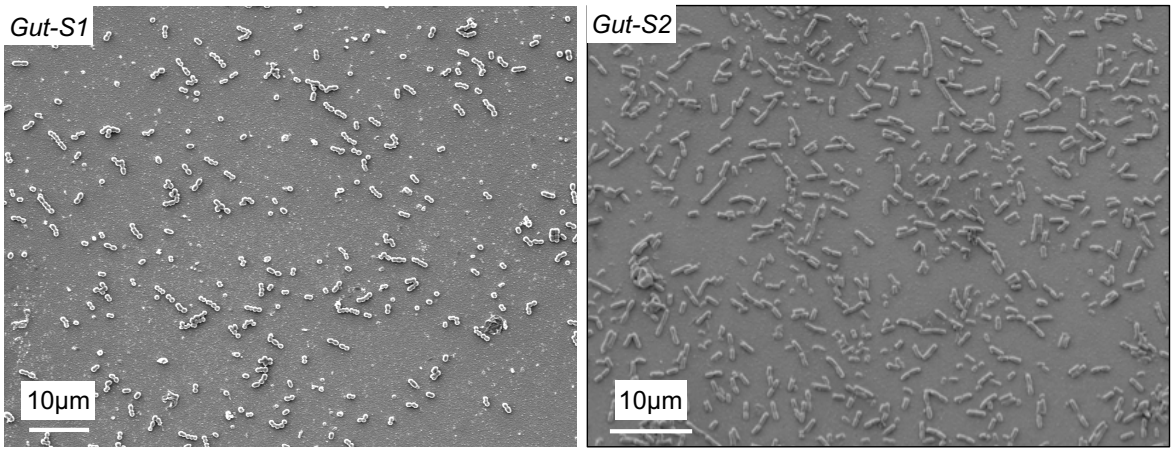

Figure 5-9. Scanning electron microscope images of *Gut*-S1 and *Gut*-S2 biofilm attached on the electrode surface after 24 hours of current production with 10 mM glucose at +0.2 V vs. Ag/AgCl (sat. KCl).

In this study, the EET ability of isolates from the human gut sample was investigated and the metabolism pathway was studied. Our data provide the evidence that the physiological role of EET coupled with fermentation is somehow distinct from that with anaerobic microbial respiration. The magnitude of anodic currents detected from these isolated strains reported here is significantly lower than those typically reported for the metal-reducing microbes usually investigated as EET model systems, which is easily missed by traditional cultivation strategies. For example, *S. oneidensis* MR-1 produces two orders of magnitude more current than *Gut-S1 and Gut-S2* [187]. The low currents observed here also pointed to the isolated

strains' lower ability to gain cellular energy from external redox active surfaces. The physiological role of this mode of energy acquisition from external substrates should be further investigated in detail.

Phylogenetic analysis showed that *Gut-S1* and *Gut-S2* were similar to *E. avium* and *K. pneumoniae,* respectively. Both strains are facultative anaerobes, but not strict anaerobes which are the majority in the human gut. *E. avium* is a Gram-positive bacterium and known as a rare human pathogen and only a few case series exist [188]. While the EET capability in the specific strain was not reported, but *K. pneumoniae* has been earlier studied for their EET capability. This gram-negative bacterium was isolated from subterranean forest sediment and investigated with glucose and starch as the carbon sources with successful current generation [189]. Also in one of the study, an electron-shuttle mechanism in *K. pneumoniae* based-microbial fuel cells has been reported [190].

As in our study, one of the isolated strains is gram-negative and the other is gram-positive, they should have different redox proteins for transferring the electrons to the outer surface. Gram-negative bacteria are known for relying on cell surface-exposed cytochromes for the oxidation or reduction of extracellular minerals [191-193]. Little is known about electroactivity in gram-positive bacteria. Compared to that of gram-negative bacteria, gram-positive bacteria's cell envelope lacks an outer membrane and the peptidoglycan layer is thicker (20–35 nm) [194]. Gram-positive bacteria are known to be poor in current production but can donate electrons to an external conductive acceptor [195] and are frequent members of the microbial community in MFCs [196]. The detailed understanding of this aspect can lead to important discoveries in devising a strategy for pathogenicity control and improvement in human health.

This study, in addition to identifying the new microbial candidates for EET, light on the role of EET associated with the fermentation distinct from that of anaerobic respiration. We believe that this new EET mode coupled with fermentation may open new windows for biotechnological applications and pathogenicity control models. It should be noted that while the focus here was on the gut microbes, but the similar relevance of EET and

electrochemically active microorganisms may be of interest in the vast range of other human pathogens and external environments.

Publications of chapter 5:

Divya Naradasu, Waheed Miran, Mitsuo Sakamoto and Akihiro Okamoto. Isolation and Characterization of Human Gut Bacteria Capable of Extracellular Electron Transport by Electrochemical Techniques. *Front. Microbiol.* 9:3267 (2019) **(published).**

Chapter 6
Summary and Prospective

Our study has identified the novel redox homeostasis mechanism of fermentation associated electron transport in the human oral-pathogen. Given RF is ubiquitous electron shuttle in the oral and gut environments, use of oxidative power outside the biofilm (such as oxygen) may be facilitated by the EET process in fermentative pathogens. The native and direct-EET capability of *S. mutans* suggests the existence of a different long-range electron transport mechanism, *i.e.,* electrically conductive biofilm matrix in oral polymicrobial biofilms. Certain environmental EET bacteria forms an electrically conductive biofilm associated with the production of pili and such conductivity was also previously reported in oral pathogenic biofilms. Assuming that these electrically conductive matrices exist in oral biofilms, *S. mutans* is able to export excess reductive energy to the outside the biofilm and utilize oxidative power. This idea is further supported by the critical impact of small electron export on the metabolic activity (Figure 6-1), because even a low level of electrical conduction by the biofilm appears to be beneficial for these bacteria.

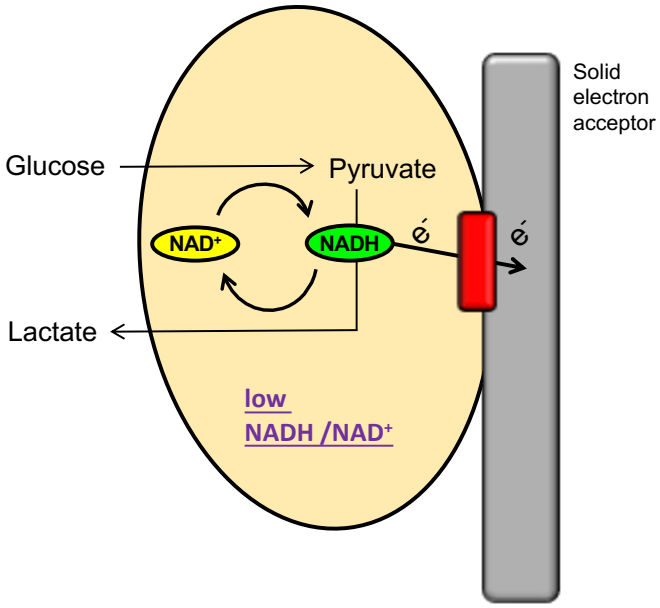

Figure 6. Schematic showing the electron export associated with glucose fermentation which helps the redox homeostasis by regenerating the NAD^+

Given that redox homeostasis and continuous regeneration of NAD+ are universal issues for a wide spectrum of fermentative bacteria that form various types of biofilms, the microbial strategy of exporting excess reductive energy may be ubiquitous. The large impact of the low electron flux on the metabolite pathway and on single-cell activity suggests the importance of electron outflow in highly reductive environments. Given that long-range electron transport is a potential mechanism in *in vivo* biofilms, occurring via electron shuttling or an electrically conductive matrix, as confirmed in environmental bacteria, the findings of the present study indicate that oxidative power outside of oral biofilms (such as that of oxygen) may greatly contribute to the *in vivo* activity and/or physiology of *S. mutans* and a wide spectrum of fermentative bacteria because redox homeostasis and continuous regeneration of NAD^+ are a universal issue in various types of biofilms. Assuming that EET plays a vital role in enhancing microbial activity in biofilms, specifically the acidic-pH dependent EET capability exhibited by the primary cavity causing pathogen *S. mutans* explains the survival mechanism of this pathogen in highly reductive environments of oral plaque, the pathway involved in electrochemical energy maintenance would be a promising target for drug-based or electrical control of pathogens in microbiomes. And such pH dependent EET can be implicated as a sensor to assess the oral health of an individual with the help of synthetic bioelectrochemical analysis.

In natural environments like sediments EET capable bacteria are known for harvesting electrons from electron donors in deeper sediment horizons and transferring these electrons along their longitudinal axes to oxygen present near the sediment-water interface [33,115,164,165,167,169]. In such environments, microbial competition for terminal electron acceptors results in a characteristic vertical redox zones formation and redox potential is the major contributor in controlling the ET rates and thus regulating ET processes. It can be mimicked in oral biofilms where redox gradients may be playing significant role in their survival and growth. OMVs having more positive redox potential than the cell surface, can act as an electron acceptor and donating electrons to more positive redox surfaces and ultimately to final electron acceptor, *i.e*., oxygen at the tooth surface. The enhanced rate of ET in our study is likely due to higher potential gradient between electron donors and OMVs

as the electron acceptor. Because OMVs can be produced by other oral pathogens as well [122-124,133] and may have different redox potentials; therefore, the redox property of these all-important organelles will greatly expand their function and importance in ET in oral biofilms and pathogenicity. This directed to further investigate the mechanisms involved in OMVs dependent EET based on redox potential using OMVs produced by other oral pathogens as well.

Based on these understandings, strategies can be devised to fine-tune the redox potential using both natural and unnatural amino acids and native and nonnative cofactors [197]. For instance, in biological reactions, cytochromes P450s are a class of enzymes that catalyze activation of O_2 and then transfer the oxo group to many organic substrates. In the absence of the target, the enzyme has a low E° which prevents its reduction by its redox partner and is thus stable [198]. Similarly, if we develop a detailed understanding of OMVs based on their redox behavior, we could mimic the design and synthetically produce OMV with a content and specificity of choice for controlling ET rates and ultimately oral pathogenicity.

While cell death and lysis are generally believed the most important source of eDNA [199,200], there is clear evidence that MVs containing eDNA can also be actively produced independently of cell lysis in oral pathogens [122,133].The MVs containing eDNA are largely responsible for enhancing the cell-surface and cell-cell interactions, assisting biofilm formation, and playing a very important role in structural integrity and stability of biofilms. Thus, MVs containing eDNA can have a very strong implication with oral pathogenicity. Studying the electro active nature of pathogens would help microbiologist to understand the energy conservation mechanisms which can provide insight to prepare a new drug targets or antibiotics in order to cure the diseases. *Aggregatibacter actinomycetemcomitans* and *Porphyromonas gingivalis* are the keystone pathogens in periodontitis whose cell surface redox enzymes can be targeted to inactivate them. The redox properties of cell surface enzymes can be utilized to sense the pathogens in oral samples by using electrode devises. Oral saliva samples from humans can be screened to detect the oral health status of a person, by detecting the redox signals in differential pulse voltammogram or current measurements.

Since the oral plaque has the electroactive bacteria with electrically conductive nanowires connecting hundreds of species together and sustaining the biofilm proliferation in oral diseases, such electroactive conductive nature can be targeted to eradicate the biofilm and the pathogens. Low electron export itself is enough for these fermentative pathogens to maintain the redox homeostasis, hence poising a small external negative potential to the biofilms will enhance the reductive environment and can finally damage the cells. Reducing the cell surface enzymes with external voltage will stop the intracellular NAD^+ regeneration leading to reductive stress in the microbes. We hope our study of electroactive oral and gut pathogens would pave paths for new horizons to help the society by reevaluating the disease study models from pathogens electroactive nature point of view and design disease control treatment methods.

References

1 Sanchez, S. & Demain, A. L. Metabolic regulation and overproduction of primary metabolites. *Microb Biotechnol* **1**, 283-319, (2008).

2 Jurtshuk, P., Jr. in *Medical Microbiology* (eds th & S. Baron) (1996).

3 Kim, B. H. & Gadd, G. M. Bacterial Physiology and Metabolism Preface. *Bacterial Physiology and Metabolism*, Xxi-Xxii, (2008).

4 Romano, A. H. & Conway, T. Evolution of carbohydrate metabolic pathways. *Research in Microbiology* **147**, 448-455, (1996).

5 Barnett, J. A. A history of research on yeasts 5: the fermentation pathway. *Yeast* **20**, 509-543, (2003).

6 Herrmann, G., Jayamani, E., Mai, G. & Buckel, W. Energy conservation via electron-transferring flavoprotein in anaerobic bacteria. *Journal of Bacteriology* **190**, 784-791, (2008).

7 Beckmann, J. D. & Frerman, F. E. Electron-transfer flavoprotein-ubiquinone oxidoreductase from pig liver: purification and molecular, redox, and catalytic properties. *Biochemistry* **24**, 3913-3921, (1985).

8 Hartel, U. & Buckel, W. Sodium ion-dependent hydrogen production in Acidaminococcus fermentans. *Arch Microbiol* **166**, 350-356, (1996).

9 Jackins, H. C. & Barker, H. A. Fermentative processes of the fusiform bacteria. *J Bacteriol* **61**, 101-114, (1951).

10 Jungermann, K., Rupprecht, E., Ohrloff, C., Thauer, R. & Decker, K. Regulation of the reduced nicotinamide adenine dinucleotide-ferredoxin reductase system in Clostridium kluyveri. *J Biol Chem* **246**, 960-963, (1971).

11 Dimroth, P. & Schink, B. Energy conservation in the decarboxylation of dicarboxylic acids by fermenting bacteria. *Arch Microbiol* **170**, 69-77, (1998).

12 Fuller, S. J. *et al.* Extracellular electron transport-mediated Fe(III) reduction by a community of alkaliphilic bacteria that use flavins as electron shuttles. *Appl Environ Microbiol* **80**, 128-137, (2014).

13 Pollock, J. *et al.* Alkaline iron(III) reduction by a novel alkaliphilic, halotolerant, Bacillus sp isolated from salt flat sediments of Soap Lake. *Appl Microbiol Biot* **77**, 927-934, (2007).

14 Lovley, D. Dissimilatory Fe(III)- and Mn(IV)-Reducing Prokaryotes. *Prokaryotes: A Handbook on the Biology of Bacteria, Vol 2, Third Edition*, 635-658, (2006).

15 Stucki, J. W., Lee, K., Goodman, B. A. & Kostka, J. E. Effects of in situ biostimulation on iron mineral speciation in a sub-surface soil. *Geochim Cosmochim Ac* **71**, 835-843, (2007).

16 Murphy, W. M. & Shock, E. L. Environmental Aqueous Geochemistry of Actinides. *Rev Mineral <D>* **38**, 221-253, (1999).

17 Roh, Y., Chon, C. M. & Moon, J. W. Metal reduction and biomineralization by an alkaliphilic metal-reducing bacterium, Alkaliphilus metalliredigens (QYMF). *Geosci J* **11**, 415-423, (2007).

18 Myers, C. R. & Nealson, K. H. Respiration-Linked Proton Translocation Coupled to Anaerobic Reduction of Manganese(Iv) and Iron(Iii) in Shewanella-Putrefaciens Mr-1. *Journal of Bacteriology* **172**, 6232-6238, (1990).
19 Nealson, K. H. & Saffarini, D. Iron and manganese in anaerobic respiration: environmental significance, physiology, and regulation. *Annu Rev Microbiol* **48**, 311-343, (1994).
20 Viamajala, S., Peyton, B. M., Apel, W. A. & Petersen, J. N. Chromate reduction in Shewanella oneidensis MR-1 is an inducible process associated with anaerobic growth. *Biotechnol Prog* **18**, 290-295, (2002).
21 Gralnick, J. A., Vali, H., Lies, D. P. & Newman, D. K. Extracellular respiration of dimethyl sulfoxide by Shewanella oneidensis strain MR-1. *Proc Natl Acad Sci U S A* **103**, 4669-4674, (2006).
22 Richardson, D. J. Bacterial respiration: a flexible process for a changing environment. *Microbiology* **146 (Pt 3)**, 551-571, (2000).
23 Peters, B. M., Jabra-Rizk, M. A., O'May, G. A., Costerton, J. W. & Shirtliff, M. E. Polymicrobial interactions: impact on pathogenesis and human disease. *Clin Microbiol Rev* **25**, 193-213, (2012).
24 Flemming, H. C. *et al.* Biofilms: an emergent form of bacterial life. *Nat Rev Microbiol* **14**, 563-575, (2016).
25 Patel, R. Biofilms and antimicrobial resistance. *Clin Orthop Relat Res*, 41-47, (2005).
26 Hall-Stoodley, L. & Stoodley, P. Evolving concepts in biofilm infections. *Cell Microbiol* **11**, 1034-1043, (2009).
27 Anwar, H., Strap, J. L. & Costerton, J. W. Establishment of aging biofilms: possible mechanism of bacterial resistance to antimicrobial therapy. *Antimicrob Agents Chemother* **36**, 1347-1351, (1992).
28 Borriello, G. *et al.* Oxygen limitation contributes to antibiotic tolerance of Pseudomonas aeruginosa in biofilms. *Antimicrob Agents Chemother* **48**, 2659-2664, (2004).
29 Costerton, J. W., Stewart, P. S. & Greenberg, E. P. Bacterial biofilms: a common cause of persistent infections. *Science* **284**, 1318-1322, (1999).
30 Gilbert, P., Maira-Litran, T., McBain, A. J., Rickard, A. H. & Whyte, F. W. The physiology and collective recalcitrance of microbial biofilm communities. *Adv Microb Physiol* **46**, 202-256, (2002).
31 Rosen, D. A. *et al.* Utilization of an intracellular bacterial community pathway in Klebsiella pneumoniae urinary tract infection and the effects of FimK on type 1 pilus expression. *Infect Immun* **76**, 3337-3345, (2008).
32 Light, S. H. *et al.* A flavin-based extracellular electron transfer mechanism in diverse Gram-positive bacteria. *Nature* **562**, 140-144, (2018).
33 Shi, L. *et al.* Extracellular electron transfer mechanisms between microorganisms and minerals. *Nature Reviews Microbiology* **14**, 651-662, (2016).
34 Rey, F. E. *et al.* Metabolic niche of a prominent sulfate-reducing human gut bacterium. *P Natl Acad Sci USA* **110**, 13582-13587, (2013).
35 Fischbach, M. A. & Sonnenburg, J. L. Eating For Two: How Metabolism Establishes lnterspecies Interactions in the Gut. *Cell Host & Microbe* **10**, 336-347, (2011).

36 Wolin, M. J. & Miller, T. L. Interactions of Microbial-Populations in Cellulose Fermentation. *Fed Proc* **42**, 109-113, (1983).
37 Nevin, K. P., Woodard, T. L., Franks, A. E., Summers, Z. M. & Lovley, D. R. Microbial Electrosynthesis: Feeding Microbes Electricity To Convert Carbon Dioxide and Water to Multicarbon Extracellular Organic Compounds. *Mbio* **1**, (2010).
38 Beck, J. D. & Offenbacher, S. Systemic effects of periodontitis: Epidemiology of periodontal disease and cardiovascular disease. *Journal of Periodontology* **76**, 2089-2100, (2005).
39 Welch, J. L. M., Rossetti, B. J., Rieken, C. W., Dewhirst, F. E. & Borisy, G. G. Biogeography of a human oral microbiome at the micron scale. *P Natl Acad Sci USA* **113**, E791-E800, (2016).
40 Wanger, G. *et al.* Electrically conductive bacterial nanowires in bisphosphonate-related osteonecrosis of the jaw biofilms. *Or Surg or Med or Pa* **115**, 71-78, (2013).
41 Bitoun, J. P., Liao, S., Yao, X., Xie, G. G. & Wen, Z. T. The redox-sensing regulator Rex modulates central carbon metabolism, stress tolerance response and biofilm formation by Streptococcus mutans. *PLoS One* **7**, e44766, (2012).
42 Tokunou, Y., Hashimoto, K. & Okamoto, A. Electrochemical Detection of Deuterium Kinetic Isotope Effect on Extracellular Electron Transport in Shewanella oneidensis MR-1. *J Vis Exp*, (2018).
43 Akihiro, O., Kazuhito, H. & Ryuhei, N. in *Recent Trend in Electrochemical Science and Technology* Ch. Chapter 13, (2012).
44 Okamoto, A., Hashimoto, K., Nealson, K. H. & Nakamura, R. Rate enhancement of bacterial extracellular electron transport involves bound flavin semiquinones. *Proc Natl Acad Sci U S A* **110**, 7856-7861, (2013).
45 Fourmond, V. *et al.* SOAS: a free program to analyze electrochemical data and other one-dimensional signals. *Bioelectrochemistry* **76**, 141-147, (2009).
46 Liu, J., Ling, J.-Q., Zhang, K., Huo, L.-J. & Ning, Y. Effect of sodium fluoride, ampicillin, and chlorhexidine on Streptococcus mutans biofilm detachment. *Antimicrob Agents Chemother* **56**, 4532-4535, (2012).
47 Phan, T. N. & Marquis, R. E. Triclosan inhibition of membrane enzymes and glycolysis of Streptococcus mutans in suspensions and biofilms. *Canadian journal of microbiology* **52**, 977-983, (2006).
48 Marsili, E. *et al.* Shewanella secretes flavins that mediate extracellular electron transfer. *Proc Natl Acad Sci U S A* **105**, 3968-3973, (2008).
49 Okamoto, A. *et al.* Uptake of self-secreted flavins as bound cofactors for extracellular electron transfer in Geobacter species. *Energy Environ. Sci.* **7**, 1357-1361, (2014).
50 Pilone, G. J. Determination of ethanol in wine by titrimetric and spectrophotometric dichromate methods: collaborative study. *J Assoc Off Anal Chem* **68**, 188-190, (1985).
51 Huang, L., Tang, J., Chen, M., Liu, X. & Zhou, S. Two Modes of Riboflavin-Mediated Extracellular Electron Transfer in Geobacter uraniireducens. *Front Microbiol* **9**, 2886, (2018).
52 Coursolle, D., Baron, D. B., Bond, D. R. & Gralnick, J. A. The Mtr Respiratory Pathway Is Essential for Reducing Flavins and Electrodes in Shewanella oneidensis. *Journal of Bacteriology* **192**, 467-474, (2010).

53 Saito, J., Hashimoto, K. & Okamoto, A. Nanoscale Secondary Ion Mass Spectrometry Analysis of Individual Bacterial Cells Reveals Feedback from Extracellular Electron Transport to Upstream Reactions. *Electrochemistry* **85**, 444-446, (2017).
54 Geertz-Hansen, H. M., Blom, N., Feist, A. M., Brunak, S. & Petersen, T. N. Cofactory: sequence-based prediction of cofactor specificity of Rossmann folds. *Proteins* **82**, 1819-1828, (2014).
55 Edgar, R. C. MUSCLE: multiple sequence alignment with high accuracy and high throughput. *Nucleic Acids Res* **32**, 1792-1797, (2004).
56 Saitou, N. & Nei, M. The neighbor-joining method: a new method for reconstructing phylogenetic trees. *Mol Biol Evol* **4**, 406-425, (1987).
57 Kumar, S., Stecher, G. & Tamura, K. MEGA7: Molecular Evolutionary Genetics Analysis Version 7.0 for Bigger Datasets. *Mol Biol Evol* **33**, 1870-1874, (2016).
58 Myers, C. R. & Nealson, K. H. Bacterial manganese reduction and growth with manganese oxide as the sole electron acceptor. *Science* **240**, 1319-1321, (1988).
59 Bond, D. R. & Lovley, D. R. Electricity production by Geobacter sulfurreducens attached to electrodes. *Appl Environ Microbiol* **69**, 1548-1555, (2003).
60 Carlson, H. K. *et al.* Surface multiheme c-type cytochromes from Thermincola potens and implications for respiratory metal reduction by Gram-positive bacteria. *Proc Natl Acad Sci U S A* **109**, 1702-1707, (2012).
61 Shi, L. *et al.* Extracellular electron transfer mechanisms between microorganisms and minerals. *Nat Rev Microbiol* **14**, 651-662, (2016).
62 Keogh, D. *et al.* Extracellular electron transfer powers Enterococcus faecalis biofilm metabolism. *mBio* **9**, (2018).
63 Naradasu, D., Miran, W., Sakamoto, M. & Okamoto, A. Isolation and Characterization of Human Gut Bacteria Capable of Extracellular Electron Transport by Electrochemical Techniques. *Front Microbiol* **9**, 3267, (2018).
64 Khan, M. T. *et al.* The gut anaerobe Faecalibacterium prausnitzii uses an extracellular electron shuttle to grow at oxic-anoxic interphases. *ISME J* **6**, 1578-1585, (2012).
65 Ajdic, D. *et al.* Genome sequence of Streptococcus mutans UA159, a cariogenic dental pathogen. *Proc Natl Acad Sci U S A* **99**, 14434-14439, (2002).
66 Ravcheev, D. A. *et al.* Transcriptional regulation of central carbon and energy metabolism in bacteria by redox-responsive repressor Rex. *J Bacteriol* **194**, 1145-1157, (2012).
67 Green, J. & Paget, M. S. Bacterial redox sensors. *Nat Rev Microbiol* **2**, 954-966, (2004).
68 Liu, X. *et al.* Redox-sensing regulator Rex regulates aerobic metabolism, morphological differentiation, and avermectin production in Streptomyces avermitilis. *Sci Rep* **7**, 44567, (2017).
69 Brekasis, D. & Paget, M. S. A novel sensor of NADH/NAD+ redox poise in Streptomyces coelicolor A3(2). *EMBO J* **22**, 4856-4865, (2003).
70 Woebken, D. *et al.* Identification of a novel cyanobacterial group as active diazotrophs in a coastal microbial mat using NanoSIMS analysis. *ISME J* **6**, 1427-1439, (2012).

71 McGlynn, S. E., Chadwick, G. L., Kempes, C. P. & Orphan, V. J. Single cell activity reveals direct electron transfer in methanotrophic consortia. *Nature* **526**, 531-535, (2015).
72 Sickmier, E. A. *et al.* X-ray structure of a Rex-family repressor/NADH complex insights into the mechanism of redox sensing. *Structure* **13**, 43-54, (2005).
73 Bitoun, J. P., Nguyen, A. H., Fan, Y., Burne, R. A. & Wen, Z. T. Transcriptional repressor Rex is involved in regulation of oxidative stress response and biofilm formation by Streptococcus mutans. *FEMS Microbiol Lett* **320**, 110-117, (2011).
74 Sztajer, H. *et al.* Autoinducer-2-regulated genes in Streptococcus mutans UA159 and global metabolic effect of the luxS mutation. *Journal of Bacteriology* **190**, 401-415, (2008).
75 Moscoviz, R., Toledo-Alarcon, J., Trably, E. & Bernet, N. Electro-Fermentation: How To Drive Fermentation Using Electrochemical Systems. *Trends Biotechnol* **34**, 856-865, (2016).
76 Doyle, L. E. & Marsili, E. Weak electricigens: A new avenue for bioelectrochemical research. *Bioresour Technol* **258**, 354-364, (2018).
77 Yang, Y., Zhou, H., Mei, X., Liu, B. & Xing, D. Dual-Edged Character of Quorum Sensing Signaling Molecules in Microbial Extracellular Electron Transfer. *Front Microbiol* **9**, 1924, (2018).
78 Schievano, A. *et al.* Electro-Fermentation - Merging Electrochemistry with Fermentation in Industrial Applications. *Trends Biotechnol* **34**, 866-878, (2016).
79 Sander, C. & Schneider, R. Database of homology-derived protein structures and the structural meaning of sequence alignment. *Proteins* **9**, 56-68, (1991).
80 Rost, B. Twilight zone of protein sequence alignments. *Protein Eng* **12**, 85-94, (1999).
81 Hirose, A. *et al.* Electrochemically active bacteria sense electrode potentials for regulating catabolic pathways. *Nat Commun* **9**, 1083, (2018).
82 Ajdic, D. *et al.* Genome sequence of Streptococcus mutans UA159, a cariogenic dental pathogen. *P Natl Acad Sci USA* **99**, 14434-14439, (2002).
83 Dzink, J. L., Socransky, S. S. & Haffajee, A. D. The predominant cultivable microbiota of active and inactive lesions of destructive periodontal diseases. *J Clin Periodontol* **15**, 316-323, (1988).
84 Genco, R. J., Van Dyke, T. E., Levine, M. J., Nelson, R. D. & Wilson, M. E. 1985 Kreshover lecture. Molecular factors influencing neutrophil defects in periodontal disease. *J Dent Res* **65**, 1379-1391, (1986).
85 Keyes, P. H. The infectious and transmissible nature of experimental dental caries. Findings and implications. *Arch Oral Biol* **1**, 304-320, (1960).
86 Deng, X., Dohmae, N., Nealson, K. H., Hashimoto, K. & Okamoto, A. Multi-heme cytochromes provide a pathway for survival in energy-limited environments. *Sci Adv* **4**, eaao5682, (2018).
87 Wanger, G. *et al.* Electrically conductive bacterial nanowires in bisphosphonate-related osteonecrosis of the jaw biofilms. *Oral Surg Oral Med Oral Pathol Oral Radiol* **115**, 71-78, (2013).

88 Hall-Stoodley, L., Costerton, J. W. & Stoodley, P. Bacterial biofilms: from the Natural environment to infectious diseases. *Nature Reviews Microbiology* **2**, 95-108, (2004).
89 Stewart, P. S. & Costerton, J. W. Antibiotic resistance of bacteria in biofilms. *Lancet* **358**, 135-138, (2001).
90 Bjarnsholt, T. The role of bacterial biofilms in chronic infections. *APMIS. Supplementum*, 1-51, (2013).
91 Skogman, M. E., Vuorela, P. M. & Fallarero, A. A Platform of Anti-biofilm Assays Suited to the Exploration of Natural Compound Libraries. *J Vis Exp*, 54829, (2016).
92 Norton, T. A. *et al.* Using confocal laser scanning microscopy, scanning electron microscopy and phase contrast light microscopy to examine marine biofilms. *Aquatic Microbial Ecology* **16**, 199-204, (1998).
93 Peeters, E., Nelis, H. J. & Coenye, T. Comparison of multiple methods for quantification of microbial biofilms grown in microtiter plates. *Journal of Microbiological Methods* **72**, 157-165, (2008).
94 Guo, L., McLean, J. S., Lux, R., He, X. & Shi, W. The well-coordinated linkage between acidogenicity and aciduricity via insoluble glucans on the surface of Streptococcus mutans. *Sci Rep* **5**, 18015, (2015).
95 Banas, J. A. Virulence properties of Streptococcus mutans. *Front Biosci* **9**, 1267-1277, (2004).
96 Liao, S. M. *et al.* Streptococcus mutans Extracellular DNA Is Upregulated during Growth in Biofilms, Actively Released via Membrane Vesicles, and Influenced by Components of the Protein Secretion Machinery. *Journal of Bacteriology* **196**, 2355-2366, (2014).
97 Baker, J. L., Faustoferri, R. C. & Quivey, R. G. Acid-adaptive mechanisms of Streptococcus mutans-the more we know, the more we don't (vol 32, pg 107, 2017). *Molecular Oral Microbiology* **32**, 354-354, (2017).
98 Pankratova, G., Leech, D., Gorton, L. & Hederstedt, L. Extracellular Electron Transfer by the Gram-Positive Bacterium Enterococcus faecalis. *Biochemistry* **57**, 4597-4603, (2018).
99 Myers, C. R. & Nealson, K. H. Bacterial Manganese Reduction and Growth with Manganese Oxide as the Sole Electron-Acceptor. *Science* **240**, 1319-1321, (1988).
100 Kumar, A. *et al.* The ins and outs of microorganism-electrode electron transfer reactions. *Nat Rev Chem* **1**, (2017).
101 Chadwick, G. L., Otero, F. J., Gralnick, J. A., Bond, D. R. & Orphan, V. J. NanoSIMS imaging reveals metabolic stratification within current-producing biofilms. *P Natl Acad Sci USA* **116**, 20716-20724, (2019).
102 Prosser, B. L., Taylor, D., Dix, B. A. & Cleeland, R. Method of evaluating effects of antibiotics on bacterial biofilm. *Antimicrob Agents Chemother* **31**, 1502-1506, (1987).
103 Li, G. *et al.* Early stage detection of Staphylococcus epidermidis biofilm formation using MgZnO dual-gate TFT biosensor. *Biosens Bioelectron* **151**, 111993, (2020).
104 Baig, S. Reviewing Personal Bacteria - The Human Microbiome Project. *Jcpsp-J Coll Physici* **22**, 3-4, (2012).

105 Conlan, S., Kong, H. H. & Segre, J. A. Species-Level Analysis of DNA Sequence Data from the NIH Human Microbiome Project. *Plos One* **7**, (2012).
106 Dewhirst, F. E. *et al.* The Human Oral Microbiome. *Journal of Bacteriology* **192**, 5002-5017, (2010).
107 Herbert, B. A., Novince, C. M. & Kirkwood, K. L. Aggregatibacter actinomycetemcomitans, a potent immunoregulator of the periodontal host defense system and alveolar bone homeostasis. *Molecular Oral Microbiology* **31**, 207-227, (2016).
108 Kreth, J., Merritt, J., Shi, W. & Qi, F. Co-ordinated bacteriocin production and competence development: a possible mechanism for taking up DNA from neighbouring species. *Molecular Microbiology* **57**, 392-404, (2005).
109 Olsen, I., Tribble, G. D., Fiehn, N. E. & Wang, B. Y. Bacterial sex in dental plaque. *J Oral Microbiol* **5**, (2013).
110 Rup, L. The Human Microbiome Project. *Indian J Microbiol* **52**, 315-315, (2012).
111 Gonzalez, D., Tzianabos, A. O., Genco, C. A. & Gibson, F. C. Immunization with Porphyromonas gingivalis capsular polysaccharide prevents P-gingivalis-elicited oral bone loss in a murine model. *Infection and Immunity* **71**, 2283-2287, (2003).
112 Peters, B. M., Jabra-Rizk, M. A., O'May, G. A., Costerton, J. W. & Shirtliff, M. E. Polymicrobial Interactions: Impact on Pathogenesis and Human Disease. *Clinical Microbiology Reviews* **25**, 193-+, (2012).
113 Wang, H. K. *et al.* Brain abscess associated with multidrug-resistant Capnocytophaga ochracea infection. *Journal of Clinical Microbiology* **45**, 645-647, (2007).
114 Brown, S. A. & Whiteley, M. A novel Exclusion mechanism for carbon resource partitioning in Aggregatibacter actinomycetemcomitans. *Journal of Bacteriology* **189**, 6407-6414, (2007).
115 Mark Welch, J. L., Rossetti, B. J., Rieken, C. W., Dewhirst, F. E. & Borisy, G. G. Biogeography of a human oral microbiome at the micron scale. *Proc Natl Acad Sci U S A* **113**, E791-800, (2016).
116 Benitez-Paez, A., Belda-Ferre, P., Simon-Soro, A. & Mira, A. Microbiota diversity and gene expression dynamics in human oral biofilms. *BMC Genomics* **15**, 311, (2014).
117 Banerjee, S. *et al.* Microbial Signatures Associated with Oropharyngeal and Oral Squamous Cell Carcinomas. *Sci Rep* **7**, 4036, (2017).
118 Hawkey, P. M., Malnick, H., Glover, S. A., Cook, N. & Watts, J. A. Capnocytophaga ochracea infection: two cases and a review of the published work. *J Clin Pathol* **37**, 1066-1070, (1984).
119 Wang, H. K. *et al.* Brain abscess associated with multidrug-resistant Capnocytophaga ochracea infection. *J Clin Microbiol* **45**, 645-647, (2007).
120 Mayatepek, E., Zilow, E. & Pohl, S. Severe intrauterine infection due to Capnocytophaga ochracea. *Biol Neonate* **60**, 184-186, (1991).
121 Kita, D. *et al.* Involvement of the Type IX Secretion System in Capnocytophaga ochracea Gliding Motility and Biofilm Formation. *Appl Environ Microbiol* **82**, 1756-1766, (2016).

122 Schwechheimer, C. & Kuehn, M. J. Outer-membrane vesicles from Gram-negative bacteria: biogenesis and functions. *Nat Rev Microbiol* **13**, 605-619, (2015).
123 Mantri, C. K. *et al.* Fimbriae-mediated outer membrane vesicle production and invasion of Porphyromonas gingivalis. *Microbiologyopen* **4**, 53-65, (2015).
124 Nakao, R. *et al.* Effect of Porphyromonas gingivalis outer membrane vesicles on gingipain-mediated detachment of cultured oral epithelial cells and immune responses. *Microbes Infect* **16**, 6-16, (2014).
125 Doyle, L. E. & Marsili, E. Weak electricigens: A new avenue for bioelectrochemical research. *Bioresource Technol* **258**, 354-364, (2018).
126 Nakamura, R., Kai, F., Okamoto, A., Newton, G. J. & Hashimoto, K. Self-constructed electrically conductive bacterial networks. *Angew Chem Int Ed Engl* **48**, 508-511, (2009).
127 Okamoto, A., Hashimoto, K., Nealson, K. H. & Nakamura, R. Rate enhancement of bacterial extracellular electron transport involves bound flavin semiquinones. *Proceedings of the National Academy of Sciences* **110**, 7856-7861, (2013).
128 McGlynn, S. E., Chadwick, G. L., Kempes, C. P. & Orphan, V. J. Single cell activity reveals direct electron transfer in methanotrophic consortia. *Nature* **526**, 531-535, (2015).
129 Sheik, A. R. *et al.* In situ phenotypic heterogeneity among single cells of the filamentous bacterium Candidatus Microthrix parvicella. *The Isme Journal* **10**, 1274, (2015).
130 Moscoviz, R., Flayac, C., Desmond-Le Quéméner, E., Trably, E. & Bernet, N. Revealing extracellular electron transfer mediated parasitism: energetic considerations. *Scientific reports* **7**, 7766-7766, (2017).
131 Lillich, T. T. & Calmes, R. Cytochromes and Dehydrogenases in Membranes of a New Human Periodontal Bacterial Pathogen, Capnocytophaga-Ochracea. *Archives of Oral Biology* **24**, 699-702, (1979).
132 Hosohama-Saito, K. *et al.* Involvement of luxS in Biofilm Formation by Capnocytophaga ochracea. *Plos One* **11**, e0147114, (2016).
133 Schwechheimer, C., Sullivan, C. J. & Kuehn, M. J. Envelope control of outer membrane vesicle production in Gram-negative bacteria. *Biochemistry* **52**, 3031-3040, (2013).
134 Ojima, Y. *et al.* Deletion of degQ gene enhances outer membrane vesicle production of Shewanella oneidensis cells. *Arch Microbiol* **199**, 415-423, (2017).
135 Okamoto, A., Hashimoto, K., Nealson, K. H. & Nakamura, R. Rate enhancement of bacterial extracellular electron transport involves bound flavin semiquinones. *P Natl Acad Sci USA* **110**, 7856-7861, (2013).
136 Keogh, D. *et al.* Extracellular Electron Transfer Powers Enterococcus faecalis Biofilm Metabolism. *MBio* **9**, e00626-00617, (2018).
137 Lovley, D. R. Happy together: microbial communities that hook up to swap electrons. *ISME J* **11**, 327-336, (2017).
138 McGlynn, S. E., Chadwick, G. L., Kempes, C. P. & Orphan, V. J. Single cell activity reveals direct electron transfer in methanotrophic consortia. *Nature* **526**, 531-U146, (2015).

139 Henderson, B., Ward, J. M. & Ready, D. Aggregatibacter (Actinobacillus) actinomycetemcomitans: a triple A* periodontopathogen? *Periodontol 2000* **54**, 78-105, (2010).
140 Bostanci, N. & Belibasakis, G. N. Porphyromonas gingivalis: an invasive and evasive opportunistic oral pathogen. *FEMS Microbiol Lett* **333**, 1-9, (2012).
141 Loesche, W. J. & Grossman, N. S. Periodontal disease as a specific, albeit chronic, infection: diagnosis and treatment. *Clin Microbiol Rev* **14**, 727-752, table of contents, (2001).
142 Fine, D. H. *et al.* Aggregatibacter actinomycetemcomitans and its relationship to initiation of localized aggressive periodontitis: longitudinal cohort study of initially healthy adolescents. *J Clin Microbiol* **45**, 3859-3869, (2007).
143 Wang, W. *et al.* Bacterial Extracellular Electron Transfer Occurs in Mammalian Gut. *Anal Chem* **91**, 12138-12141, (2019).
144 Myers, C. R. & Myers, J. M. Localization of cytochromes to the outer membrane of anaerobically grown Shewanella putrefaciens MR-1. *J Bacteriol* **174**, 3429-3438, (1992).
145 Marsili, E., Rollefson, J. B., Baron, D. B., Hozalski, R. M. & Bond, D. R. Microbial biofilm voltammetry: direct electrochemical characterization of catalytic electrode-attached biofilms. *Appl Environ Microbiol* **74**, 7329-7337, (2008).
146 Litwin, J. A. Transition metal-catalysed oxidation of 3,3'-diaminobenzidine [DAB] in a model system. *Acta Histochem* **71**, 111-117, (1982).
147 Brown, S. A. & Whiteley, M. A novel exclusion mechanism for carbon resource partitioning in Aggregatibacter actinomycetemcomitans. *J Bacteriol* **189**, 6407-6414, (2007).
148 Mizoguchi, K. *et al.* The regulatory effect of fermentable sugar levels on the production of leukotoxin by Actinobacillus actinomycetemcomitans. *FEMS Microbiol Lett* **146**, 161-166, (1997).
149 Nelson, K. E. *et al.* Complete genome sequence of the oral pathogenic Bacterium porphyromonas gingivalis strain W83. *J Bacteriol* **185**, 5591-5601, (2003).
150 Rey, F. E. *et al.* Metabolic niche of a prominent sulfate-reducing human gut bacterium. *Proc Natl Acad Sci U S A* **110**, 13582-13587, (2013).
151 Farhana, A. *et al.* Reductive stress in microbes: implications for understanding Mycobacterium tuberculosis disease and persistence. *Adv Microb Physiol* **57**, 43-117, (2010).
152 Chen, L. *et al.* Electron Communication of Bacillus subtilis in Harsh Environments. *iScience* **12**, 260-269, (2019).
153 Takahashi, N., Ishihara, K., Kato, T. & Okuda, K. Susceptibility of Actinobacillus actinomycetemcomitans to six antibiotics decreases as biofilm matures. *J Antimicrob Chemother* **59**, 59-65, (2007).
154 Li, G. *et al.* Early stage detection of Staphylococcus epidermidis biofilm formation using MgZnO dual-gate TFT biosensor. *Biosensors and Bioelectronics*, (2019).
155 Rifkin, S. C. & Evans, D. H. Analytical Evaluation of Differential Pulse Voltammetry at Stationary Electrodes Using Computer-Based Instrumentation. *Analytical Chemistry* **48**, 2174-2180, (1976).

156 Gray, H. B. & Winkler, J. R. Electron flow through metalloproteins. *Bba-Bioenergetics* **1797**, 1563-1572, (2010).
157 Gray, H. B. & Winkler, J. R. Electron transfer in proteins. *Annu Rev Biochem* **65**, 537-561, (1996).
158 Hartshorne, R. S. *et al.* Characterization of an electron conduit between bacteria and the extracellular environment. *P Natl Acad Sci USA* **106**, 22169-22174, (2009).
159 Hartshorne, R. S. *et al.* Characterization of Shewanella oneidensis MtrC: a cell-surface decaheme cytochrome involved in respiratory electron transport to extracellular electron acceptors. *Journal of Biological Inorganic Chemistry* **12**, 1083-1094, (2007).
160 Clarke, T. A. *et al.* Structure of a bacterial cell surface decaheme electron conduit. *P Natl Acad Sci USA* **108**, 9384-9389, (2011).
161 Cologgi, D. L., Lampa-Pastirk, S., Speers, A. M., Kelly, S. D. & Reguera, G. Extracellular reduction of uranium via Geobacter conductive pili as a protective cellular mechanism. *P Natl Acad Sci USA* **108**, 15248-15252, (2011).
162 El-Naggar, M. Y. *et al.* Electrical transport along bacterial nanowires from Shewanella oneidensis MR-1. *P Natl Acad Sci USA* **107**, 18127-18131, (2010).
163 Reguera, G. *et al.* Extracellular electron transfer via microbial nanowires. *Nature* **435**, 1098-1101, (2005).
164 Summers, Z. M. *et al.* Direct Exchange of Electrons Within Aggregates of an Evolved Syntrophic Coculture of Anaerobic Bacteria. *Science* **330**, 1413-1415, (2010).
165 Burdorf, L. D. W., Hidalgo-Martinez, S., Cook, P. L. M. & Meysman, F. J. R. Long-distance electron transport by cable bacteria in mangrove sediments. *Mar Ecol Prog Ser* **545**, 1-8, (2016).
166 Nielsen, L. P. Ecology: Electrical Cable Bacteria Save Marine Life. *Current Biology* **26**, R32-R33, (2016).
167 Bjerg, J. T. *et al.* Long-distance electron transport in individual, living cable bacteria. *P Natl Acad Sci USA* **115**, 5786-5791, (2018).
168 Bjerg, J. T., Damgaard, L. R., Holm, S. A., Schramm, A. & Nielsen, L. P. Motility of Electric Cable Bacteria. *Appl Environ Microb* **82**, 3816-3821, (2016).
169 Mark Welch, J. L., Dewhirst, F. E. & Borisy, G. G. Biogeography of the Oral Microbiome: The Site-Specialist Hypothesis. *Annu Rev Microbiol* **73**, 335-358, (2019).
170 Liu, J. *et al.* Metalloproteins Containing Cytochrome, Iron-Sulfur, or Copper Redox Centers. *Chem Rev* **114**, 4366-4469, (2014).
171 Gallant, C. V., Sedic, M., Chicoine, E. A., Ruiz, T. & Mintz, K. P. Membrane morphology and leukotoxin secretion are associated with a novel membrane protein of Aggregatibacter actinomycetemcomitans. *J Bacteriol* **190**, 5972-5980, (2008).
172 Shi, L. *et al.* Extracellular electron transfer mechanisms between microorganisms and minerals. *Nat Rev Microbiol* **14**, 651-662, (2016).
173 Lovley, D. R. & Phillips, E. J. P. Novel Mode of Microbial Energy Metabolism: Organic Carbon Oxidation Coupled to Dissimilatory Reduction of Iron or Manganese. *Appl. Envir. Microbiol.* **54**, 1472-1480, (1988).

174 Fedorovich, V. *et al.* Novel electrochemically active bacterium phylogenetically related to Arcobacter butzleri, isolated from a microbial fuel cell. *Applied and Environmental Microbiology* **75**, 7326-7334, (2009).
175 Logan, B. E. & Regan, J. M. Isolation and Analysis of Novel Electrochemically Active Bacteria. *Nature Reviews Microbiology*, (2009).
176 Rowe, A. R. *et al.* In situ electrochemical enrichment and isolation of a magnetite-reducing bacterium from a high pH serpentinizing spring. *Environmental Microbiology* **19**, 2272-2285, (2017).
177 Zuo, Y., Xing, D., Regan, J. M. & Logan, B. E. Isolation of the exoelectrogenic bacterium Ochrobactrum anthropi YZ-1 by using a U-tube microbial fuel cell. *Applied and Environmental Microbiology* **74**, 3130-3137, (2008).
178 Kumar, P., Chandrasekhar, K., Kumari, A., Sathiyamoorthi, E. & Kim, B. Electro-Fermentation in Aid of Bioenergy and Biopolymers. *Energies* **11**, 343-343, (2018).
179 Zhou, L. *et al.* Microbial Electricity Generation and Isolation of Exoelectrogenic Bacteria Based on Petroleum Hydrocarbon-contaminated Soil. *Electroanalysis* **28**, 1510-1516, (2016).
180 Khan, M. T. *et al.* The gut anaerobe Faecalibacterium prausnitzii uses an extracellular electron shuttle to grow at oxic-anoxic interphases. *ISME Journal* **6**, 1578-1585, (2012).
181 Edwards, C. A., Duerden, B. I. & Read, N. W. Metabolism of mixed human colonic bacteria in a continuous culture mimicking the human cecal contents. *Gastroenterology* **88**, 1903-1909, (1985).
182 Okamoto, A., Tokunou, Y., Kalathil, S. & Hashimoto, K. Proton Transport in the Outer-Membrane Flavocytochrome Complex Limits the Rate of Extracellular Electron Transport. *Angew Chem Int Edit* **56**, 9082-9086, (2017).
183 Saito, J., Hashimoto, K. & Okamoto, A. Flavin as an Indicator of the Rate-Limiting Factor for Microbial Current Production in Shewanella oneidensis MR-1. *Electrochim Acta* **216**, 261-265, (2016).
184 Lim, J. K., Mayer, F., Kang, S. G. & Muller, V. Energy conservation by oxidation of formate to carbon dioxide and hydrogen via a sodium ion current in a hyperthermophilic archaeon. *Proc Natl Acad Sci U S A* **111**, 11497-11502, (2014).
185 Bretschger, O. *et al.* Current production and metal oxide reduction by Shewanella oneidensis MR-1 wild type and mutants. *Appl Environ Microbiol* **73**, 7003-7012, (2007).
186 Marsili, E. *et al.* Shewanella secretes flavins that mediate extracellular electron transfer. *Proc. Natl. Acad. Sci. USA* **105**, 3968-3973, (2008).
187 Xu, S., Jangir, Y. & El-Naggar, M. Y. Disentangling the roles of free and cytochrome-bound flavins in extracellular electron transport from Shewanella oneidensis MR-1. *Electrochim Acta* **198**, 49-55, (2016).
188 Lee, P. P., Ferguson, D. A. & Laffan, J. J. Vancomycin-resistant Enterococcus avium infections: Report of 2 cases and a review of Enterococcus avium infections. *Infectious Diseases in Clinical Practice* **12**, 239-244, (2004).
189 Zhang, L. X. *et al.* Microbial fuel cell based on Klebsiella pneumoniae biofilm. *Electrochem Commun* **10**, 1641-1643, (2008).

190 Deng, L., Li, F., Zhou, S., Huang, D. & Ni, J. A study of electron-shuttle mechanism in Klebsiella pneumoniae based-microbial fuel cells. *Chinese Science Bulletin* **55**, 99-104, (2010).
191 Stams, A. J. M. & Plugge, C. M. Electron transfer in syntrophic communities of anaerobic bacteria and archaea. *Nature Reviews Microbiology* **7**, 568-577, (2009).
192 Wegener, G., Krukenberg, V., Riedel, D., Tegetmeyer, H. E. & Boetius, A. Intercellular wiring enables electron transfer between methanotrophic archaea and bacteria. *Nature* **526**, 587-590, (2015).
193 White, G. F. *et al.* Mechanisms of Bacterial Extracellular Electron Exchange. *Advances in Microbial Physiology* **68**, (2016).
194 Beeby, M., Gumbart, J. C., Roux, B. & Jensen, G. J. Architecture and assembly of the Gram-positive cell wall. *Mol Microbiol* **88**, 664-672, (2013).
195 Pankratova, G. & Gorton, L. Vol. 5 193-202 (2017).
196 Rabaey, K., Boon, N., Siciliano, S. D., Verhaege, M. & Verstraete, W. Biofuel cells select for microbial consortia that self-mediate electron transfer. *Appl Environ Microbiol* **70**, 5373-5382, (2004).
197 Yu, Y., Hu, C., Xia, L. & Wang, J. Y. Artificial Metalloenzyme Design with Unnatural Amino Acids and Non-Native Cofactors. *Acs Catal* **8**, 1851-1863, (2018).
198 Hosseinzadeh, P. & Lu, Y. Design and fine-tuning redox potentials of metalloproteins involved in electron transfer in bioenergetics. *Bba-Bioenergetics* **1857**, 557-581, (2016).
199 Mincione, G. *et al.* Role of the extracellular DNA (eDNA) associated with the Outer Membrane Vesicles (OMVs) in Helicobacter pylori biofilm development. *Helicobacter* **21**, 125-125, (2016).
200 Grande, R. *et al.* Helicobacter pylori ATCC 43629/NCTC 11639 Outer Membrane Vesicles (OMVs) from Biofilm and Planktonic Phase Associated with Extracellular DNA (eDNA). *Frontiers in Microbiology* **6**, (2015).

List of publications

2. **Divya Naradasu**, Waheed Miran, Mitsuo Sakamoto and Akihiro Okamoto. "Isolation and Characterization of Human Gut Bacteria Capable of Extracellular Electron Transport by Electrochemical Techniques". *Front. Microbiol.* 9:3267 (2019)

3. **Divya Naradasu,** Alexis Guionet, Toshinori Okinaga, Tatsuji Nishihara, Akihiro Okamoto. "Electrochemical Characterization of Current Producing Human Oral-pathogens by Whole-Cell Electrochemistry". *ChemElectroChem*, (2020). https://doi.org/10.1002/celc.202000117.

4. Shu Zhang*, Miran Waheed*, **Divya Naradasu*,** Siyi Guo and Akihiro Okamoto. "A Human Pathogen *Capnocytophaga Ochracea* Exhibits Current Producing Capability". *Electrochemistry*, (2020)**.** * equal authors

Acknowledgement

This thesis deals with the studies accomplished by the author under the direction of Professor Dr. Kazuhito Hashimoto, Professor Hiroshi Ishikita and Associate professor Dr. Okamoto akihiro in his laboratory at the University of Tokyo and at NIMS, Tsukuba

First of all, I would like to express my sincere thanks to the professor. Dr. Kazuhito Hashimoto for the invaluable guidance and constant encouragement throughout the course of this research.

It is a great pleasure to express my gratitude to professor. Hiroshi Ishikita for his kind guidance and discussion regarding this work.

I would also like express my gratitude for Associate professor, Independent scientist
Dr. Okamoto akihiro for his kind guidance and insightful discussion regarding this work.

I am greatly thankful to the MEXT Japanese government scholarship and National Institute for Materials Science (NIMS) for giving the opportunity, support and for providing the scholarship to do my Ph.D. work in japan.

Finally, I would like to thank my father Naradasu Subbarao, my beloved mother Naradasu Padma and my sister Naradasu Jyothi for their warm encouragement and their continuous support.